Cellulose-based amorphous solid dispersions enhance rifapentine delivery characteristics and dissolution kinetics *in vitro*

By

Christopher J. Winslow

Thesis submitted to the Faculty of Virginia Polytechnic Institute and State University in partial fulfillment of the requirements for the degree of

Masters of Life Science

In

Food Science and Technology

Approved by:
Andrew P. Neilson
Kevin Edgar
Cristina Fernandez-Fraguas

June 12th, 2017
Blacksburg, Virginia

Keywords: Amorphous solid dispersion, bioavailability, tuberculosis, cellulose, rifapentine, dissolution, bioavailability, 3-formylrifamycin, solubility

Cellulose-based amorphous solid dispersions enhance rifapentine delivery characteristics and dissolution kinetics *in vitro*

Christopher J. Winslow

Abstract [Academic]

The efficacy of rifapentine, an oral antibiotic used in the treatment of tuberculosis, is reduced due to its degradation at gastric pH and low solubility at intestinal pH. We aimed to improve delivery properties *in vitro* by incorporating rifapentine into pH-responsive amorphous solid dispersions with cellulose derivatives including: hydroxypropylmethylcellulose acetate succinate (HPMCAS), cellulose acetate suberate (CASub), and 5-carboxypentyl hydroxypropyl cellulose (CHC). Most amorphous solid dispersions reduced rifapentine release at gastric pH, with the best performing polymer CASub showing >31-fold decrease in area under the curve compared to rifapentine alone. Lower solubility at gastric conditions was accompanied by a reduction in the acidic degradation product 3-formylrifamycin, as compared to rifapentine alone. Certain formulations also showed enhanced apparent solubility and stabilization of supersaturated solutions at intestinal pH, with the best performing polymer HPMCAS showing almost a 4-fold increase in total area under the curve compared to rifapentine alone. These *in vitro* results suggest that delivery of rifapentine via amorphous solid dispersion with cellulose polymers may improve bioavailability *in vivo.*

Cellulose-based amorphous solid dispersions enhance rifapentine delivery characteristics and dissolution kinetics *in vitro*

Christopher J. Winslow

Abstract [Public]

Rifapentine is an antibiotic that is used in the treatment of tuberculosis. Although it is an effective drug, it has limitations caused by digestion and its low ability to dissolve in water. The environment of the human stomach, which contains strong acid, can destroy the drug making it ineffective against the bacteria that cause tuberculosis. The low ability to dissolve in water is also a problem because in order for the drug to be absorbed, it must be dissolved first. Improving these characteristics of this drug could lead to advancements in the treatment and elimination of tuberculosis. The strategy we used to enhance the characteristics of this drug is called amorphous solid dispersion. This system holds the drug in a very easy to absorb form and releases it as such. Many amorphous solid dispersion formulations in combination with other drugs have shown improved ability to dissolve the drugs and protection of drugs from destruction in harsh conditions such as the stomach acid. Various derivatives of natural cellulose (a chain of sugars, called a polysaccharide, which is a major component of all plants) were used as part of this system, to stabilize the drug and to help dissolve it. We found that these amorphous solid dispersions did help to release and dissolve the drug in large concentrations and protect the drug from the stomach acid. Since we have seen positive results here, the next step is to use these systems in an animal study.

Acknowledgements

I would first like to thank my family, especially my mom, for consistently providing support and encouragement for all that I do and for providing me great role models to follow. I would also like to thank my friends from here at Virginia Tech as well as back home. I could not have done this without the love and support of my friends and family. I would like to thank my advisor, Dr. Andrew Neilson, for providing me this opportunity. I can't say how much it means to have this opportunity and truly don't know where I would be without it. Thank you for all of your support as well, over the last two years as I have grown tremendously as a scientist. I have had the opportunity to improve skills in the laboratory as well as in communication and writing, which will help me wherever I go. I would like to thank the members of the Neilson lab group, both old and new (Andrew Gilley, Tommy Haufe, Andrew Smithson, Caroline Ryan, Laura Griffin, and Reem Ajlan) for helping me to not only develop skills and learn professionally but also for always keeping it fun; couldn't have asked for a better group. I also thank my committee members Dr. Cristina Fernandez-Fraguas and Dr. Kevin Edgar for choosing to work with me and continuously providing feedback and guidance in research. I also appreciate the work of Dr. Edgar's students, Brittany Nichols and Diana Novo; my project would not be possible without them. The Food Science department here at Virginia Tech has been a huge part of my time here and I have really enjoyed being part of it. The faculty and staff are always friendly and willing to help with whatever you need. My fellow grad students are some of the best friends I have ever made and I really appreciate all of the good times we have had and will truly miss it here. I have always felt welcome and supported here and truly appreciate the opportunity to further my education with such a fine department.

Table of Contents

Attributions

The following individuals made invaluable contributions to this research. Dr. Andrew Neilson provided facilities and project materials as well as guidance in research. Dr. Kevin Edgar and Dr. Cristina Fernandez-Fraguas provided guidance and support in research. Brittany Nichols and Diana Novo made the various cellulose polymers and ASDs and provided solid-state characterization data. Laura Mosquera-Giraldo and Dr. Lynne S. Taylor supported research and provided information for the amorphous solubility of rifapentine. Ann Norris (Department of Sustainable Biomaterials, Virginia Tech) performed PXRD analyses.

Abbreviations

Amorphous solid dispersion (ASD), tuberculosis (TB), hydroxypropyl methyl cellulose acetate succinate (HPMCAS), cellulose acetate suberate (CASub), 5-carboxypentyl hydroxypropyl cellulose (CHC), maximum concentration (C_{max}), area under the curve (AUC), rifapentine (RPT), rifampicin (RIF), 3-formylrifamycin (3-FR), X-ray Powder Diffraction (PXRD), differential scanning calorimetry (DSC), polyvinylpyrrolidone (PVP)

Chapter 1: Introduction

Introduction

Rifapentine (RPT) is a semi-synthetic drug belonging to the rifamycin group of antibiotics and used in the treatment of tuberculosis (TB) (FDA, 2010). This drug has shown great promise for the elimination of *Mycobacterium tuberculosis* from human subjects (Rosenthal et al., 2006). Though this is one of the most effective TB drugs that have been discovered, there are still many challenges encountered during treatment. One of the major challenges is that treatment time is too long for many patients to follow and another is that oral bioavailability needs to be improved. Oral bioavailability is variable which may be caused by acid-lability because the drug is degraded at gastric pH, poor solubility at small intestine pH because this is the major site of absorption, crystalline nature of the drug, and/or ingestion with various foods (Dooley et al., 2015; Patil-Gadhe et al., 2014; Tam, Chan, Lam, Dickinson, & Mitchison, 1997). However, even with these challenges, RPT is still an effective treatment for TB and with enhancement of delivery characteristics it could become even more effective against this illness (Rosenthal et al., 2006).

As mentioned, this drug is not yet optimally formulated for maximum efficacy. Amorphous solid dispersion (ASD) has shown incredible promise for improving drug delivery characteristics. With this strategy we see major benefits of increased solution concentrations for many poorly water-soluble drugs and can also see protection from degradation for certain drugs in combination with certain polymers (Gilley et al., 2017; Pereira et al., 2013). As ASD technology and research continues to advance, we see this strategy working for increasingly more drugs. ASD is essentially a rigid matrix of polymers that hold the drug in its amorphous/ molecular

form and then release the amorphous form into solution, enhancing the concentrations achievable (Shah et al., 2014). Though this delivery strategy is not optimal for every drug, the bioavailability of many drugs especially those that are poorly water-soluble, is improved through it. ASDs can further be improved by the modification of the polymers used in the system. There has been particular interest in the use of cellulose polymers, largely due to their low toxicity and the relative ease of modification (e.g. ability to be made pH responsive) (Li et al., 2009). Merging the benefits of ASD with the effectiveness of RPT as an antibiotic could provide the perfect synergy for the elimination of TB from the planet due to a decrease in variability dose to dose, protection from degradation, and higher delivery of the drug with smaller doses.

Research Objectives and Specific Aims

The long-term goal of this research is to develop a drug delivery strategy for RPT that helps to eradicate TB from the planet. The c*entral question* is: Can the oral bioavailability of RPT be increased by ASD? The *central objective* of this research is to determine whether the gastric stability and small intestinal release of RPT can be improved through ASD using cellulose-based polymers. The *central hypothesis* is that if pH responsive amorphous solid dispersions are used to deliver RPT, then gastric stability will increase and supersaturated solutions can be achieved in the small intestine; the rationale is that optimizing behavior at these two pH environments will likely improve bioavailability *in vivo*. In order to achieve our central objective and test our central hypothesis, the following specific aims are proposed:

- **Specific Aim 1:** Prepare ASDs of RPT with cellulose-derived polymers.

- **Specific Aim 2:** Determine the impact of these ASDs on dissolution kinetics at gastric pH *in vitro,* compared to crystalline RPT.
- **Specific Aim 3:** Determine the impact of these ASDs on dissolution kinetics at small intestinal pH *in vitro*, compared to crystalline RPT.

The studies that will be performed to test the hypothesis will be *in vitro* dissolution experiments. The dissolution studies will be performed with RPT by itself and RPT in ASD matrices of different cellulose polymers, at different concentrations. The dissolution studies will further be performed at different pH values, including fasted stomach pH at 1.2, small intestine pH at 6.8, and a pH shift from 1.2→6.8, simulating the pH change during gastrointestinal transit from the stomach to the small intestine (Pereira et al., 2013). This question is important because the improvements from this ASD delivery system could potentially lead to an increase in bioavailability *in vivo* (Gilley et al., 2017; Shah et al., 2014). Increased bioavailability is important because it leads to lower effective doses of the drug thereby providing a higher kill of bacteria and decreasing treatment cost while also decreasing side effects and patient variability (White, 2013). With this system we may see shorter and more effective treatments for TB. Seeing positive results may ultimately help to eradicate TB from the planet.

Chapter 2: Literature Review

Tuberculosis

Introduction

TB has been a worldwide problem for centuries, with evidence pointing to documented infections in Egypt over 5000 years ago, although the cause was not discovered until 1882 by Robert Koch (Daniel, 2006). Now, 135 years after its discovery, TB continues to plague the world. TB is an infection caused by the bacterium *Mycobacterium tuberculosis (WHO, 2014).* These bacteria are acid-fast, aerobic, non-motile, and non-sporulating (Rastogi, Legrand, & Sola, 2001). Once acquired, the bacteria can reside in the lungs of infected individuals and can be easily spread from the carrier through coughing, sneezing, or even speaking (WHO, 2014). After being expelled, others can contract the infection themselves by inhaling the bacteria. In addition to other factors, the ease of spread of TB has caused an estimated 1/3 of the current global population to be infected (Dye et al., 1999). According to the World Health Organization (WHO), there were 9 million new cases of TB and 1.5 million deaths due to TB in 2013 alone (WHO, 2014).

TB has been shown to have a larger presence in less developed areas (Fig. 2.1), and is the leading cause of death due to infectious disease in developing countries (Rastogi, Legrand, & Sola, 2001). Currently, the highest presence of this illness is in Asia and Africa (Rastogi, Legrand, & Sola, 2001; WHO, 2014).

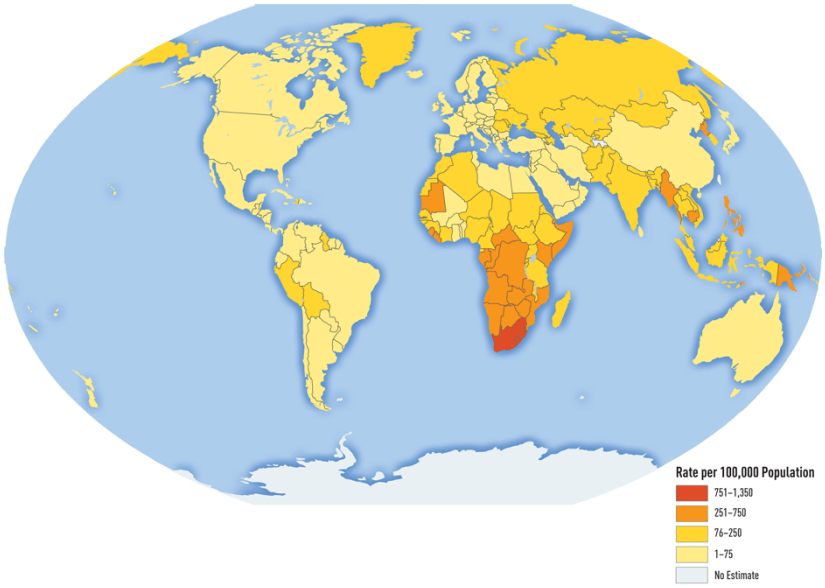

Figure 2.1: Prevalence of TB in 2012 organized by the CDC and data collected by WHO https://wwwnc.cdc.gov/travel/yellowbook/2016/infectious-diseases-related-to-travel/tuberculosis (LoBue, 2015).

The mortality rate of TB is estimated by WHO and the Institute for Health Metrics and Evaluation to be anywhere between 13.9-20.9%, but other estimates suggest it is closer to 23% (Dye et al., 1999; WHO, 2014). However, these estimates are global averages and it is important to note that the rate is extremely variable, ranging from an estimated 1.5% in parts of the Americas to over 50% in some parts of Africa (WHO, 2014).

Not only is TB a problem because of its high mortality rate, but also due to the amount of latent infections. It is estimated that two billion people are currently latently infected (Ginsberg, 2010). Being latently infected means that TB is present and surviving in a seemingly healthy carrier person. Although they do not show symptoms of the infection, they do have a risk of developing the active form of the disease (WHO, 2014, 2015). When the active form is developed, these subjects become sick as well as infectious. Immunocompromisation is the most important factor

when determining whether latently infected patients will develop the active form (LoBue, 2015). Since such a large portion of the infected population is latently infected, it is extremely difficult to eliminate and even find all of the carriers of TB.

Although this infection is curable and the accepted treatments are effective when followed scrupulously, there are issues especially due to the length of the treatment. The treatment has an average length of 6-9 months, which is difficult for many subjects to maintain, especially in developing countries (Rastogi, Legrand, & Sola, 2001). Not completing the treatment leads to the obvious, however not the only, problem that the infected individual remains infected. The rigor and length of the treatment can lead to drug resistant bacteria because many patients stop following the treatments strictly, or even at all. Drug resistance occurs if the regimen is not followed strictly and the bacteria are exposed to the drug but not in high enough concentrations to kill the organisms. This pushes the organisms to develop new methods to survive and thrive in the environment through mutations and these are the organisms that do survive, gain greater resistance, and can pass on their genes (Rastogi, Legrand, & Sola, 2001). TB is considered to be multidrug resistant when treatment with isoniazid and rifampicin (RIF) (currently used in the first-line treatment) is ineffective or takes too long, thus requiring treatment with higher potency drugs (WHO, 2014).

Current Treatment Protocols

The U.S. Centers for Disease Control (CDC) recognizes that TB can be treated in a variety of ways, but the currently recognized first-line treatment involves the use of multiple drugs and spans the time of 6-9 months (CDC, 2016). The preferred first-line treatment for TB involves

daily doses of isoniazid, rifampicin (also known as rifampin) (RIF), ethambutol, and pyrazinamide over 8 weeks (56 doses) and continues with either daily doses of isoniazid and RIF for 18 weeks (126 doses) or isoniazid and RIF twice weekly for 18 weeks (36 doses) (CDC, 2016). As mentioned, it is difficult to treat and cure TB because it takes months of multiple drugs to be effective, which is a difficult regime for many patients to follow. In fact, not following the treatment correctly has caused so many problems that one of the only ways to ensure that the doses are taken and taken when they should be is through directly observed therapy/treatment short course (DOTS) which can involve a regimen as strict and intense as physically watching each patient ingest each dose of medicine (Volmink & Garner, 2007).

Rifapentine vs Rifampin

Though both are rifamycin antibiotics, RPT (Fig. 2.2A) has been selected as a possible treatment over RIF (Fig. 2.2B) for several reasons, two of which are 1) it is generally recognized as a more effective drug and 2) there are not as many strains of bacteria resistant to RPT when compared to RIF (Dooley et al., 2012; Duanmu, Liu, Jiang, Wang, & Fu, 2005; Emary, Toren, Mathews, & Huh, 1998; Hastings, Watkins, & White, 2002; Lemke, 1995; Rosenthal et al., 2006). RPT is expected to increase patient compliance because it has a longer elimination half-life, which allows less frequent treatments (Lemke, 1995). Essentially, RPT persists longer in the blood than RIF before it gets cleared from the system, which allows a longer exposure time for the drug to combat the bacteria (Hastings et al., 2002). RPT has also been associated with shorter treatment times and can possibly be given in higher doses than stated by FDA without harmful effects; which would also reduce treatment time, as well as bacterial drug resistance (Dooley et al., 2012). Several studies suggest that RPT treatment is more active against TB when compared to

certain regimens with RIF (Duanmu et al., 2005; He, Wang, Liu, & Chen, 1996; Rosenthal et al., 2006); up to 9 fold more effective (He et al., 1996). The mechanism of action of RPT is inhibition of DNA-dependent RNA polymerase in bacterial cells, without affecting mammalian cells or enzymes (Patil-Gadhe et al., 2014).

Rosenthal *et al.* found that after two months of treatment, a regimen containing RPT twice weekly was more effective than the standard regimen including RIF daily (Rosenthal et al., 2006). Additionally, a stable cure was achieved after 4 months with RPT versus 6 months with RIF. Evidence has also been shown that giving higher dosages of RPT has shortened treatment time in mice, especially when in combination with certain drugs (Van den Boogaard, Kibiki, Kisanga, Boeree, & Aarnoutse, 2009). Structures of RIF and RPT can be seen below:

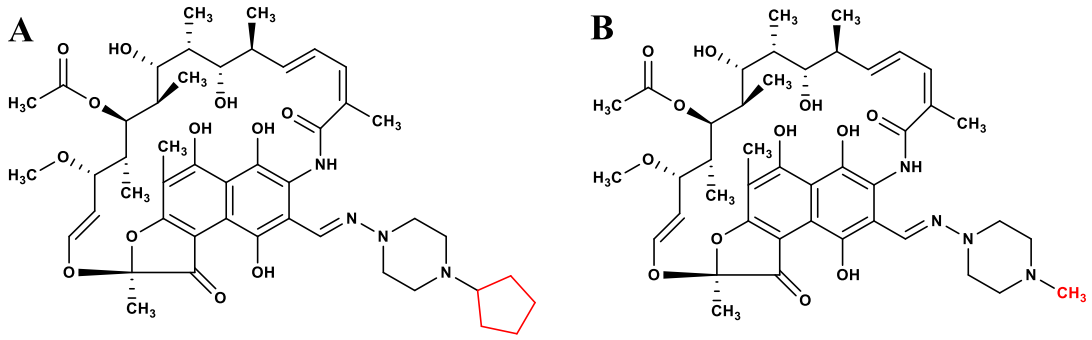

Figure 2.2: Structural similarity of A) rifapentine (RPT) and B) rifampicin (RIF); notice that the only difference between the molecules is the attachment of a cyclopentyl ring or methyl group (both highlighted in red).

Bioavailability

Introduction

Neilson *et al.* explain concepts of bioavailability in "Bioavailability and Metabolism of Bioactive Compounds from Foods," which is summarized below (Neilson et al., 2012). Bioavailability is used to describe the portion of an administered or consumed dose (of drug, xenobiotic, or nutrient) that reaches the bloodstream in an unmodified form and is therefore able to act on the target action site (Brenner & Stevens, 2009; Zhao, Xia, & Huang, 2015). Bioavailability is measured through the compound's pharmacokinetic behavior and is described by the graph of blood (or other specific tissue) concentration over time after an administered dose (Fig. 2.3). The common values associated with pharmacokinetic behavior are C_{max}, T_{max}, AUC, and $t_{1/2}$ (Neilson et al., 2012). C_{max} is representative of the peak concentration and shows the maximum concentration the drug reaches in the body (Urso, Blardi, & Giorgi, 2002). The peak time, known as T_{max}, is the time at which the drug is at its highest concentration (Urso, Blardi, & Giorgi, 2002). AUC, or area under the curve, refers to the total area under the curve of the graph of drug concentration in the blood over time, is expressed in units of (time·concentration), and represents total exposure to the drug (Urso, Blardi, & Giorgi, 2002). $T_{1/2}$ is the elimination half-life, this is the time that it takes to clear ½ of the compound from the body or specific tissue of interest. The corresponding values can be used to indicate *in vitro* bioavailability simply by measuring solution concentration rather than blood concentration. These pharmacokinetic values are indicated in the figure below:

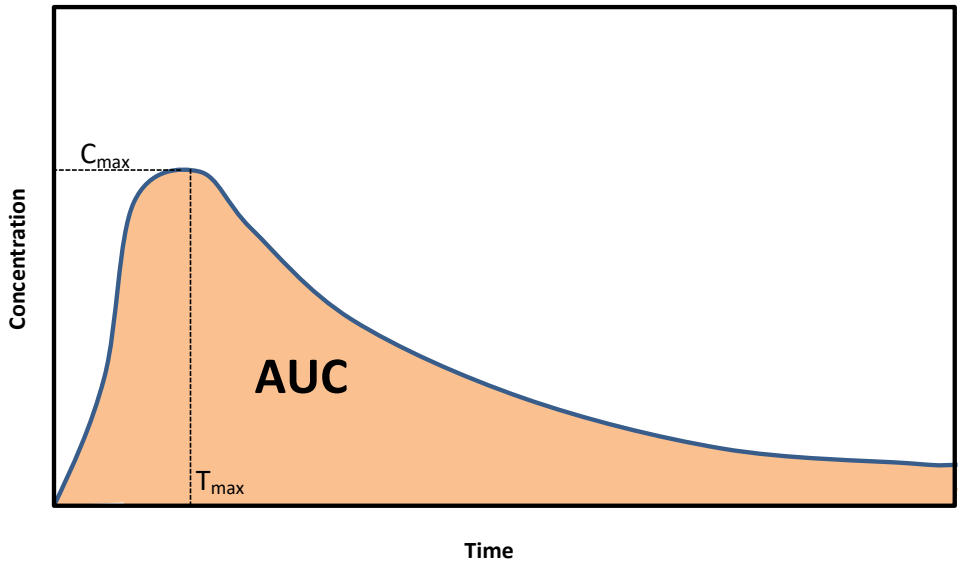

Figure 2.3: Shows a typical pharmacokinetic curve, concentration represents measured concentration in the blood.

Bioavailability is most often determined using the total area under the curve. An intravenous (IV) injection, though it may not always truly be 100% bioavailable, is interpreted as such in order to be used as a comparison for determining absolute bioavailability (Toutain & Bousquet-Mélou, 2004). Absolute bioavailability is used to determine effectiveness of an extravenous form of the drug compared to the intravenous form (e.g. an oral formulation may have 80% absolute bioavailability which actually is relative to an IV injection) (Toutain & Bousquet-Mélou, 2004; Wesch, 2011). However, there may be cases where IV injection is not possible or a compound undergoes extensive metabolism after IV administration and in these cases relative bioavailability is used instead (Wesch, 2011). Relative bioavailability compares two different extravenous forms of the drug (e.g. an oral solution relative to a pill) (Toutain & Bousquet-Mélou, 2004; Wesch, 2011).

The FDA uses the biopharmaceutical classification system (BCS) to classify each drug, in terms of solubility and permeability. This developed system consists of: Class I, II, III, and IV drugs, which are further explained in table 2.1 below (McClements, Li, & Xiao, 2015). Based on this system RPT is considered a BCS class II drug, meaning that solubility is an issue in final bioavailability whereas permeability is not (Agrawal & Panchagnula, 2005).

Table 2.1: Biopharmaceutical classification system (BCS) used by the FDA to classify drugs and/or nutraceuticals

Characteristic	High Solubility[1]	Low Solubility[1]
High Permeability[2]	Class I	Class II
Low Permeability[2]	Class III	Class IV

[1] solubility relates to solubility in gastrointestinal fluids
[2] permeability relates to permeability across epithelial cell membranes

Also important to note when discussing bioavailability is the issue of bioaccessibility. Bioaccessibility is a prerequisite for bioavailability and is known as the amount of a nutrient that is available for absorption in the GI tract by the enterocytes after digestion and release from food components (Bender, 2009; Etcheverry, et al., 2012; Hedrén et al., 2002). Compounds must be released, be stable, be soluble, and be able to diffuse across membranes in order to be absorbed and to be considered bioaccessible (Neilson et al., 2012). Poor bioaccessibility can severely limit bioavailability, which is especially important in food matrices. Both bioavailability and bioaccessibility can be studied through *in vitro* and *in vivo* methods (Etcheverry et al., 2012).

Xenobiotic Bioavailability

Food matrices contain macromolecules as well as essential micronutrients (vitamins and minerals) that are used within the body. There are also xenobiotics contained in some foods. A

xenobiotic is generally described as any substance that the body (or another living system) recognizes as foreign (Bender, 2009; Daintith, 2008). These may or may not be a part of the normal diet and include many substances such as phytochemicals, drugs, pesticides, toxins, and food additives. These foreign compounds are subjected to the same metabolic processes of digestion within the body because there is no way for the body to know if they are helpful or harmful; as long as compounds are substrates for the enzymes, the metabolic processes attempt to neutralize their effects (Neilson et al., 2012).

Digestion and Metabolism

Digestion is the process that the body uses to break down whole food or other ingested materials (drugs, supplements, phytochemicals) into nutrients and other absorbable material, through both physical and chemical means (Neilson et al., 2012). An orally administered drug, such as RPT, must survive each step of digestion and metabolism, much like any food component.

Both the National Institute of Diabetes & Digestive & Kidney Diseases in "The Digestive System & How it Works" and Mike Boland in "Human digestion- a processing perspective," describe the process of digestion, which is summarized in the following paragraphs (Boland, 2016; Wallace, 2013). Digestion begins with mechanical separation, or mastication, of foods in the mouth; although there are some enzymatic reactions (especially salivary amylase for the hydrolysis of starch) it is mostly about size reduction of the food and mixing with saliva so the food can be more easily broken down and absorbed in future steps. Saliva is important because it contains glycoproteins called mucins that aid in keeping the food together while swallowing and lubricating during transport of the food. Salivary proteins in saliva are also known to interact

with certain compounds and one such example is the perception of astringency that is thought to be caused by the precipitation of proteins in the presence of tannins (Lee, Ismail, & Vickers, 2012). After chewing and swallowing, the food is transported into the esophagus. After this point, the movement of the food is involuntary and the body controls the flow through peristaltic movement. From the esophagus, the food travels through the esophageal sphincter into the stomach where the food is mixed with gastric fluid, consisting of mostly hydrochloric acid (HCl), and some digestive enzymes (Martinsen, Bergh, & Waldum, 2005; Jolliffe, 2009). Due to the acid found in the stomach this environment often has a very low pH of about 2, however it is important to note that the pH can vary with age, health status, and food consumed. This environment promotes gastric enzymes to catalyze further breakdown food, such as pepsin to breakdown proteins or gastric lipase for fats. The major function of the stomach is further mechanical breakdown and mixing of food before it moves to the major regions of absorption. This harsh environment can be a challenge for some substances to survive. The stability of the compounds here is a major factor in determining the amount that can ultimately be absorbed (Neilson et al., 2007).

The partially digested food moves through the pyloric sphincter and into the small intestine where the majority of digestion occurs. Upon entering the small intestine, there is a drastic pH change. The pH shifts from highly acidic to a more neutral pH of about 6.8. This occurs because bicarbonate from the pancreas is mixed with HCl from the stomach to neutralize the pH (Kaunitz & Akiba, 2006). Processes here include further breakdown of macromolecules and absorption of most nutrients. The food materials move through the small intestine and are mixed with other digestive juices that contain enzymes from the liver and pancreas, which further digest

compounds that have not yet been degraded or absorbed (Neilson et al., 2012). As the food travels, it passes finger-like ridges, called villi, in the lining of the digestive tract. The villi are lined with intestinal cells called enterocytes containing additional ridges, called microvilli which increase the surface area (Fig. 2.4). This is where most of the absorption occurs, which explains why the high surface area is used (to enhance ability for absorption). The usable nutrients are absorbed through the intestinal lining and into the enterocytes.

In order to enter the enterocyte, the food components must also pass through the unstirred water layer where they must be soluble, and a mucosal layer that protects the enterocytes. Though the mucous layer does not significantly impede absorption for all substances, some compounds can be immobilized here or their absorption can be reduced (Crespy et al., 2003; Gonzales, 2015). It is also important to note that the permeability of this layer can be altered such as the decrease in permeability seen with the introduction of certain dietary fiber components (Mackie et al., 2016). Once compounds pass through these barriers they can enter the enterocytes and have the opportunity to actually be absorbed into the bloodstream. Compounds can cross the membrane by way of passive diffusion, facilitated diffusion, or active transport. The body more specifically uses a combination of endocytosis, tight junctions that may allow paracellular diffusion and carrier-mediated transport for transport across the membrane (Crespy et al., 2003). For passive diffusion and paracellular transport, the main driving force for absorption is the transmembrane concentration gradient (Avdeef, 2012; Tang & Goodenough, 2003; Van Itallie & Anderson, 2006; Washington, 2001). This means that the compound moves from an area of high concentration to an area of low concentration and hence more of a compound will be absorbed if more is present at the apical membrane (Avdeef, 2012; Tang & Goodenough, 2003; Van Itallie

& Anderson, 2006; Washington, 2001). Solubility is extremely important for absorption in these cases because only compounds that are soluble will contribute to increasing this gradient (Raina, Zhang, Alonzo, & Wu, 2014).

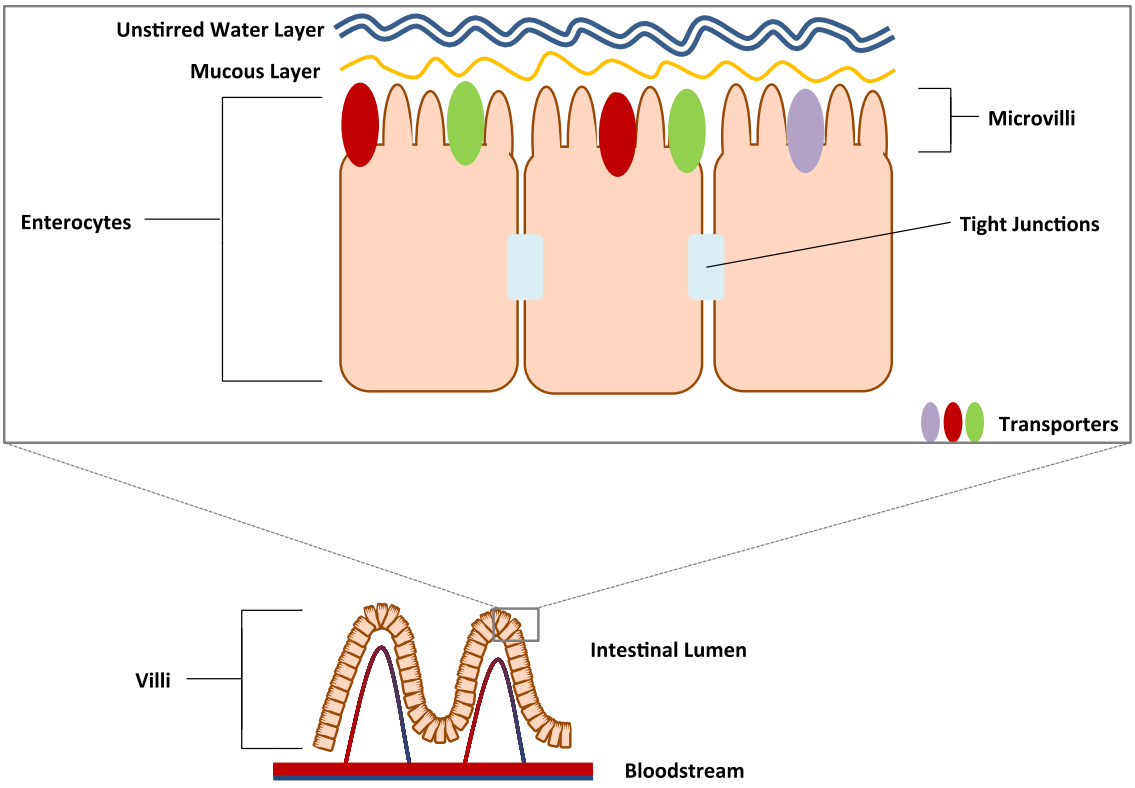

Figure 2.4: A schematic of the small intestinal epithelium showing the enterocytes and various protective layers.

Lipids and lipophilic compounds are absorbed by a somewhat different process. In order to enter the enterocytes, lipophilic compounds and lipids must first be solubilized in an aqueous environment. The formation of micelles (Fig. 2.5) aids in this process and allows passage through the unstirred water layer. Micelles are formed by relatively small amphipathic molecules, such as monoglycerides and fatty acids, or molecules that have both a hydrophilic (polar) and hydrophobic (nonpolar) end. Above a certain concentration, the critical micelle

concentration, the molecules associate together with their like ends towards each other (Cui, Mao, Liu, Yuan, & Du, 2008). Micelles are able to pass through aqueous environments because they form a structure that shows aqueous characteristics on the outside. The molecules of fat form a sphere that is hydrophobic on the inside and hydrophilic on the outside, which happens because some fat molecules have hydrophilic, polar heads that form an outside barrier and hydrophobic, nonpolar tails that tightly pack into the center, in order to minimize the thermodynamic energy of displacing water molecules. The formation of micelles is aided by the coingestion of dietary fats which provide structural components for the micelles (Neilson et al., 2012). Micelles allow lipids to pass the unstirred water layer of the enterocytes; once they pass this, the micelles break apart at the apical surface, releasing the lipid particles onto the surface and allowing uptake by the enterocytes.

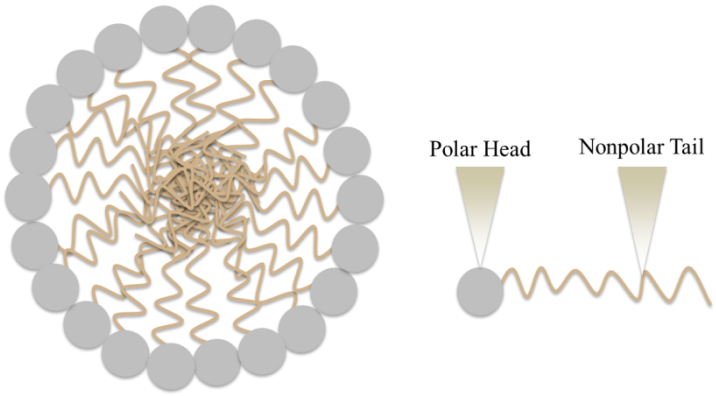

Figure 2.5: Shows a micelle in an aqueous environment with the polar heads outside towards the aqueous phase and the nonpolar tails tightly packing into the center of the structure.

Ingestion of dietary fats also promotes production of bile salts, which are a key component in fat digestion (Neilson et al., 2012). Bile salts are especially important for triglycerides (the main constituents of fat found in food) because triglycerides are large and very nonpolar. Though bile salts are used in the formation of micelles as well, they are different from conventional

surfactants in that they have hydrophilic and hydrophobic faces versus heads and tails. Bile salts function to solubilize and transport fat and make fat droplets easier to absorb both by emulsifying to increase surface area and by allowing lipase to attach to their surface (Maldonado-Valderrama, Wilde, Macierzanka, & Mackie, 2011).

Xenobiotic Metabolism

Inside the enterocytes, there is a series of metabolic reactions that may modify xenobiotics and other absorbed compounds. If the ingested compound is a substrate for a particular enzymatic reaction it is therefore used in that process (Kucukatay, Bor-Kucukatay, Atsak, & Aysel, 2007). These reactions mainly occur and exist to detoxify and attempt to deactivate xenobiotic compounds in order to excrete them without causing bodily harm. The metabolic processes however, do not always succeed in fulfilling their functions and sometimes actually activate the xenobiotics, by producing compounds that are more biologically active either in a helpful or harmful manner, which is known as bioactivation (Lackie, 2010; McClements et al., 2015; Monks, Jones, Bai, & Lau, 2004). Furthermore, compounds with health benefits may be extensively metabolized and deactivated, negating their benefits. There are cases where compounds can be unaltered by certain steps of these metabolic reactions; which depends on whether they are substrates for the enzyme that catalyzes that step (Neilson et al., 2012). One example is if a compound includes many different hydroxyl groups it may not undergo phase I metabolism (explained below).

Phase I metabolism is the first step of the intracellular metabolic mechanisms. These reactions make xenobiotics more reactive through hydroxylation and oxidation/reduction reactions; this

allows the reactions in phase II to proceed much easier (McClements et al., 2015; Neilson et al., 2012). Phase I metabolism is done by the cytochrome P450 superfamily (Neilson et al., 2012). Phase II metabolism exists to minimize xenobiotic toxicity and increase hydrophilicity (with the exception of methylation) and includes the processes of glucuronidation, sulfation, and methylation (Crespy et al., 1999; Kohri et al., 2001). The increased hydrophilicity allows easier excretion. In phase III metabolism, enterocytes employ efflux transporters to remove the xenobiotics from the cell interior, they act by either pumping the compounds back into the intestine, into the bloodstream, or into the interstitial fluid between cells (Lambert, Sang, & Yang, 2007; Neilson et al., 2012). The main transporters in phase III metabolism are powered by the use of ATP and consist of P-glycoproteins (Pgp), multidrug resistant proteins (such as MDR1), and organic anion-transporting polypeptides (such as OATP2) (Brinkmann & Eichelbaum, 2001; Lambert et al., 2007; Tirona & Kim, 2002).

If compounds enter the bloodstream, they can proceed into the liver by way of the portal vein before circulating the body. The liver is similar to the enterocytes in that it is abundant with these detoxifying enzymes (Neilson et al., 2012). Metabolism that occurs in the enterocytes or the hepatocytes, before absorbed compounds enter general circulation is known as “first pass” metabolism (Neilson et al., 2012).

Unabsorbed compounds can travel through the small intestine into the large intestine. In the large intestine there are trillions of native colonic bacteria in a symbiotic relationship with the gut (Kamada, Seo, Chen, & Nunez, 2013). These bacteria ferment the materials that pass by and allow further breakdown of some compounds. Some reactions can even produce beneficial

substances such as vitamins that the body will absorb. The unabsorbed compounds and other particles left over after nutrients have been harvested are prepared for excretion (Brenner & Stevens, 2009).

The removal of absorbed foods, drugs, and/or their metabolized compounds, known as excretion, occurs largely through the urine (Brenner & Stevens, 2009). However, there are also excretion pathways through fecal matter, sweat, exhaled air, tears, bile, saliva, and even breast milk (if being produced) (Brenner & Stevens, 2009; Rollins & Klaassen, 2012). If being excreted through the urine, the compound is brought to the kidneys for a filtration process, termed glomerular filtration; secretion process called tubular secretion; or reabsorption; based on various conditions such as: pH, size, binding, chemical structure, and hydrophobicity (Brenner & Stevens, 2009; Rollins & Klaassen, 2012). Biliary excretion (through bile) can be an important method for clearing compounds as well, but can also lead to enterohepatic recycling where the drug may be hydrolyzed into an active compound by intestinal bacteria (Brenner & Stevens, 2009; McClements et al., 2015; Rollins & Klaassen, 2012). This process can be affected by individual specific GI tract factors such as: transit time, pH, intestinal surface area, disease, and use of other medications (Brenner & Stevens, 2009; Rollins & Klaassen, 2012; Sherwin, Fukuda, Brunner, Goebel, & Vinks, 2011). The biliary pathway of excretion leads to excretion through fecal matter (Rollins & Klaassen, 2012).

Rifapentine and Rifampin Metabolism

RPT and RIF, like any other xenobiotic, must survive the digestive processes. Due to the fact that information for RIF is much more widely available than for RPT a large portion of this

section covers RIF; however due to their structural similarity, it is assumed that RPT will exhibit similar behavior to RIF in most cases. The first challenge for drugs such as these is the acidic stomach due to its low pH and metabolic enzymes (Agrawal & Panchagnula, 2005). In fact, RPT degradation has been shown to be highest at a pH of 2, commonly found in the stomach (Prasad, Bhutani, & Singh, 2006). These drugs are acid labile due to the hydrazone linkage that connects part of the molecule (Fig. 2.6) (Kalia & Raines, 2008; Pereira et al., 2013).

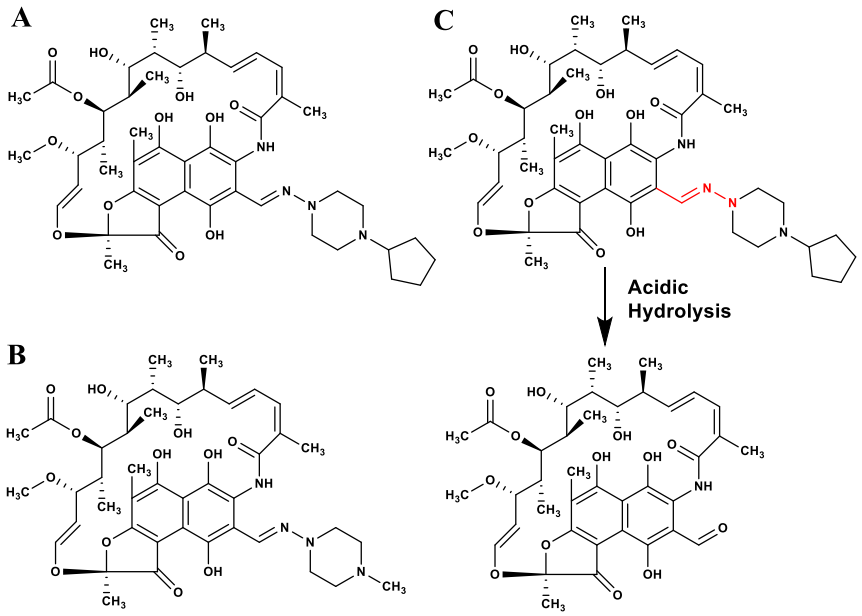

Figure 2.6: Chemical structures of A) rifapentine and B) rifampin and C) shows rifapentine (top) being hydrolyzed to form 3-formylrifamycin (bottom); red color highlights the acid-labile hydrazone linkage.

These compounds are particularly vulnerable at this pH because typically the protonation of nitrogen in similar compounds increases solubility, thereby increasing exposure to the acid and promoting a greater amount of degradation (Pereira et al., 2013). This means that the dose taken does not get fully absorbed in the active form, which can be compensated for with the use of

higher doses but means that a large portion of the drug is wasted and there could be additional side effects.

RIF has been shown to have a low permeability from the stomach, high permeability from the small intestine, and moderate permeability from the large intestine (Agrawal & Panchagnula 2005; Gonçalves et al., 2012). The problem in the small intestine, the major site of absorption and permeability, is RIF solubility which is low to moderate at best (Fig. 2.7) (Agrawal & Panchagnula, 2005).

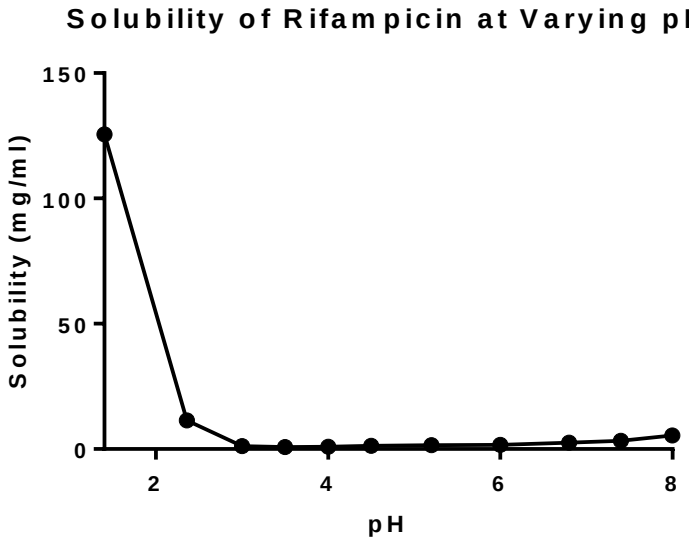

Figure 2.7: A graph of RIF equilibrium solubility from pH 1.4-8.0, data collected by Agrawal et al. Lowest solubility is seen at 3.5, with slight increases in basic pH; RIF is highly soluble at highly acidic pH (Agrawal & Panchagnula, 2005).

In Caco-2 cell culture models, Goncalves *et al*. found that RIF permeability increased at pH 6.8 versus 5.8 or 7.4 (Gonçalves et al., 2012). This permeability remained the same with the addition of a mucous layer as well as with the addition of bovine serum albumin (BSA) (Gonçalves et al.,

2012). This further contributes to the hypothesis that increasing solubility at this pH would increase absorption.

It has been shown that RIF may saturate first pass metabolism at a dose of 300-450 mg (Dooley et al., 2012). At concentrations above these, the effect of the drug would be much greater because the phase I, II, and III metabolism systems (especially efflux transporters) would be saturated. This would thereby limit drug deactivation/excretion and allow a greater response per dose, due to the drug flooding the systems. If these same effects are seen with RPT it would be especially useful because RPT would otherwise undergo extensive first pass metabolism (Patil-Gadhe et al., 2014).

Some common metabolites that are produced by RIF and RPT are: 25-desacetyl-rifampin and 25-desacetyl rifapentine, 3-formyl-25-desacetyl-rifamycin, and 3-formyl-rifamycin (Emary et al., 1998; Winchester, Podany, Baldwin, Robbins, & Fletcher, 2015). These structures for RPT can be seen in Fig. 2.8 (below):

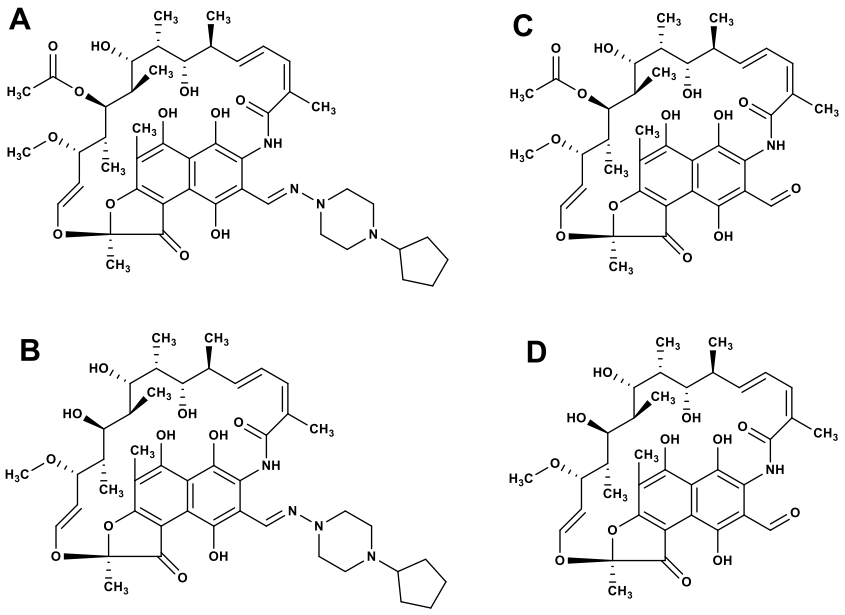

Figure 2.8: Adapted from Emary et al. 1998, shows the common metabolites of A) rifapentine (RPT). B) 25-desacetyl-rifapentine is a common enzymatic hydrolysis product whereas C) 3-formylrifamycin is commonly attributed to acidic degradation and D) 3-formyl-25-desacetyl-rifamycin would represent a combination of the two (Emary et al., 1998).

25-desacetyl-rifampin is commonly found in the liver after digestion of RIF (Jamis-Dow, Katki, Collins, & Klecker, 1997). RIF has been found to be deacetylated through the action of B-esterases (Jamis-Dow et al., 1997). Desacetyl-rifampin and desacetyl-rifapentine, which are microbiologically active compounds, can be found in the feces as such or in urine as glucuronidated forms (Lemke, 1995). 3-formyl-rifamycin (3-FR) may be produced in the urine through a spontaneous reaction and is produced as a major metabolite due to degradation in the stomach (Acocella, 1978; Agrawal & Panchagnula 2005; Kalia & Raines, 2008; Pereira et al., 2013; Prasad et al., 2006).

RPT is more biologically active than RIF and has a half-life over four times as long because it binds to plasma proteins (Kalra, Gaur, Nainwal, Singh, & Jain, 2011; Lemke, 1995). Ehret *et al.*

found that acute RIF administration caused induction of multidrug resistant protein and P-glycoprotein efflux transporters in Caco-2 intestinal cell culture models (Ehret, Levin, Narasimhan, & Rathinavelu, 2007). Since P-glycoproteins contribute to biliary as well as renal excretion by transporting xenobiotics back into the intestine, it is possible that this drug would cause interferences with other drugs as well (Ehret et al., 2007). A summary of pharmacokinetic parameters for RIF and RPT can be seen in Table 2.2.

Table 2.2: A summary of human pharmacokinetic parameters of rifampin (RIF) and rifapentine (RPT) after oral administration of a 600 mg dose, collected by various sources (FDA, 2010; A. Keung, Eller, McKenzie, & Weir, 1999; Ribera et al., 2007; Ruslami et al., 2007; Sirgel et al., 2005; Weiner et al., 2004; Xu et al., 2013).

Source	Drug	Administration	C_{max}* (µg /mL)	AUC* (µg*h/mL)	$T_{1/2}$* (h)
Ribera *et al*., 2006	RIF	Steady-state	8.9	42.1[24]	N/A
Ruslami *et al*., 2007	RIF	Steady-state	15.6	79.7[24]	2.2 (1.3-6.3)
Xu *et al*., 2013	RIF	Single-dose	11.4	91.4[24]	3.7
Xu *et al*., 2013	RIF	Single-dose	11.4	93.3[∞]	3.7
Sirgel *et al*., 2005	RIF	Single-dose	13	100[∞]	N/A
FDA (Priftin), 2010	RPT	Steady-state	15.05	320[72]	13.19 1.38
Weiner *et al*., 2003	RPT	Steady-state	12.2	296[∞]	14.4 (13-16)
Keung *et al*., 1999	RPT	Steady-state	24.3	367[∞]	11.9 (16)
Keung *et al*., 1999	RPT	Single-dose	15.8	386[∞]	14.1 (15)
Sirgel *et al*., 2005	RPT	Single-dose	13.19	397[∞]	N/A

[∞]AUC from 0-∞ hours

[24]AUC from 0-24 hours, a good estimation of 0-∞ hours for RIF due to $T_{1/2}$

[72]AUC from 0-72 hours, a good estimation of 0-∞ hours for RPT due to $T_{1/2}$

*Averages are shown with no ranges given for cleanliness and consistency between sources

Bioavailability of Rifapentine

Oral bioavailability of RPT has been shown to be variable (Patil-Gadhe et al., 2014; Tam et al., 1997). It is surprisingly difficult to find consistent information about absolute oral bioavailability for RPT in the literature. The FDA even states that absolute oral bioavailability has not yet been determined, despite being in use for many years (FDA, 2010). However, the Curry International Tuberculosis Center states it to be 70% with increases after meal consumption (CITC, 2012). The FDA states oral bioavailability relative to an oral solution to be 70% (FDA, 2010). Based on the problems RPT faces with acidic degradation and solubility, this is higher bioavailability than one would expect (which again points to the variability).

It is important to note that many bioavailability measurements have been taken after meals, which can further complicate things because meal composition is one of the major contributing factors to the variable bioavailability of RPT (Chan et al., 1994; CITC, 2012; Zvada et al., 2010). It is common to find studies that suggest the bioavailability is increased after certain meals, especially meals containing high fat (Chan et al., 1994; CITC, 2012; Patil-Gadhe et al., 2014; Zvada et al., 2010). One study even suggests that the bioavailability can be increased by over 85% after consuming the correct meal, while others state increases of around 35-40% (Chan et al., 1994; FDA, 2010; Zvada et al., 2010). Either of these numbers would lead to a significantly different bioavailability and hence drug efficacy.

Another factor that may impact this variable bioavailability is the crystalline state of RPT. Being a crystalline solid means that the molecules are arranged in a specific 3-dimensional order with a

definite repeating structure and maintain a rigid structure (Chakrabarty, 2010). Crystals can form and are maintained in order to minimize the free energy of the system (Chakrabarty, 2010). The crystalline state is usually the lowest energy state, therefore the most thermodynamically stable product. Crystals, being in a low energy state, make dissolution difficult due to the large amount of energy required to overcome the high heat of crystallization (Li et al., 2013). In addition to this, RIF shows crystal polymorphism in solid oral doses, which means that there are multiple stable forms of the crystal structure of this drug (Agrawal, Ashokraj, Bharatam, Pillai, & Panchagnula, 2004). The polymorphs include form I, form II, and the amorphous form (Agrawal, Ashokraj, Bharatam, Pillai, & Panchagnula 2004). We see changes in crystal structure especially with the use of different solvents for crystallization (Occelli, Nebuloni, & Cavalleri, 1990). This could be part of the reason that we see variation in bioavailability between manufacturers, possibly due to different methods of synthesis and crystallization practices (Tam et al., 1997). As with any drug, a final factor that we see causing variable bioavailability is due to intersubject variability, with age and pH of the digestive tract having large effects (Agrawal, 2003; Brenner & Stevens, 2009; Keung, Eller, & Weir, 1998; Rollins & Klaassen, 2012; Sherwin et al., 2011). Removal of crystal structure prior to administration and reduction in variability after meal consumption are some of the benefits of strategies such as amorphous solid dispersion (ASD) (further explained later).

Strategies to Increase Bioavailability of Drugs/Nutraceuticals

Overview

Nutraceuticals are food components that have health values above and beyond basic nutrition, but which are not drugs. These are usually isolated from natural food systems (such as grape or

cocoa polyphenols) or eaten as a whole food matrix to provide beneficial health effects. The biopharmaceutical classification system (BCS) (explained previously in Table 2.1) is an important consideration for drugs and even nutraceuticals in bioavailability determination and delivery strategy selection. Regarding BCS, it is interesting to note that we often see drugs in class II and III vs I and IV, because, for example, a drug that has a high aqueous solubility is often limited by permeability due to its high polarity and lack of lipophilicity (Martinez & Amidon, 2002). If the class of the drug is determined first, it is much easier to determine the best strategies for delivery. Drugs are often made more bioavailable by the use of formulation strategies or chemical modification (Pouton, 2006). Of these, formulation strategies are often selected over chemical modification because the approval process for a new drug is long and difficult. Using formulation strategies can help to minimize some of the cost and time required for developing new chemicals, which are the biggest limiting factors in drug manufacturing (Gomez-Orellana, 2005).

Food and Drug Matrix Design

One delivery strategy that has been considered and tested is the design of an actual food matrix for drug (or especially nutraceutical) delivery. A specific diet, food, or delivery matrix design can have an effect on the bioavailability of drugs and nutrients (McClements, 2015). In fact, as mentioned previously, RPT itself is affected by food intake and bioavailability can be greatly increased after certain meals, especially meals containing high amounts fat (Patil-Gadhe et al., 2014; Zvada et al., 2010). Although this may not always be the main strategy employed for use with drugs, food matrix design is important to consider for some drugs, and is especially important for nutraceuticals.

Size Reduction

One seemingly simple strategy that has been employed to promote absorption is particle size reduction. Decreasing particle size often increases dissolution rate through reducing energy needed to break the crystal structure and solubilize the drug, which is important because dissolution rate can often be a limiting factor in absorption (Agrawal, 2003; Agrawal, Ashokraj, Bharatam, Pillai, & Panchagnula, 2004). One example is the increased peak concentration and area under the curve that Fu *et al*. found with smaller particle sizes of nimodipine (Fu et al., 2012). However, the beneficial effects of size reduction may level off after a certain size is reached. Though this strategy may be effective for some drugs, there are limitations. The size to which the drug or nutraceutical can be reduced is strongly dependent on the technology available (Karavas, Ktistis, Xenakis, & Georgarakis, 2006; Pouton, 2006). Micronization for drug particle size reduction can be used freely but only leads to particle sizes of 2-5 um which may not be small enough for an effective system (Pouton, 2006). Additionally, if the compound can be reduced to an effective size, powders with small particle size generally have poor flow and wettability characteristics, increasingly large electrostatic forces, and can agglomerate (Karavas et al., 2006).

Encapsulation

Encapsulation is a system in which the material, in this case drug or nutraceutical, is physically surrounded by an outer coating (Desai & Jin Park, 2005). This system can be used for time-release and location-release within the body, and to protect against degradation (Desai & Jin Park, 2005). There are a wide variety of encapsulation techniques and methods for the

manufacture of each type of encapsulated dosage form; this can allow diverse delivery characteristics based on the end goal of the formulation (Fang & Bhandari, 2010). Liposomes are one form of encapsulation, and these are interesting because they have the ability to hold hydrophilic, hydrophobic, and amphipathic compounds due to their lipid bilayer membrane formation (Fang & Bhandari, 2010; Mozafari et al., 2008). This system is similar to a cell with a lipid bilayer; essentially the hydrophobic interactions drive the hydrophobic phases of the phospholipid molecules together inside of the hydrophilic phases, which cause this membrane to form. Liposomes can vary in effectiveness and characteristics depending on the material being encapsulated and the solution that is used during manufacture (Fang & Bhandari, 2010). Mozafari *et al.* lists several studies that show health advantages of liposomes and states that these can be prepared from natural materials (Mozafari et al., 2008). However, some methods of producing liposomes lead to hydrolysis of lipids or even deactivation of the drug and some drugs have difficulty in release or loading into liposomes (Tazina, Kostin, & Oborotova, 2011).

Inclusion encapsulation is another technique; this uses mostly cyclodextrins as the membrane material. In this system, the inside of the cyclodextrin is usually hydrophobic and the outside is hydrophilic which makes it ideal to encapsulate nonpolar, hydrophobic compounds (Fang & Bhandari, 2010). This strategy shows improvements in water solubility however, the effectiveness is strongly dependent on the material being encapsulated (Fang & Bhandari, 2010).

Nanoparticles have also been used as an encapsulation strategy and lipid nanocapsules can be adjusted to different sizes based on the intended use (Fang & Bhandari, 2010). One problem with nanocapsules is the possible formation of aggregates, which would mean the particles are no

longer nano size and are converted back to micron size, thereby partially negating the advantages of nanosizing (Mozafari et al., 2008).

Solid lipid nanoparticles are an alternative to liposomes (Li et al., 2009; Yadav et al., 2014). This formulation embeds the drug or nutraceutical inside a solid fat that is encased by a single layer of phospholipids. Solid lipid nanoparticles offer advantages of: site-specific delivery, time-release delivery, easy production, and great biocompatibility (Yadav et al., 2014). However the solid lipid matrix may cause problems due to the highly crystalline nature of the fat which can limit the amount of drug allowed in the system and even eject the drug if fat crystal formation occurs too vigorously in the system (Yadav et al., 2014).

Prodrugs

Prodrugs are inactive precursors for a drug that are hydrolyzed or transformed by other chemical processes into an active form, during the normal metabolic process. The precursor oftentimes "covers" charged or highly polar groups so they are more easily absorbed, acts as an enhancement to transporter-mediated uptake, or adds permeability to the drug (Gomez-Orellana, 2005). Some of the benefits that have been seen with the use of prodrugs are: possible increase of permeability and absorption in the gut and potential increase in half-life (which lowers dose frequency) (Gomez-Orellana, 2005). The downsides to this strategy are: they can decrease drug solubility, can entrap drugs and not properly release them, and the drug can accumulate in the tissues or cells in which it is modified, along with the major downsides of approval cost and time of development because a prodrug is considered a new drug and therefore requires a new drug application (Gomez-Orellana, 2005).

Salt Formation

Salt formation is a strategy that has been very effective. This system is so extensively employed that it is currently the most common strategy for increasing drug solubility (Serajuddin, 2007). However, this strategy generally only works for acidic or basic drugs and may not be practical in some cases due to the chemical and/or physical properties of the drug (Karavas et al., 2006; Serajuddin, 2007). Additionally, the salt formed may not have sufficient solubility and therefore will not increase bioavailability in some cases (Serajuddin, 2007). Salt formation can be a complicated process and solubility of these formulations is very pH dependent and some formulations can have issues with stability (Karavas et al., 2006; Serajuddin, 2007). If the salt formation is not optimized for the specific compound, it is a much less effective system.

Amorphous Solid Dispersion (ASD)

This technique is used to increase dissolution and improve release of a compound. An ASD allows the selected compound to temporarily overcome the unfavorable thermodynamics of the crystalline form by holding it in the amorphous form. The amorphous (i.e. non-crystalline) form of the drug allows a greater solution concentration and dissolution which improves bioavailability but this form can easily and relatively quickly recrystallize (Konno, Handa, Alonzo, & Taylor, 2008). This is why ASD is used; it employs a rigid matrix of polymers to hold the particles in the amorphous form, and ideally can also prevent recrystallization (Fig 2.9).

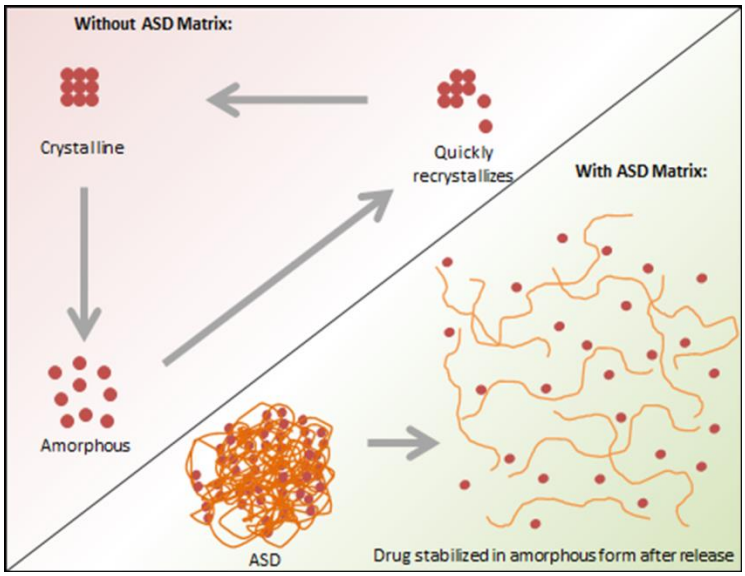

Figure 2.9: Drug crystallinity/amorphism with/without the use of ASD.

Crystallization is all about minimizing the free energy of the system. The thermodynamically favored form is typically the crystalline form because it is a much lower energy state. In solution, when thermodynamic solubility is exceeded, it means that there is a larger amount of solute than should be soluble at that temperature and pressure (Sun & Lee, 2013). This yields a high free energy and crystallization is what minimizes this free energy. Crystallinity is a problem because if this happens to the drug, then it will not be as readily absorbed. Crystals (in an undissolved form) may travel through the digestive tract without the opportunity to be absorbed because they cannot impact the transmembrane gradient and are not able to reach the apical membrane in soluble form, therefore leading to high amounts of excretion (Raina, Zhang, Alonzo, & Wu 2014). The larger the crystals, the lower the bioavailability due to reduced dissolution (Wolen, Carmichael, Ridolfo, Thompkins, & Ziege, 1979). However, the drug being in a high concentration in a soluble form leads to increased absorption due to enhanced passive absorption (Corrigan, Farvar, & Higuchi, 1980; Raina, Zhang, Alonzo, & Wu, 2014).

An ASD allows the drug to be released in soluble form, providing benefits mentioned earlier, while at the same time (ideally) preventing crystallization. These ASD formulations, ideally, are designed to inhibit crystal formation both in the solid form during storage and in solution (Konno et al., 2008). The drug in the dispersion is amorphous, and after the carrier dissolves and/or swells, the drug is essentially released in its molecular form. This bypasses the large energy barrier that would be required to break the crystal structure; because the energy had already been put into the ASD when it was formed (Leuner & Dressman, 2000). If the drug is allowed to remain in its amorphous state, it can supersaturate the intestine with the compound, driving absorption and possibly overwhelming metabolic enzymes and efflux transporters, and will be absorbed in a larger quantity than if crystalline drug were present (Ilevbare, Liu, Edgar, & Taylor, 2012). Supersaturation means that the intestines would be holding more solute than would normally be possible at those specific conditions, the drug is in solution at a higher concentration than its thermodynamic solubility (Schaschke, 2013; Sun & Lee 2013). Since the thermodynamic solubility is exceeded, this increased measured concentration is termed "apparent solubility." Though this high apparent solubility creates favorable conditions for crystallization, the compound will be absorbed faster than it will crystallize due to the polymer matrix inhibiting or at least slowing crystallization and stabilizing the amorphous drug in solution. The increase in apparent solubility gives rise to greater bioaccessibility and transmembrane concentration gradient, which facilitates improved absorption and better bioavailability (Leuner & Dressman, 2000).

One extremely important property of amorphous compounds to consider is their glass transition temperature (T_g). This is different than a melting temperature (T_m) which would be seen as a

liquid is cooling and there is a phase transition from a liquid to a crystalline solid matrix. For amorphous forms we see a T_g instead of a T_m; above the T_g polymers can assume a pliable rubbery state and below they assume a brittle, glassy state (Shah et al., 2014). Though non-crystalline, this glassy state shows characteristics of a solid; this rigid state is able to prevent movement and stabilize the polymers and hence trap the drug and decrease risk of crystallization in the ASD (Ediger & Harrowell, 2012). Though relatively stable, this state allows a higher separation of molecules and heat content compared to the crystalline state and is therefore recognized as a higher energy form. This means that there is less energy required for dissolution, therefore resulting in a faster and more complete dissolution compared to the crystalline form (Shah et al., 2014). T_g is also a key parameter considered in the long-term storage stability of an ASD and a general consideration is that an ASD will prevent recrystallization if it is stored 50˚C below the T_g of the polymer (Yu, 2001).

There are definitely many advantages to using ASDs. ASD allows a smaller particle size (molecular) and hence increased surface area of the particles (Karavas et al., 2006; Leuner & Dressman, 2000; Pouton, 2006). Particle size reduction is an important strategy on its own but is included as part of this process (Vasconcelos, Sarmento, & Costa, 2007). The very obvious advantage is an increase in apparent solubility due to extremely small particle size and higher dissolution rate, which translates to much more drug being absorbed and a higher bioavailability (Gilley et al., 2017). We also see that these ASD polymers can be modified to have different release characteristics and drug interactions based on differences in the polymers used (Gilley et al., 2017; Li et al., 2009). One such example that is important for the scope of this study is that carboxylic acid groups can provide a release that is pH responsive due to protonation/

deprotonation under certain pH conditions (Gilley et al., 2017; Li et al., 2009). With this system applied to RPT we could see both protection from degradation in the stomach and increase apparent solubility at small intestine pH, where absorption is highest (Agrawal, 2003). One final advantage is that patients prefer to take medicines in pill form versus liquid form, which is possible through this strategy and may help to increase patient compliance (Karavas et al., 2006).

Of course there are disadvantages to using ASD as well. These systems have had some problems with shelf life, due to crystallization from manufacturing processes or storage humidity and temperature; though mostly only seen in older systems because long-shelf life is now a requirement for approval of these systems (Pouton, 2006; Vasconcelos et al., 2007). More modern ASD systems, such as those observed by Theil *et al*. containing nifedipine, have been shown to be stable in their amorphous form for over 25 years of storage at temperatures stored at just 30˚C below their T_g (Theil et al. 2017). If problems of crystallization in the ASD do occur, it would likely be from storage condition abuse, such as being stored in a highly humid environment where water may act as a plasticizer, increasing mobility of drug and leading to recrystallization and agglomeration (Konno et al., 2008; Pouton, 2006). Large-scale manufacturing processes have been a challenge for some of these systems (Pouton, 2006; Serajuddin, 1999). However, with advances in technologies such as hot-melt extrusion and spray-drying these are mostly overcome, with the exception of manufacturing new and novel polymers that do not have a commercial process fully developed (Shah et al., 2014). The supersaturation of the compound in the intestine can lead to crystallization of the drug if nucleation and crystal growth do occur, which can happen if the polymer formulation is not optimal (Ilevbare et al., 2012; Konno et al., 2008; Pouton, 2006).

Manufacture of ASDs

ASDs can be made in a variety of ways and their use continues to expand with the development in processing technology and further understanding of the ASD delivery system. Shah *et al*., in the book "Amorphous Solid Dispersions: Theory and Practice," explain these different processing technologies and divide these methods into two broad categories: solvent-based technology and fusion-based technology, which are summarized in the following paragraphs (Shah et al., 2014). Of the solvent-based technologies, the most common method used in the scale-up production of ASDs is spray-drying and of the fusion-based methods, melt extrusion is the most common (Huang & Dai, 2014).

The basis of spray-drying is to combine the polymer and drug in one volatile solvent system and then to remove the solvent rapidly in a controlled environment (Huang & Dai, 2014; Shah et al., 2014). Solvent and polymer selection are very important to this method and can determine the final characteristics of the ASD. The major benefits of spray-drying include: the efficiency, it is a well-understood and common process, high surface area of final particles, and high scalability (Shah et al., 2014). Though spray-drying is common, we often see the use of another simpler method of solvent evaporation termed film casting, especially in the small-scale production of ASDs, because spray-drying can lead to higher yield losses with small amounts of solution. This simple solvent evaporation involves many of the same principles as spray-drying with the major difference in this method being that the solvent is allowed to dry much more slowly. These formulations are often left to air dry, while the solvent evaporates. Film casting is a high-yield process, requiring minimal amount of materials that is often used for pre-screening in the production of ASDs. This process can relatively easily translate to spray-drying if scale-up is

required. The major drawback of these solvent-based methods is actually the use of the solvent itself (Shah et al., 2014). If solvent is not fully removed we can see problems with consumer safety as well as stability of the ASD.

Hot-melt extrusion is the most common commercial fusion-based process in the manufacture of ASDs. Essentially this process heats the drug and polymers to a liquid state where they can be mixed freely and then extruded together, giving an ASD. Unlike solvent-based technologies, this strategy offers the major benefit of being a solvent free method (Shah et al., 2014). However, this strategy can mostly be applied only to polymers and drugs with relatively low melting points. Non-ideal polymers and drugs may also require the use of certain additives such as: plasticizers, surfactants, and flow aids which may affect stability and delivery of the final product (Huang & Dai, 2014). This process can be difficult at lab-scale and scale-up ability from here can be limited, however if correctly scaled we can see a continuous process that offers a nearly complete final product.

Polymers that have been studied

The properties of the dispersing polymers have proven very important for the development of ASDs. These substances are important because there are many diverse types that can be selected and modified to provide favorable characteristics such as: increasing apparent solubility, pH responsiveness, preventing crystallization, time release, and prolonged release if necessary (Liu, Taylor, & Edgar, 2015). The polymers selected for ASDs must have minimal toxicity, be soluble themselves in the desired region of drug release, and form favorable interactions with the drug or nutraceutical being used (Liu et al., 2015).

Polymers that have been used include water-soluble synthetic polymers and cellulose derivatives. Some examples include: poly(vinylpyrrolidinone) (PVP), hydroxypropyl methylcellulose (HPMC), hydroxypropylmethylcellulose acetate succinate (HPMCAS), carboxymethylcellulose acetate butyrate (CMCAB), cellulose acetate phthalate (CAPhth), cellulose acetate adipate propionate (CAAdP), and poly(ethylene glycol) (PEG) (seen in Fig. 2.10) (Konno et al., 2008; B. Li et al., 2013).

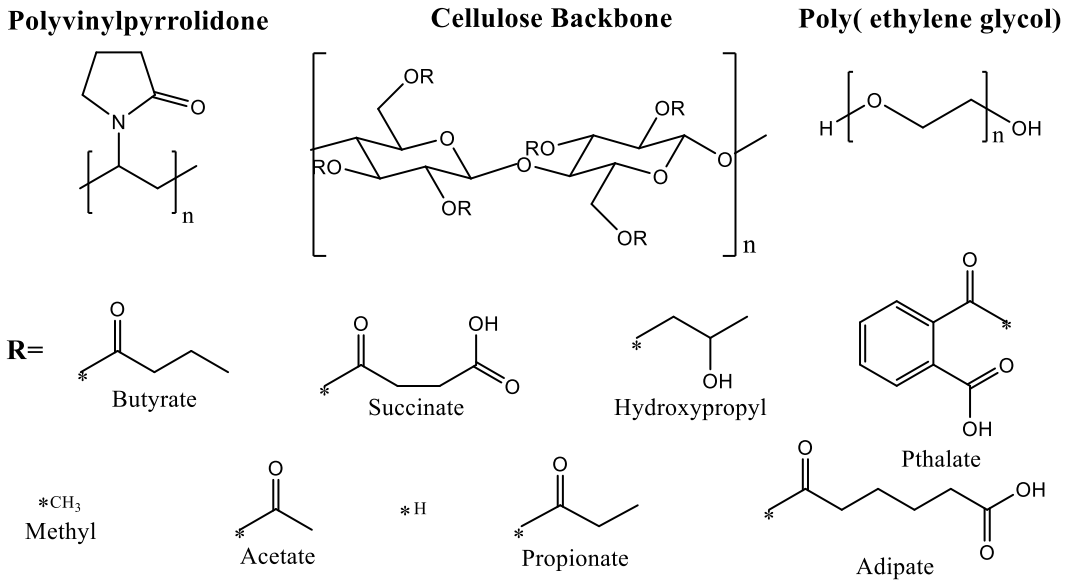

Figure 2.10: Common polymers used in ASD. Top row of polymers shows two common synthetic polymers as well as the natural cellulose backbone. The structures below represent some of the possible R groups that could be attached to a modified cellulose polymer of HPMC, HPMCAS, CMCAB, CAPhth, or CAAdP.

Cellulose derivatives have been selected for several reasons including availability, ease of modification for compatibility with drug and delivery characteristics, low toxicity/ high biocompatibility, high T_g allowing stability in storage, and have previously shown evidence for effective use in ASD (Gilley et al., 2017; B. Li et al., 2013; Liu, 2014). Cellulose polymers have

also been shown to prevent crystallization and drug mobility during storage (Liu et al., 2014). Carboxylic acid groups can provide a pH responsive release because in an acidic environment they are largely protonated and have a neutral charge, but in a more neutral or basic environment (above their pK_a) the protons are stripped giving an overall negative charge forcing the polymers to repel each other thereby causing swelling of the dosage form and releasing the compound at the desired pH (Fig 2.11) (Gilley et al., 2017; Li et al., 2009; Yang et al., 2005).

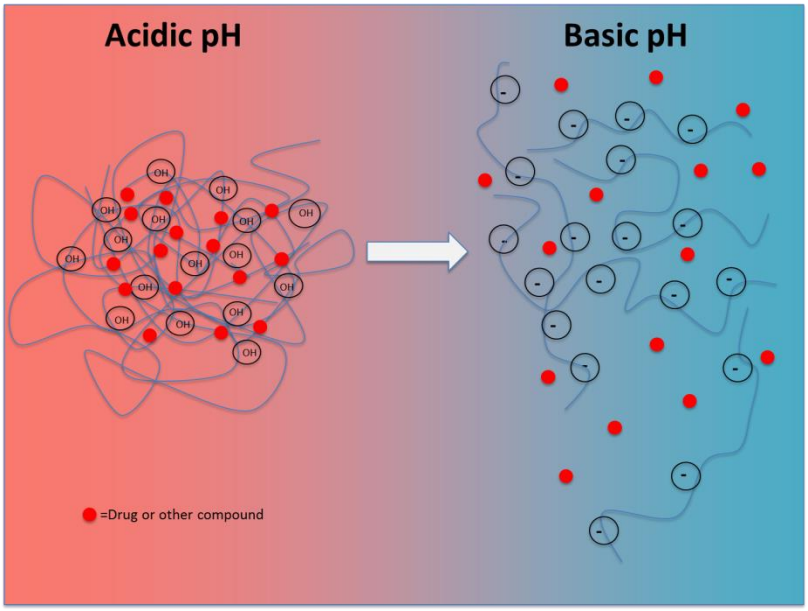

Figure 2.11: Polymers of carboxylic acid derivatives swelling and repelling each other due to electrostatic repulsion at basic pH, releasing drug into solution.

Li *et al*. conducted studies with quercetin in ASDs and found that carboxylated cellulose derivatives prevent recrystallization but can give a slow release of the dispersion (Li et al., 2013). They also found that PVP can be added to the mixtures to prevent crystallization and compound degradation. ASDs using PVP gave fast and complete drug release while the cellulose derivatives gave a slow release that was pH responsive. In this study, the cellulose derivatives did not protect the quercetin against alkaline chemical degradation while PVP did, but this is not

the case for all compounds as their lab did have evidence from other experiments showing that the cellulose polymers did protect curcumin by limiting formation of the ionic transition state required for the mechanism of degradation (Li et al., 2013). Konno *et al.* performed studies with felodipine and ASDs using PVP, HPMC, and HPMCAS (Konno et al., 2008). They found that HPMCAS gave the greatest supersaturation over the longest time and that PVP inhibited crystals the least but still showed an effect. Finally, they showed that polymers used in ASD can enhance solution concentration, relative to the amorphous form of the drug by itself.

ASD and Rifapentine

A drug such as RPT would require a polymer that is pH responsive, protecting the drug from release at the low pH of the stomach and then releasing the drug into a supersaturated solution at the pH of the small intestine. This ideal polymer would also prevent crystallization, stabilize the supersaturated solution, be able to be easily produced, and be nontoxic. ASD would likely help give RPT desirable release characteristics. The solubility of RPT at gastric pH causes problems because it is susceptible to acidic degradation, whereas at the more neutral pH of the small intestine, the lack of solubility causes problems with absorption (Kalia & Raines, 2008; Pereira et al., 2013). Using ASD could protect RPT from degradation in the stomach and enhance the solubility in the small intestine.

ASDs may also have an impact on metabolism and efflux. Achieving high enterocyte concentrations of the drug may facilitate saturation of this system, meaning that the efflux may be overwhelmed (Agrawal & Panchagnula 2005). Above saturated concentration, the efflux rate will not be able to out compete the influx rate. The efflux transporters would be operating at

maximum capacity and unable to further increase efflux despite increases in the drug gradient. This allows the compound to flood the enterocytes and be absorbed at a much larger concentration. This higher amount of absorption and bioavailability could lead to a reduction in variability both dose to dose and patient to patient, a reduction in side effects, and finally more patients treated per aid dollar due to the lower amount of drug required (White, 2013). The product of ASD and RPT could ultimately lead to a shorter and more effective treatment for TB.

Limitations and Concerns

RPT can be prone to oxidation and is light sensitive, which could cause problems during storage and with shelf-life (Lemke, 1995; Srivastava, Waterhouse, Ardrey, & Ward, 2012). RPT has been shown to have variable bioavailability possibly due to production by different manufacturers, crystallization with different solvents, crystal polymorphism, fed vs fasted state, and inter subject variability (Agrawal, 2003; Agrawal, Ashokraj, Bharatam, Pillai, & Panchagnula 2004; Agrawal & Panchagnula 2005; Tam et al., 1997; Yew, 2002; Kun Zhou, Li, Luo, & Zheng, 2010). These concerns could be minimized with an effective ASD system that would reduce intersubject and interdose variability.

For the use of any drug, drug resistant bacteria can become a problem, given the right situations. The bacteria that cause TB have already shown the ability to adopt drug resistance (Anderson, Groundwater, Todd, & Worsley, 2012; Rastogi, Legrand, & Sola, 2001). This may continue to be a problem until a more effective and rapid drug delivery system is developed. In the unlikely event that widespread resistance is accumulated before an effective strategy is developed, RPT may not be powerful enough to stop the bacteria. However, with the creation of a rapid and

effective delivery system leading to a much higher kill of the bacteria, we will see a reduction in this risk.

Even with *in vitro* studies that mimic human digestion, it is impossible to fully encompass each exact detail that is present in the gut, especially since the conditions change constantly; this is why animal models are often used as the best predictor of human oral bioavailability (Ting et al., 2015). This is not possible with this research due to time constraints. However, even animal studies have limitations and are not always ideally correlated with humans and as always there is inter-subject variability, such as differences in pH, that can affect the significance of the results in human trials (Brenner & Stevens, 2009; Rollins & Klaassen, 2012; Sherwin et al., 2011).

The best drug delivery system for RPT has not yet been discovered and there is still a lot of work to be done to find the best system. RPT has shown promising results for defeating TB but it is degraded in the acidic stomach and its bioavailability has been shown to be variable. ASD has shown promising results in combination with other drugs, but has not been tried extensively with this drug. Putting these two together could potentially lead to a drug delivery system that shows excellent antimicrobial activity and is very efficiently used within the body, which would reduce cost and waste for the drug.

Conclusions

TB is a deadly infection that causes over a million deaths each year. It is problematic because *Mycobacterium tuberculosis,* the bacteria that cause the illness, is relatively difficult to kill. The resistant nature of the bacteria in combination with the ease of spread, possibility of latent

infection, and current treatments make it difficult to eliminate. Though TB has been a problem for thousands of years, it is still difficult to treat and cure with the current treatment protocols. This treatment often requires over 6 months of daily dosing with multiple drugs which decreases patient compliance and therefore can lead to antibiotic resistance. RPT has shown great promise in improving the current treatment and has essentially cut treatment times in half while also increasing patient compliance due to less frequent dosing and decreasing bacterial resistance with the use of higher doses. Although a very effective drug, RPT faces challenges in delivery. Oral bioavailability is limited because this drug is both acid-labile, being degraded in the gastric environment and is relatively poorly soluble at small intestine pH, where it is absorbed. ASD has shown amazing potential to improve these drug delivery characteristics. We have seen great benefits for the improvement of solubility as well as the protection of drugs from degradation. The use of ASD with this drug could lead to optimal delivery characteristics of RPT and ultimately lead to a more effective delivery of the drug. This would in turn reduce cost and time of treatment which would increase patient compliance and reduce antibiotic resistance, ultimately leading to the elimination of TB.

Chapter 3: Cellulose-based amorphous solid dispersions enhance rifapentine delivery characteristics *in vitro*

Christopher J. Winslow[a], Brittany L.B. Nichols[b], Diana Novo[b], Laura Mosquera-Giraldo[e], Lynne S. Taylor[e], Kevin J. Edgar[c,d], Andrew P. Neilson[a,]*

[a]Department of Food Science and Technology, Virginia Tech, Blacksburg, VA 24060, USA; Christopher Winslow - apples12@vt.edu; Andrew Neilson - andrewn@vt.edu
[b]Department of Chemistry, Virginia Tech; Brittany Nichols - brittan@vt.edu; Diana Novo - dnovo001@vt.edu
[c]Department of Sustainable Biomaterials, Virginia Tech; Kevin Edgar – kjedgar@vt.edu
[d]Macromolecules Innovation Institute, Virginia Tech;
[e]Department of Industrial and Physical Pharmacy, Purdue University, West Lafayette, IN 47907, USA; Lynne Taylor - lstaylor@purdue.edu; Laura Mosquera-Giraldo- lmosquer@purdue.edu

***Corresponding author:** Dr. Andrew P. Neilson, Dept. of Food Science and Technology at Virginia Tech
1013 Integrated Life Science Building, Blacksburg, VA 24060, USA; E-mail: andrewn@vt.edu; Phone: 1 (540) 231-8391; Fax: 1 (540) 231-9293

ABSTRACT

The efficacy of rifapentine, an oral antibiotic used in the treatment of tuberculosis, may be reduced due to its degradation at gastric pH and low solubility at intestinal pH. We aimed to improve delivery properties *in vitro* by incorporating rifapentine into pH-responsive amorphous solid dispersions with cellulose derivatives including: hydroxypropylmethylcellulose acetate succinate (HPMCAS), cellulose acetate suberate (CASub), and 5-carboxypentyl hydroxypropyl cellulose (CHC). Most amorphous solid dispersions reduced rifapentine release at gastric pH, with the best performing polymer, CASub showing >31-fold decrease in area under the curve compared to rifapentine alone. Lower solubility at gastric conditions was accompanied by a reduction in the acidic degradation product 3-formylrifamycin, as compared to rifapentine alone. Certain formulations also showed enhanced apparent solubility and stabilization of supersaturated solutions at intestinal pH, with the best performing HPMCAS formulation showing almost a 4-fold increase in total area under the curve compared to rifapentine alone. These *in vitro* results suggest that delivery of rifapentine via amorphous solid dispersion with cellulose polymers may improve bioavailability *in vivo.*

Keywords: Amorphous solid dispersion, cellulose, rifapentine, dissolution, bioavailability, 3-formylrifamycin, solubility

Chemical compounds studied in this article: Rifapentine (PubChem CID: 6323497, rifampicin (PubChem CID: 5458213), 3-formylrifamycin (PubChem CID: 6438444), hydroxypropylmethylcellulose acetate succinate (PubChem CID: 121950)

1. Introduction

Rifapentine (RPT, Fig. 3.1A) is a semi-synthetic rifamycin antibiotic used to treat tuberculosis (TB) (Anderson, Groundwater, Todd, & Worsley, 2012). Though rifampin (also known as rifampicin) (RIF, Fig. 3.1B), a similar drug, is currently used in the first-line treatment of TB, RPT has several benefits over RIF. RPT is generally recognized as a more effective drug because there is less potential for bacterial resistance, it persists longer in the blood (providing less frequent dosing and increased patient compliance), and has shown shorter treatment times to resolve the infection (Dooley et al., 2012; Duanmu et al., 2005; Emary et al., 1998; Hastings et al., 2002; He et al., 1996; Lemke, 1995; Rosenthal et al., 2006). One of the major challenges in the delivery of RPT and RIF is their instability during gastric transit. The acidic pH of the stomach degrades these drugs due to their acid-labile hydrazone linkage (Figure 3.1C) (Agrawal & Panchagnula 2005; Kalia & Raines, 2008; Pereira et al., 2013; Prasad et al., 2006). RPT and RIF are particularly vulnerable to degradation at acidic pH because the protonation of nitrogen in acidic conditions results in a net positive charge, which can impart solubility for some compounds and thus would increase exposure to the acid (Pereira et al., 2013). Degradation of RPT and RIF produces 3-formylrifamycin (3-FR, Fig. 3.1C).

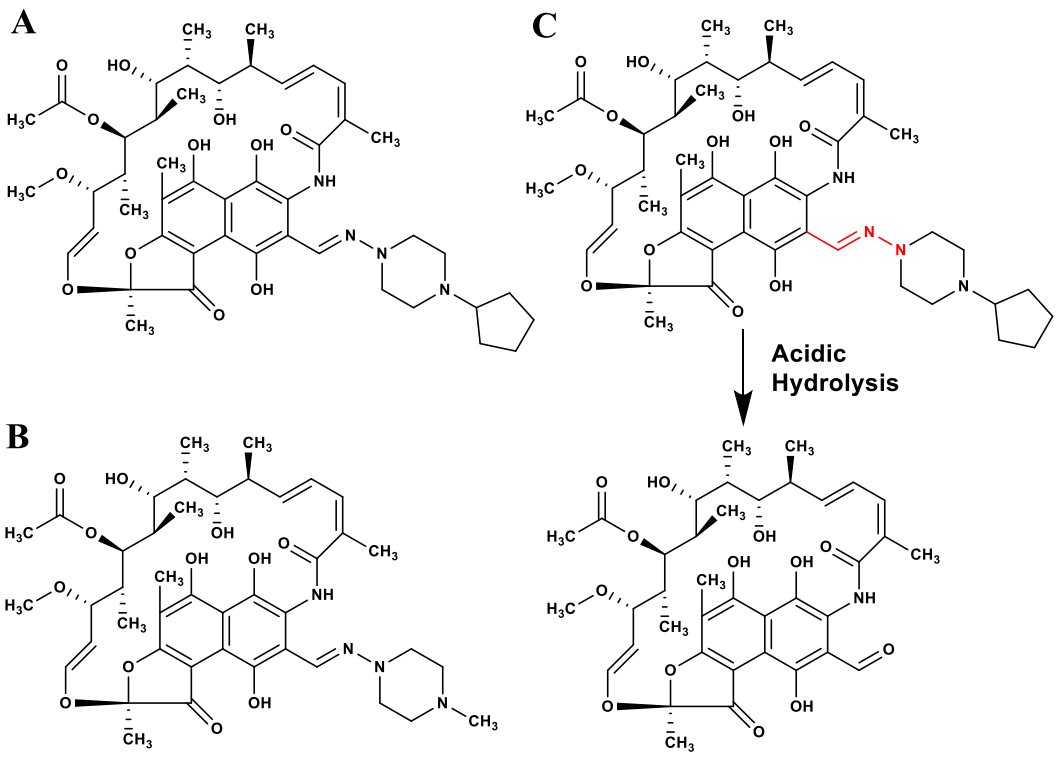

Figure 3.1: Structures of A) rifapentine and B) rifampin. C) Rifapentine (top) is hydrolyzed in acid to form 3-formylrifamycin (bottom); the acid-labile hydrazone bond is highlighted in red.

RPT and RIF have poor solubility at the near-neutral pH of the small intestine, limiting their absorption (Agrawal, 2003; Ostrovskii et al., 2016). Therefore, RPT and RIF face the dual problem of acidic degradation in the stomach and poor solubility in the absorptive region of the gut. Strategies to enhance their intestinal dissolution may therefore be counterproductive by also enhancing acid solubility, and thus degradation, before absorption occurs in the small intestine. Therefore, strategies are needed to inhibit dissolution in acid while enhancing dissolution at near-neutral intestinal pH.

The use of amorphous solid dispersion (ASD) as a vehicle has shown great promise for enhancing delivery of bioactive molecules that have poor water solubility (Gilley et al.,

2017; Konno et al., 2008; Pereira et al., 2013). ASD uses a polymeric matrix to hold the drug in its amorphous form, preventing crystallization during storage and delivery (Konno et al., 2008). This strategy overcomes the inherent heat of crystallization, and thus the large amount of energy usually required to dissolve the drug is not necessary *in vivo*. This temporarily overcomes the inherent thermodynamic solubility, and can result in supersaturation and also inhibit recrystallization out of solution over the timeframe of digestive transit. Supersaturation in the intestine enhances enterocyte absorption by drastically increasing the transmembrane concentration gradient. Increased absorption can subsequently saturate and overwhelm efflux transporters and detoxification enzymes, potentially reducing the percentage of the drug metabolized and/or effluxed back into the intestinal lumen and thus enhancing transcellular flux of the native drug into the bloodstream (Ilevbare et al., 2012).

Choosing the optimal polymer has proven essential for development of ASDs. The polymer must be compatible with the drug and provide favorable drug-polymer interactions (Gilley et al., 2017; Liu et al., 2015; Pereira et al., 2013; Vasconcelos et al., 2007). Cellulose derivatives have been of particular importance for ASD formulations because of their availability, stability due to drug-polymer interactions and high glass transition temperature (T_g) limiting drug mobility, relative ease of modification, and biocompatibility (Gilley et al., 2017; Li et al., 2013; Liu, 2014; Liu et al., 2015; Shah et al., 2014). The incorporation of organic (weak) acid functional groups to the cellulose scaffold can enhance the performance of the ASD by providing pH responsive behavior (Gilley et al., 2017; Li et al., 2009; Shah et al., 2014). At acidic stomach pH, the weak

acid residues are essentially 100% protonated, resulting in a net neutral charge and the ASD remains intact due to lack of electrostatic repulsion (Gilley et al., 2017; Li et al., 2009; Pereira et al., 2013). However, at near-neutral intestinal pH (i.e. well above the pK_a of the acid residues), the acid residues are largely deprotonated, resulting in a net negative charge (Gilley et al., 2017; Li et al., 2009; Pereira et al., 2013). The resulting electrostatic repulsion causes the modified cellulose to swell, releasing the drug into solution (Gilley et al., 2017; Li et al., 2009; Pereira et al., 2013). Therefore, pH-responsive modified cellulose can potentially inhibit drug release in acid and enhance dissolution at near-neutral pH, thus providing ideal delivery properties for RPT and RIF (Li et al., 2013). We have previously used ASD to achieve supersaturation and protection from degradation of nutraceuticals and drugs (Gilley et al., 2017; Li et al., 2013).

The objective of this study was to determine whether the use of ASD with commercially available and novel cellulose derivatives [hydroxypropyl methylcellulose acetate succinate (HPMCAS), cellulose acetate suberate (CASub), and 5-carboxypentyl hydroxypropyl cellulose (CHC), Fig. 3.2] would reduce RPT dissolution and prevent acidic degradation at gastric pH, and enhance dissolution at small intestinal pH, *in vitro*. We compared the protection and release characteristics of these formulations to RPT alone. We hypothesized that ASD would both protect RPT from release at gastric pH and release RPT into stabilized supersaturated solutions at intestinal pH.

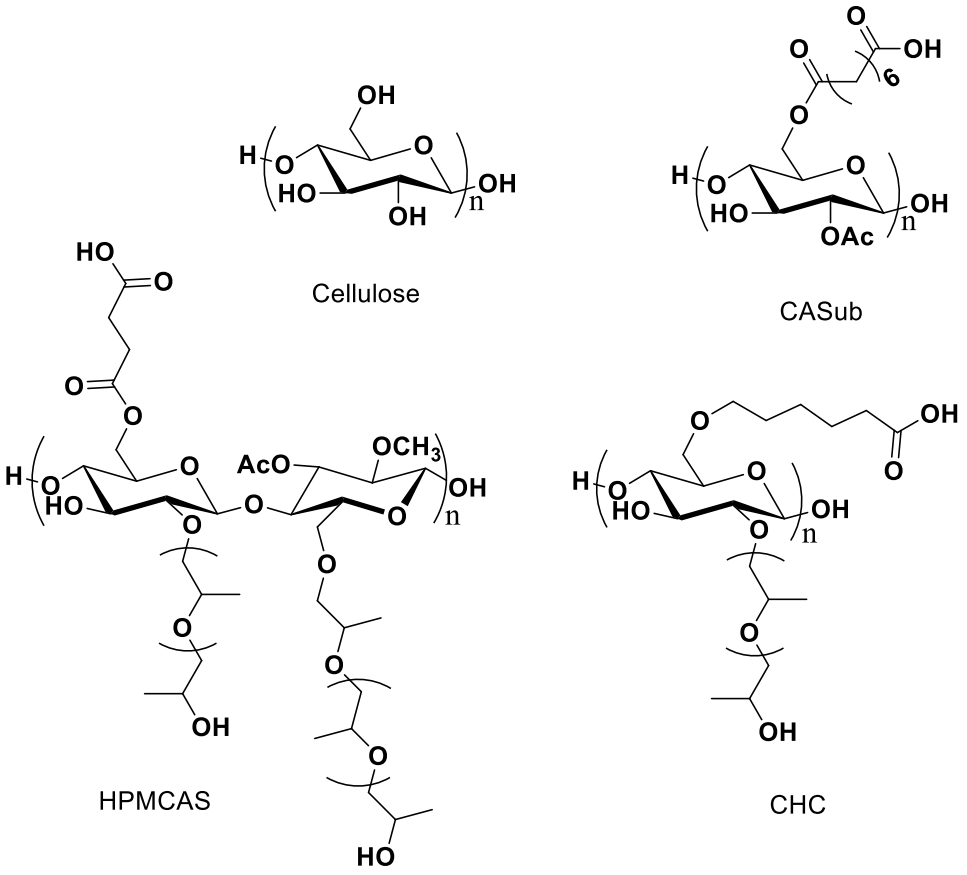

Figure 3.2: Structures of cellulose, hydroxypropyl methylcellulose acetate succinate (HPMCAS), cellulose acetate suberate (CASub), and 5-carboxypentyl hydroxypropyl cellulose (CHC). The cellulosic structures are not meant to convey regioselective substitution; depictions of substituent location are merely for convenience and clarity of depiction.

2. Experimental

2.1 Materials

RPT (powder) (98.2% purity) was purchased from Attix Pharmaceuticals (Toronto, ON, Canada). HPMCAS (wt %: methoxyl 20-24%, hydroxypropyl 5-9%, acetyl 5-9%, succinoyl 14-18%; Mw = 18,000) was from Shin-Etsu Chemical Co., Ltd (Tokyo, Japan). Cellulose acetate (CA-320S, DS (acetate) = 1.82, Mn = 50,000) was from Eastman

Chemical Company. Hydroxypropyl cellulose (HPC, Mw ~ 100,000) was purchased from Acros Organics (Geel, Belgium). For a full list of materials see Appendix A.

2.2 Synthesis of ASD polymers

CASub (Mw ~22500 g/mol, DS 2.72) and CHC (Mw 70,400 g/mol, DS 2.20) were synthesized as previously reported in Liu *et al.* 2014 and Dong *et al.* 2016, respectively. See Appendix A for full details.

2.3 Preparation of ASDs

ASD microparticles with formulations of 90:10, 75:25, and 50:50 (polymer:RPT) were prepared using HPMCAS, CASub, and CHC. ASDs were prepared by film casting and cryogenic grinding. Full details can be found in Appendix A. Our convention for naming treatments is to list the % polymer, with the remainder being drug. For example, 90% HPMCAS/10% RPT is referred to as "90 HPMCAS" in most of the text, or simply "90" in most figures. RPT-only treatments are referred to as RPT in the text and figures.

2.4 ASD Characterization

X-ray powder diffraction (PXRD) and differential scanning calorimetry (DSC) were used to characterize the physical state of the RPT-loaded ASDs and RPT only, and were performed as described in Appendix A. These results can be seen in Fig. 3.4 and Supplementary Fig. 4 in Appendix A. ASD RPT content was confirmed by UPLC-MS/MS and can be seen in Appendix A: Supplementary Table 1.

PXRD patterns were measured with a Bruker D8 Discover X-ray Defractometer (Billerica, MA) with a Lynxeye detector and a KFL CU 2K X-ray source. Samples were run with a 1 mm slit window between a scan range of 10˚ to 50˚ 2θ.

DSC analyses were performed on a Trios TA Instrument (New Castle, DE) with dry samples (5 mg) loaded into TzeroTM aluminum pans. A heat/cool/heat experiment was done for each sample and the 2nd heating scan was used. Each sample was equilibrated at 25˚C for 5 min., and then heated to 145˚C at 10˚C/min. Sample was kept at isothermal temperature for 1 min. After this, quench cooling occurred at 50˚C/ min. until -50˚C was reached. Finally, sample was heated to 190˚C at 15˚C/min. T_g values were recorded as the step-change inflection point from second heat scans.

2.5 Determination of Rifapentine Solubility

A pilot study was performed to determine RPT solubility in order to guide design of the dissolution experiments. An excess of RPT (2mg/mL total load, not fully dissolved) was added to pH 6.8 phosphate buffer and solution concentration was measured over 8 hours. Samples were centrifuged and diluted appropriately. Samples were then prepared for UPLC-MS/MS and analyzed. For full methodological details, see Appendix A.

The amorphous solubility of RPT was determined in order to evaluate the effectiveness of the ASDs compared to the solution concentrations of amorphous RPT alone. This was determined through the stabilization of RPT with HPMCAS-MF and quantified by HPLC, full details can be found in Appendix A.

2.6 *In Vitro* Dissolution

In vitro dissolution testing was performed to evaluate RPT dissolution concentrations and kinetics achieved via ASD delivery, compared to crystalline RPT alone. Dissolution experiments were performed under non-sink conditions to facilitate observation of potential RPT supersaturation. To achieve non-sink conditions, each dissolution flask contained 8.2 mg RPT per 10 mL buffer, obtained by varying the amount of ASD added. This amount ensured that all treatments were given equal possibility of 5X supersaturation. Dissolution experiments were performed to mimic normal human fasting gastric and small intestine pH conditions, buffered at pH 1.2 and 6.8 respectively, and were adapted from Gilley *et al*. with modifications (Gilley et al., 2017). Additionally, a dissolution study to mimic human digestion was performed, switching from gastric to intestinal pH, with methods adapted from Pereira *et al*. (Pereira et al., 2013). For full methodological details see Appendix A.

2.7 Determination of Rifapentine Degradation

After initial dissolution studies, 90 HPMCAS was chosen as a "proof of concept" treatment to determine whether the decreased RPT dissolution observed for this formulation was accompanied by decreased acid degradation (3-FR formation). RPT was intentionally degraded in 1 N HCl. Degraded RPT was analyzed by MS/MS to confirm the presence of 3-FR and develop a UPLC-MS/MS method for quantification. Levels of 3-FR were measured and compared between RPT and 90 HPMCAS dissolution samples at pH 1.2. Samples were prepared and analyzed by UPLC-MS/MS. For full methodological details see Appendix A.

2.8 Determination of Storage Stability after Neutralization and Freezing

In order to validate our 3-FR results, we investigated whether the production of 3-FR occurred primarily during dissolution or post-dissolution (during storage and/or sample prep). We investigated whether neutralization and storage at −80°C effectively limited acid hydrolysis of RPT to 3-FR in pH 1.2 dissolution samples. RPT was treated similarly to gastric pH dissolution experiments (n=4) for 1 hour. Samples were either neutralized or non-neutralized and analyzed fresh or after one week of storage at −80°C, by UPLC-MS/MS, and 3-FR levels were statistically analyzed to determine differences. For full details see Appendix A.

2.9 UPLC-MS/MS

ASD loading and dissolution sample concentrations were measured by UPLC-MS/MS. RIF was employed as an internal standard (IS). Full method details are found in Appendix A.

2.10 Data Analysis and Statistics

Dissolution results are reported as observed RPT or 3-FR solution concentration vs. time. Pseudo-pharmacokinetic parameters were calculated from these values, using pharmacokinetic plug-ins in Microsoft Excel (Redmond, WA): area under the (concentration × time) curve (AUC), and maximum solution concentration (C_{max}). Data were graphed and statistically analyzed using Prism v. 6.0d (GraphPad, la Jolla, CA). Statistical significance between loading treatments within each polymer were determined

using one-way ANOVA with Tukey's HSD *post hoc* test between all treatment groups. Significance was defined *a priori* as $P<0.05$. Dixon's Q-test ($\alpha = 0.05$) was used to identify any outliers, which were excluded as necessary.

3. Results and Discussion

Three polymers that show strong promise for use in ASD formulation were employed in this study. HPMCAS is a commercial polymer, while CASub and CHC have been developed by our groups for use in ASD (Gilley et al., 2017; Konno et al., 2008; Li et al., 2013; Liu, 2014). Benefits of these polymers include the ability to provide pH responsive delivery and inhibition of crystallization, as well as the likelihood of biocompatibility (Gilley et al., 2017; Li et al., 2009; Shah et al., 2014). Polymer properties are summarized in Table 3.1 (below). Each polymer used was loaded with different concentrations of RPT (50%, 25%, and 10% RPT by weight, i.e. 50%, 75% and 90% polymer by weight). The ratio of drug to polymer in the ASD is an important factor for logistics in manufacture, cost of manufacture, and delivery characteristics (such as release, solubility enhancement, and inhibition of recrystallization).

Parameter[A]	Polymer		
	HPMCAS[1,2]	**CASub[3]**	**CHC[4]**
T_g (°C)	120	144	94.0
DS (COOH)	~0.230	0.900	1.00
DS other	Me+Hp*=2.17 Ac=0.31-0.51 Suc=0.12-0.33	Ac=1.82 Sub=0.90	Hp*=2.2 (MS=4.4)
DS total	2.60	2.72	2.20
Mw (g/mol)	18,000	~22,500	70,400
Mn (g/mol)	12,600	21.2[B]	69,000
Solubility Parameter	22.4	22.6	Uncalculated
Water Solubility (mg/mL)	23.4	0.300	43.5
DP	70.0	63.0	129

Table 3.1: A summary of polymer properties as reported by 1) Liu, 2015, 2) Li, 2013, 3) Liu, 2014, and 4) Dong, 2016. Abbreviations: methoxy (Me), hydroxypropyl (Hp), acetate (Ac), succinate (Suc), suberate (Sub).
**molar substitution (MS) used for hydroxypropyl due to chain extension ability*
[A]Parameters defined: T_g (glass transition temperature), DS (degree of substitution), Mw (molecular weight), Mn (average molecular weight), DP (degree of polymerization).
[B]Relative to polystyrene standards

3.1 Determination of RPT Solubility

Reliable aqueous RPT solubility estimates proved to be difficult to find. Most estimates are vague and suggest an aqueous solubility of "<1 mg/mL," with the exception of one simulated computer model suggesting solubility as low as 0.0213 mg/mL (Adooq, 2016; Enogene; Ostrovskii et al., 2016; Tetko et al., 2005). To determine the solubility of RPT, we observed dissolution of excess RPT over 8 h under non-sink conditions (Fig. 3.3). This was necessary to determine the amount of RPT needed for each dissolution flask to ensure non-sink conditions and consistency in dissolution experiments. The

highest concentration reached was 0.164 ± 0.00254 mg/mL (mean ± SEM), and we employed this value moving forward.

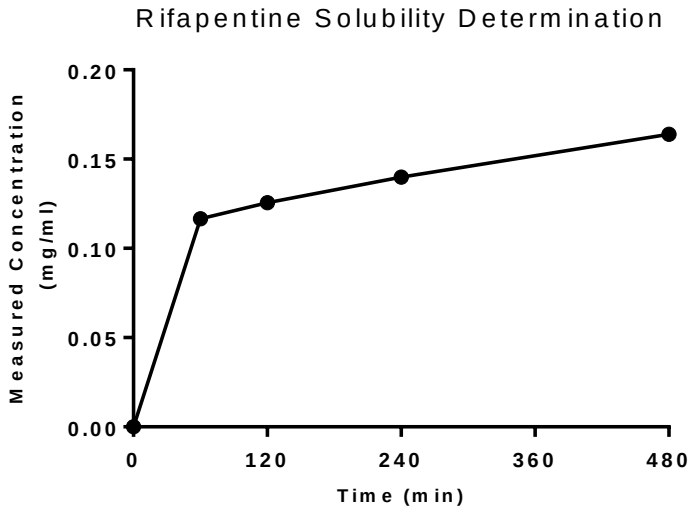

Figure 3.3: Solution concentration of RPT in aqueous pH 6.8 phosphate buffer over 8 hours, points represent mean ± SEM, n=16. Note: error bars are plotted but are too small to be visible.

While the observed solution concentration appears to still be increasing at 8 h, and thus equilibrium solubility was not likely reached, this period provides a realistic timeframe for which the drug would be in transit in the human body. Therefore, our solubility estimate appears rational for use in these dissolution experiments.

Amorphous compounds show a much higher solution concentration when compared to their crystalline counterparts (Ilevbare et al., 2012). The amorphous solubility can be difficult to measure because, although the amorphous form initially allows achievement of much higher concentrations compared to the crystalline form, it quickly recrystallizes out of solution to minimize free energy (Shah et al., 2014). For this reason, it is necessary

to use a polymer in solution with the amorphous drug in order to stabilize this form. The amorphous solubility of RPT was determined in order to compare to the crystalline solubility as well as evaluate the effectiveness of ASDs at reaching and stabilizing amorphous RPT concentration. The amorphous solubility of RPT was measured as 0.436 ± 0.0053 mg/mL in 100 mM sodium phosphate buffer pH 6.8 with 5 µg/ml HPMCAS-MF. This value is almost 3-fold higher than our solubility estimate of crystalline RPT (Fig. 3.3). This value gives insight as to just how much the use of the amorphous form may increase measured solution concentrations in the dissolution experiments.

3.2 Solid State Characterization of RPT loaded ASDs

3.2.1 DSC

DSC was used to further confirm dispersion morphology of RPT and the RPT-loaded ASDs (Fig. 3.4A). T_g values are 120 °C (HPMCAS), 144 °C (CA Suberate) and 94 °C (CHC). The observation of a T_g is important to confirm the amorphous nature of the system. It is clear that DSC analysis of the pure drug shows a melting peak (T_m) at 175 ˚C, which is indicative of crystallinity. The drug acted as a plasticizer for the ASD polymers which is indicated by a decrease in the T_g of the polymers. A high T_g is important for the stability of the ASDs during storage; when stored well below the T_g the drug is essentially immobilized in a brittle, glassy solid that prevents mobility of the drug particles thereby preventing crystallization (Yu, 2001). The absence of peaks corresponding to enthalpy of crystallization and melting in the DSC curves of ASDs confirm the amorphous character of RPT in these dispersions.

3.2.2 PXRD

PXRD was used to determine whether dispersions were amorphous as well. All PXRD spectra showed only amorphous halos for RPT-loaded ASDs (Fig. 3.4B). These data strongly confirm the amorphous nature of the solid dispersions prepared as no crystalline peaks corresponding to crystalline drug were observed. RPT only, on the other hand, demonstrated characteristics indicative of crystallinity, with the peaks indicating diffraction off of a defined crystal structure (Zhou, Li, & Zheng, 2010). The clear, sharp peaks present in the crystalline sample can be easily distinguished from the amorphous halo in Fig. 3.4B.

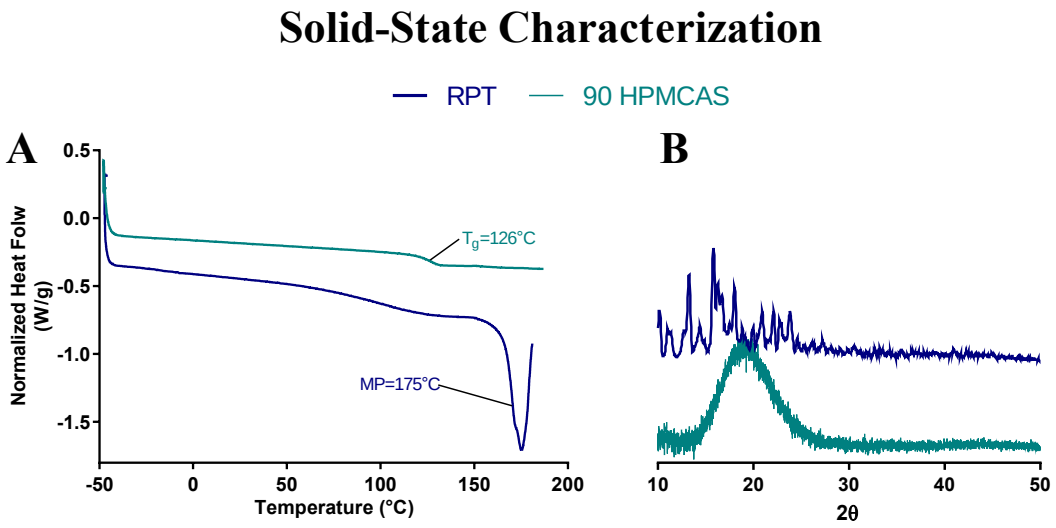

Figure 3.4: A) Representative DSC analysis and B) PXRD analysis, confirming the amorphous nature of RPT in the 90 HPMCAS ASD as opposed to the crystallinity of RPT alone. Other DSC and PXRD analysis of all RPT loaded ASD formulations can be seen in Appendix A: Supplementary Figure 4.

3.3 UPLC Verification of RPT ASD Content

Each RPT-loaded ASD was analyzed for % RPT by weight and these calculated values were used to determine the amount of ASD required to provide 8.2 mg of RPT per flask. RPT content was determined to be within 3% of target for most formulations, with the largest deviation, 50 CHC, showing a 6.5% difference from target formulation. These results can be seen in Appendix A: Supplementary Table 1.

3.4 Gastric *In Vitro* Dissolution Studies

Results of gastric dissolution experiments with RPT alone and RPT-loaded ASDs are shown in Fig. 3.5.

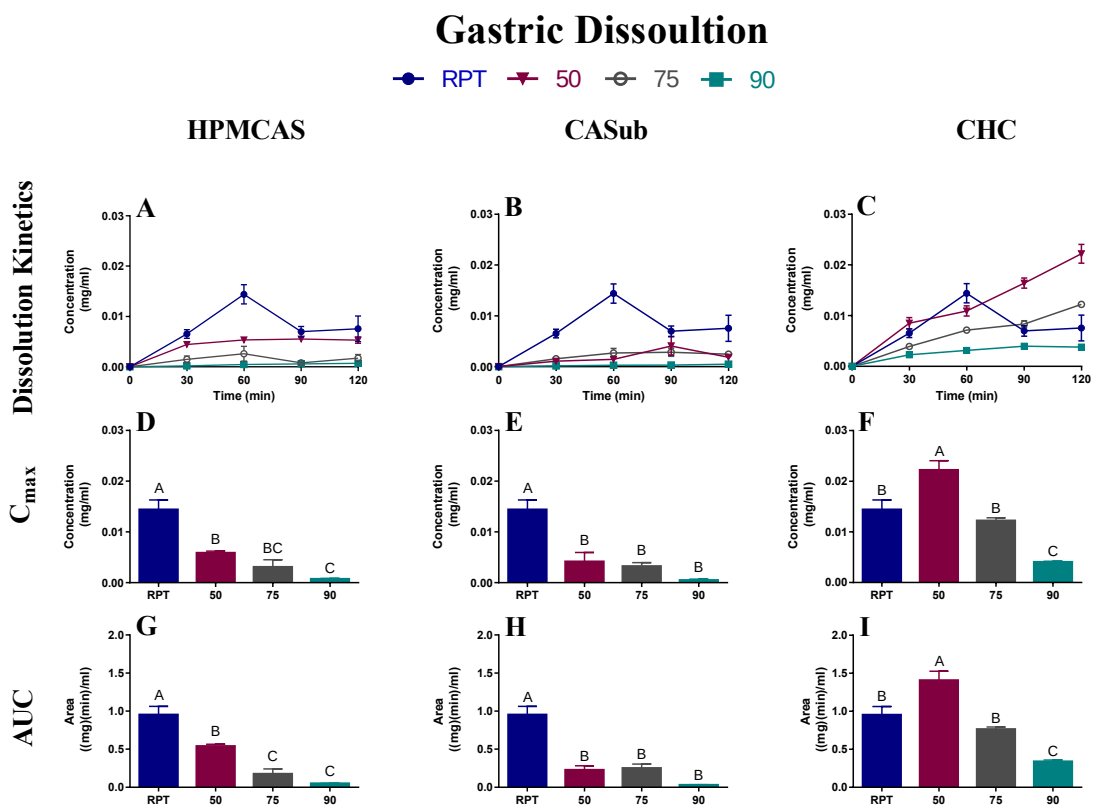

Figure 3.5: Results of gastric (pH 1.2) dissolution experiments. Performance of RPT-loaded ASDs polymers vs. RPT alone: HPMCAS (A, D, G), CASub (B, E, H) and CHC (C, F, I) as measured by dissolution concentrations over time (A-C), observed maximal concentration (C_{max}, D-F) and area under the dissolution curve (AUC, G-I). Values represent mean ± SEM (n=3-4). Values for each polymer not sharing a common superscript are statistically significantly different (1-way ANOVA with Tukey's post hoc test for all possible comparisons, $p<0.05$). These results have been provided in tabular form in Appendix A: Supplementary Table 2. In the bar graphs, RPT: RPT only (0% polymer), 50: 50% polymer, 75: 75% polymer, 90: 90% polymer, with the remainder of these formulations being RPT. All dissolution experiments employed equal masses of RPT.

When interpreting these results, note that the positive (desired) result at gastric pH is a measured solution concentration lower than RPT alone, as the goal is to reduce the dissolution at gastric pH in order to protect RPT from acid hydrolysis. In general, the low release of the ASDs compared to RPT is attributed to the protonated, neutral nature of the

carboxylic acids causing a low solubility of the polymer at this pH (Shah et al., 2014). The carboxylic acid groups at this pH are not ionized because they are below their pK_a which restricts the ASD from swelling and releasing the RPT (Pereira et al., 2013).

All HPMCAS ASD formulations performed significantly better than RPT alone with a general order of significance, most effective to least effective: 90>75>50. The dissolution kinetics over time show a clearly lower measured concentration for all ASD formulations compared to RPT. All ASDs showed significantly lower C_{max} than RPT with 90 HPMCAS showing >17-fold decrease, 75 HPMCAS showing >4-fold decrease, and 50 HPMCAS showing >2-fold decrease in measured concentration. AUC was also significantly reduced with the use of HPMCAS ASDs, with the same general order of significance. The 90 HPMCAS formulation showed >19-fold decrease and the 75 HPMCAS showed >5-fold decrease in AUC compared to RPT.

All CASub ASD formulations showed much lower solution concentrations than RPT and generally showed lower solution concentrations compared to HPMCAS as well. Though CASub ASDs were not significantly different from each other in C_{max} they did show a general downward trend of lower C_{max} with higher % polymer in the formulation. This could be due to the relative hydrophobicity of the polymer (more hydrophobic than HPMCAS). With greater concentration of a hydrophobic polymer, you would expect to see a lower concentration released in aqueous media, due to its lower solubility. Considering C_{max} compared to RPT, 90 CASub showed >22-fold decrease, 75 CASub showed > 4-fold decrease, and 50 CASub showed >3-fold decrease in soluble

concentration. Again, AUCs were reduced compared to RPT alone. Though CASub ASD formulations did not show statistically significant differences between themselves due to SEMs, there were large differences in the means; 90 CASub showed an AUC >31-fold lower, while 75 and 50 CASub showed just over a 3-fold decrease compared to RPT. Again, pointing to higher amount of polymer performing the best for CASub at gastric pH.

CHC ASD formulations also showed decreasing RPT solution concentration with increasing amount of polymer in the formulation. Not all formulations performed optimally at this pH. 75 CHC showed no significant differences from RPT only, while 50 CHC showed significantly higher measured concentrations compared to RPT. However, 90 CHC showed desirable results compared to RPT with a C_{max} and AUC >3-fold lower and >2-fold lower, respectively, than RPT; this illustrates the importance of the ratio of polymer to drug in the ASD, whose influence can vary by the polymer used. In general, we see a higher measured concentration of RPT with this polymer compared to either HPMCAS or CASub. The relatively high hydrophilicity of this polymer due to the large amount of hydroxypropyl groups was likely a large contributing factor to these results because hydrophilic polymers are known to increase drug release (Dong et al., 2016).

3.5 Rifapentine Degradation

Protection from acidic hydrolysis is extremely important for RPT as a drug. Limiting the amount of hydrolysis to 3-FR could lead to a drug that has reduced cost due to the higher dose availability. After initial dissolution studies, 90 HPMCAS was chosen due to its

ideal gastric dissolution properties as a “proof of concept” treatment to determine whether decreased RPT dissolution was accompanied by reduced acid degradation to 3-FR. Since it was previously determined that our standard protocol of neutralization and freezing effectively eliminated the hydrolysis of RPT to 3-FR (Appendix A: Supplementary Figure 3) samples were analyzed to quantify 3-FR concentration. 3-FR was detected in all tested samples at pH 1.2, though concentrations were substantially lower in treatments employing ASD. The 90 HPMCAS formula significantly decreased measured 3-FR concentrations compared to RPT alone (Fig. 3.6D-F). Therefore, it appears that protection from release was accompanied by a reduction in 3-FR formation, suggesting that pH-responsive ASDs can significantly protect RPT from acid degradation. It is also important to note that the 90 HPMCAS dissolution treatment did not show a significantly higher measured concentration of 3-FR compared to RPT analyzed directly from the bottle (Appendix A: Supplementary Figure 3). This indicates that the 90 HPMCAS ASD essentially showed no degradation due to the actual dissolution experiment and that measured 3-FR concentration in the samples was primarily due to that found in the untreated RPT itself. Though untested, it is possible that there may be even more dramatic decreases in degradation for CASub ASDs, as CASub more effectively inhibited RPT release than HPMCAS. MS (Fig. 3.6A) and MS/MS (Fig. 3.6B) spectra from direct infusion of the intentionally degraded RPT can be seen below. 3-FR was identified by its parent pseudomolecular ion ($[M-H]^-$) of 724 m/z, which was isolated to determine the MS/MS (daughter ion) spectrum. 3-FR had a longer retention time than RPT or RIF, and a representative chromatogram can be seen in Fig. 3.6C.

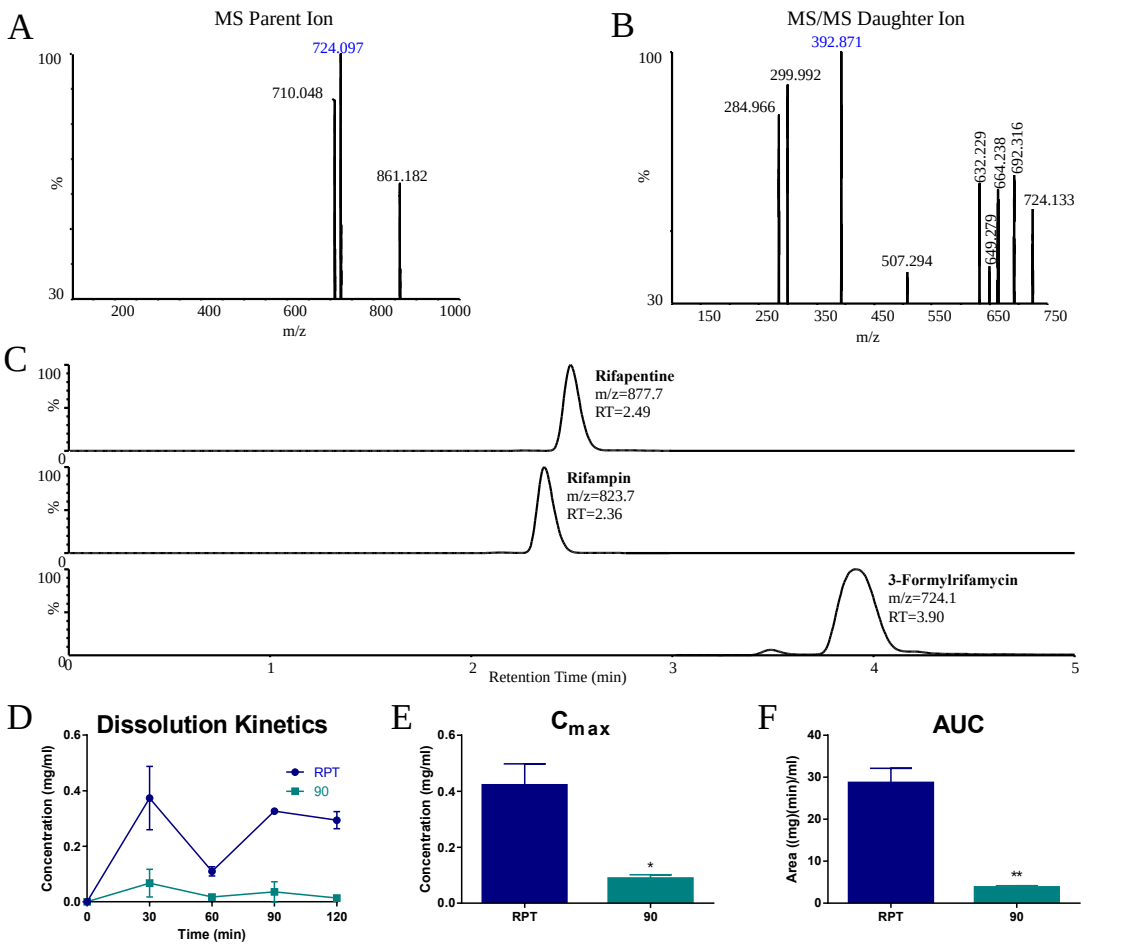

*Figure 3.6: Identification of RPT degradation product 3-FR from intentionally acid-degraded RPT (A-C), and characterization of 3-FR formation in gastric dissolution samples employing RPT only and RPT in 90% HPMCAS ASD (D-F). A) MS (parent ion) spectrum for 3-FR[1] [note the peak for 3-FR (m/z=724) in blue text], B) MS/MS (daughter) spectrum for 3-FR[1] [note main daughter fragment at 392 (blue), and other prominent fragments at 299, and 264]. C) Representative MRM chromatograms for RPT, RIF, and 3-FR. D) Measured concentration of 3-FR in gastric dissolution[2,3]. E) Measured C_{max} of 3-FR (n=3) in gastric dissolution [2,3]. F) Measured AUC of 3-FR[2,3]. Values of D, E, and F represent mean ± SEM (n=3). Values with * represent significant differences (t-test, $p<0.05$) and ** represent highly significant differences (t-test, $p<0.01$).*

[1]Graph y-axes start at 30% for ease of interpretation

[2]3-FR was quantified as RPT equivalents

[3]Only RPT alone and 90 HPMCAS formulation were compared

3.6 Small Intestinal *In Vitro* Dissolution Studies

The results of small intestinal dissolution experiments are shown in Fig. 3.7.

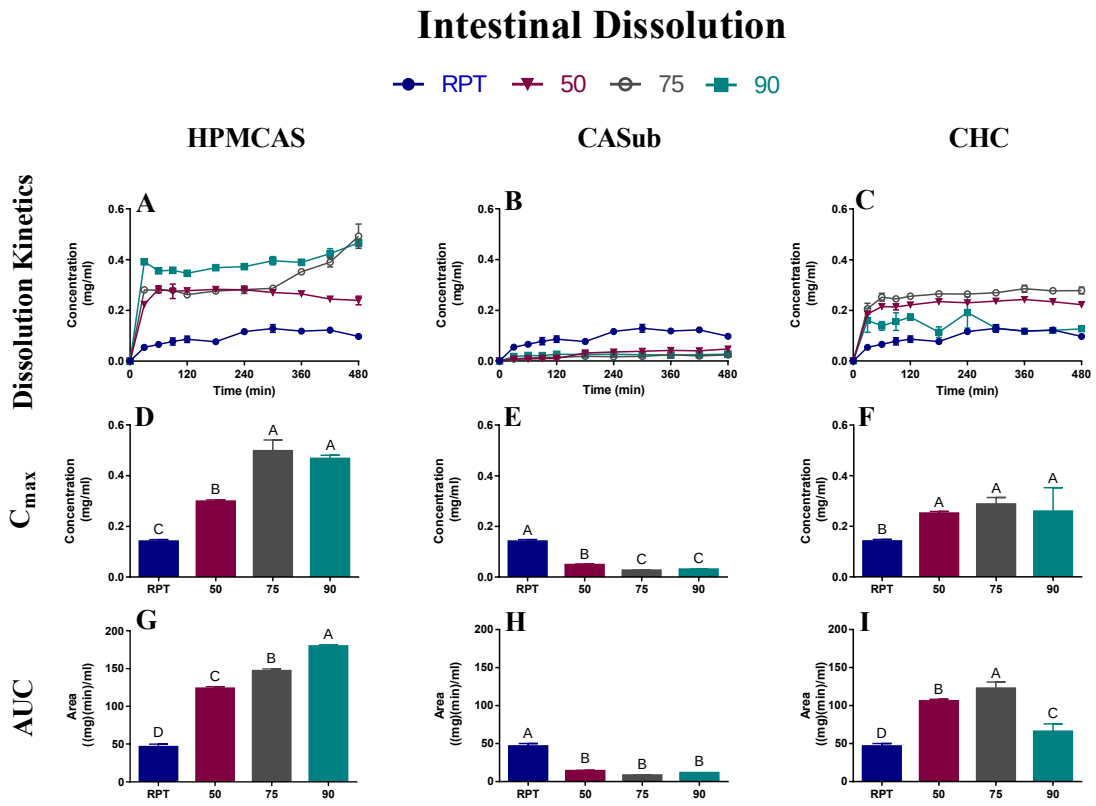

Figure 3.7: Results of small intestinal (pH 6.8) dissolution experiments. Performance of RPT-loaded ASDs from various polymers: HPMCAS (A, D, G), CASub (B, E, H) and CHC (C, F, I) as measured by dissolution concentrations over time (A-C), observed maximal concentration (C_{max}, D-F) and area under the curve (AUC, G-I). Values represent mean ± SEM (n=3-4). Values for each polymer not sharing a common superscript are statistically significantly different (1-way ANOVA with Tukey's post hoc test for all possible comparisons, $p<0.05$). These results have been provided in tabular form in Appendix A: Supplementary Table 3. In the bar graphs, RPT: RPT only (0% polymer), 50: 50% polymer, 75: 75% polymer, 90: 90% polymer, with the remainder of these formulations being RPT. All dissolution experiments employed equal masses of RPT.

When interpreting these results, note that a positive (desired) result at intestinal pH shows measured solution concentrations greater than RPT. In general, the high release of the ASDs compared to RPT is attributed to ionized nature of the carboxylic acids causing a higher solubility of the polymer at this pH (Shah et al., 2014). The carboxylic acid groups at this pH are ionized because they are above their pK_a causing the negatively charged groups to repel each other thereby causing swelling and release of the RPT (Pereira et al., 2013).

All HPMCAS ASD formulations performed significantly better than RPT alone at this pH, with a general order of significance, most effective to least effective: 90>75>50. The dissolution kinetics over time show a clearly higher measured concentration for all ASD formulations, at each time point, compared to RPT alone. All HPMCAS ASDs showed significantly higher C_{max} than RPT alone. 90 and 75 HPMCAS showed >3-fold increases compared to RPT, both significantly higher than 50 HPMCAS, showing >2-fold increase compared to RPT. AUCs proved significantly higher with the use of HPMCAS ASDs as well, showing similar increases as with C_{max} and indicating an increased total drug exposure with the use of ASD, which suggest that these formulations would provide a more effective transmembrane concentration the of drug *in vivo*. RPT in the 90 HPMCAS was stabilized just below the amorphous solubility (0.436 ± 0.0053 mg/mL) for the entire course of the dissolution, showing extremely effective stabilization. However, the C_{max} of both the 90 and 75 formulations actually exceeded the amorphous solubility of RPT briefly at end of the dissolution, reaching 0.466 ± 0.0140 and 0.497 ± 0.0435 mg/mL respectively. The highly effective nature of the HPMCAS polymer is attributed to the

ideal balance of hydrophobicity/hydrophilicity allowing stabilization of amorphous RPT at this pH and the variety of chemical substituents attached that allow diverse drug-polymer interactions also helping to aid in stabilization (Ilevbare et al., 2012).

CASub ASDs showed much lower measured RPT concentration than RPT only at intestinal pH. RPT showed significantly higher C_{max} and AUC than all CASub formulations. This means that the drug was not effectively released from the ASD and therefore increased apparent solubility was not observed. This was likely due to an issue with release from the system and not due to crystal formation as CASub was developed as an effective crystallization inhibitor and relatively hydrophobic polymers have been shown to inhibit crystallization through stabilization of (relatively lipophilic) drugs (Liu et al., 2014; Ting, Nayale, Jones, Bates, & Reineke, 2015). The low amount of RPT release is expected to have resulted from the relative hydrophobicity of the polymer as well as drug-polymer interactions between the CASub and RPT. As CASub alone does not appear to facilitate higher RPT concentrations under small intestinal conditions, the addition of polyvinylpyrrolidone (PVP), a synthetic water-soluble polymer, to the formation may be able improve release and dissolution (Gilley et al., 2017; Marks, Wegiel, Taylor, & Edgar, 2014). PVP may improve this formulation by increasing hydrophilicity and aqueous solubility leading to a more rapid and increased dissolution profile of the system, in addition to weakening of the interactions between CASub and the drug, allowing greater release (Liu et al., 2014). It is important to note however that this increase in dissolution with the addition of PVP would likely be seen at gastric pH

conditions as well, meaning that it could not be used exclusively, due to the likelihood of RPT degradation.

All CHC ASDs showed significantly higher measured concentrations compared to RPT. Interestingly, the 90 CHC did not perform as well as the other CHC formulations. This was unexpected because general trends with other polymers suggested that the highest percent polymer would provide the best performance. This differing trend, along with the lower measured solution concentration of RPT compared to the HPMCAS ASDs is attributed to the hydrophilicity of the CHC ASD polymer. If a polymer is too highly hydrophilic, it is expected to interact more strongly with the aqueous solvent rather than stabilizing the drug in solution (Ilevbare et al., 2012). Essentially this reduces the polymer-drug interactions required to stabilize the supersaturation and hence allows crystallization of the drug. This can be seen with the 90 CHC which, compared to the 50 and 75 formulations, did not show stabilization over the full course of the dissolution; likely due to the polymer interacting more strongly with the solvent versus stabilizing the drug. Though there were not significant differences between polymer concentrations and it is difficult to distinguish a clear trend regarding C_{max}, all formulations did perform significantly better than RPT. Our highest C_{max} for CHC was achieved by the 75 formulation, showing >2-fold increase in measured concentration compared to RPT. The AUC results showed that all formulations significantly increased measured concentrations compared to RPT, and all treatments were significant between one another. The order of significance most effective to least effective was 75>50>90, which again was an unexpected result. Though 90 CHC still did show a significant increase in

AUC compared to RPT, it was not as high as the 50 and 75 formulations which showed >2-fold increases in AUC compared to RPT. The CHC ASDs were able to stabilize supersaturated solutions at roughly half that of the amorphous solubility of RPT.

3.7 pH Switch *In Vitro* Dissolution Experiments

The results of pH switch dissolution experiments are shown in Fig. 3.8. These dissolution experiments involve a change in pH from acidic to neutral, mimicking gut transit *in vivo*. This models the impact of gastric events on subsequent small intestinal dissolution, as opposed to examining digestive regions in isolation.

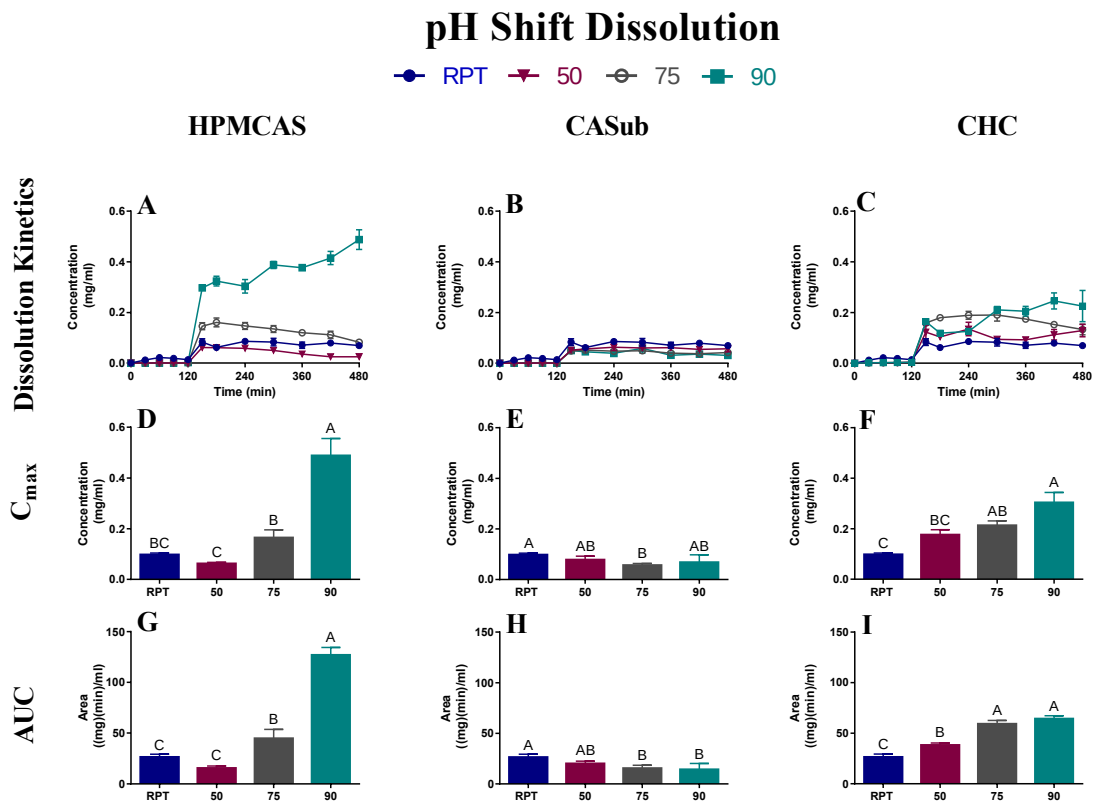

Figure 3.8: Results of pH shift (pH 1.2 → 6.8) dissolution experiments. Performance of RPT-loaded ASDs from various polymers: HPMCAS (A, D, G), CASub (B, E, H) and CHC (C, F, I) as measured by dissolution concentrations over time (A-C), observed maximal concentration (C_{max}[1], D-F) and area under the curve (AUC[1], G-I). Values represent mean ± SEM (n=3-4). Values for each polymer not sharing a common superscript are statistically significantly different (1-way ANOVA with Tukey's post hoc test for all possible comparisons, $p<0.05$). These results have been provided in tabular form in Appendix A: Supplementary Table 4. In the bar graphs, RPT: RPT only (0% polymer), 50: 50% polymer, 75: 75% polymer, 90: 90% polymer, with the remainder of these formulations being RPT. All dissolution experiments employed equal masses of RPT.

[1]C_{max} and AUC were quantified only for pH 6.8 (120-480 min.) with 120 min. being treated as a zero point.

90 HPMCAS was clearly the best performer, with excellent results, which was consistent with findings from small intestinal dissolution experiments. It is important for these polymers to provide both protection from degradation in gastric conditions and complete,

rapid release in the small intestine for optimal delivery. The delivery system is much less effective if characteristics at both pH values are not optimal. Both 75 and 50 HPMCAS showed large decreases in C_{max} reached in the pH shift dissolution experiments compared to those seen in the isolated pH 6.8 dissolution experiments (Fig. 3.7), indicating that starting in acidic conditions likely does affect delivery of the drug with these ASD concentrations. 75 HPMCAS however still showed positive results in this dissolution; though the concentrations were affected, they still reached almost double that of RPT. It is interesting to note that 50 HPMCAS remained similar to RPT alone and even decreased to lower measured concentrations than RPT towards the end of the dissolution. Though this was a surprise, it was expected that the 50 formulation would behave most similarly to RPT alone, due to the ratio of drug: polymer. The differences in behavior for this pH switch dissolution are attributed to the starting acidic conditions. It is possible that the ASDs with lower amounts of polymer did not sufficiently protect RPT from degradation, therefore leading to lower overall concentrations available when switched to intestinal pH. However, 90 and 75 HPMCAS formulations do still lead to enhanced characteristics.

CASub performed for the most part as expected based on results from previous dissolution experiments. Again we see slight differences in behavior and measured concentration after simulated digestion, compared to each isolated pH (1.2 and 6.8) alone. Overall increases in the amount of polymer in the formulation led to decreases in measured RPT solution concentration.

CHC showed improved results in the pH switch dissolution experiments compared to the isolated intestinal dissolution. 75 and 90 CHC showed significantly higher C_{max} and AUC compared to RPT. Though 50 CHC did show increases in measured concentration compared to RPT, the differences were not significant. This polymer in these pH switch dissolution experiments followed the trend for increasing amount of polymer leading to a better delivery system.

3.8 Summary of Results

At gastric pH, all formulations of HPMCAS and CASub protected RPT from release and showed significantly lower C_{max} and AUC compared to RPT alone (Fig. 3.5), while only one formulation of CHC effectively protected RPT from release. Our best performing polymer at gastric pH, 90 CASub, showed an AUC > 31-fold lower than RPT. Decreased soluble concentration of RPT at gastric pH was accompanied by a significantly lower amount of the degradation product 3-FR, as seen in Fig. 3.6, for the HPMCAS formulation (the only formulation tested for 3-FR production). At intestinal pH, HPMCAS and CHC ASDs afforded increased RPT apparent solubility and stabilized supersaturated solutions compared to RPT alone. CASub could likely show increased solution concentrations with the addition of PVP to enhance release (Gilley et al., 2017; Marks et al., 2014). Our best performing polymers at intestinal pH, 90 HPMCAS and 75 HPMCAS, showed > 3-fold RPT increases compared to RPT only. These measured RPT concentrations, especially for 90 HPMCAS, were very close to that of the amorphous solubility of RPT showcasing the excellent performance. 5-fold supersaturation was likely an acceptable limit for this experiment as we did not reach concentrations higher

than 4-fold saturation in any dissolution experiments; it is possible that these polymers may have reached their achievable limit without additional modification. However, 5X supersaturation is again an experimental limit, not a theoretical one and the use of different polymers could exceed this (Gilley et al., 2017).

ASD appears to be an effective strategy for RPT delivery, assuming the correct polymer is selected. The results suggest that hydrophilic/hydrophobic character of the ASD polymers affect the dissolution kinetics of RPT and that an ideal balance of the two is required to see positive results at both pH conditions. At gastric pH, the more ideal polymers were more hydrophobic whereas at intestinal pH the more ideal polymers were more hydrophilic. Due to its ideal balance of hydrophobic and hydrophilic character, HPMCAS showed the best delivery characteristics at both pH conditions. CASub appears to have had too strong of drug-polymer interactions, not allowing release and CHC appeared to have to weak of drug-polymer interactions, interacting more favorably with the aqueous solvent and allowing crystallization of the drug. This study helps to illustrate the potential benefits of ASD formulation, as well as the importance of selecting the best polymer for the drug. HPMCAS showed the most promise, both protecting the drug from degradation at gastric pH and achieving stabilized supersaturation at small intestine pH. There was a general trend showing that increasing the amount of polymer in the ASD led to a more effective delivery system. This is because with an increasing amount of polymer in the system, the properties of the ASD begin to mirror the characteristics of the polymer more closely than the drug itself.

4 Conclusions

In this study, the effect of ASD on RPT dissolution kinetics with one commercial and two novel cellulose polymers was explored. Overall, the results support the hypothesis that the use of ASD with these various polymers would both protect RPT from release at gastric pH and release RPT into stabilized supersaturated solutions at intestinal pH *in vitro*. These results also help to illuminate some of the properties of polymers used in ASD and show how they may affect dissolution kinetics. The use of terminal carboxylic acid groups did provide a pH-responsive nature to the ASDs; however the addition of carboxylic acid groups was not the only important factor in predicting a successful delivery of RPT. Increasing the amount of polymer in the formulation generally led to a better delivery system. However, it is extremely important that the correct polymer is selected. The results suggest that ASD can protect RPT from degradation in gastric conditions. This was due to the minimal release afforded by the ASD systems. It is hypothesized that the hydrophobicity of the polymers at this pH was the main factor in decreasing the amount of RPT release. ASDs also afforded greatly increased solution concentration of RPT at intestinal pH, showing measured concentrations that even slightly exceed that of the amorphous solubility. The high release of the drug from the system at this pH was attributed to the relative hydrophilicity of the polymers after ionization. However, a too highly hydrophilic polymer may not stabilize the drug effectively, leading to crystallization. Therefore a balance of hydrophilicity and hydrophobicity (as seen with HPMCAS) is expected to be the most important factor in stabilization of supersaturated solutions of RPT at intestinal pH. The results of this study

require more detailed experiments to further predict other structure-property relationships that may affect final delivery of RPT in ASD.

ASD as a delivery strategy shows great promise for delivering RPT *in vivo*. Our model suggests that it may be possible to lower the required effective dose of RPT by reducing acidic degradation and increasing absorption, ultimately leading to a more effective treatment of TB. These increases in RPT solution concentration suggest that the use of this system may be able to provide a much higher transmembrane gradient *in vivo*, thereby increasing absorption and bioavailability. The net sum of reduced degradation and enhanced intestinal dissolution could be improved bioavailability, *in vivo*. This may minimize the amount of drug needed to achieve effective dosing, as well as provide higher circulating levels of the drug *in vivo*. In addition to improving efficacy, reducing antibiotic resistance, and therapeutic duration, this may reduce costs associated with the treatment of TB. This much more effective delivery system for RPT could help to reduce TB burden worldwide.

5 Acknowledgements

Funding for this research was provided in part by an Enhanced Drug Delivery Project Seed Funding grant from the Institute for Critical Technologies and Applied Science (ICTAS). Funding for this work was also provided, in part, by the Virginia Agricultural Experiment Station and the Hatch Program of the National Institute of Food and Agriculture, United States Department of Agriculture. We are grateful to the VT Macromolecules Innovation Institute for their support and to VT ICTAS for their material

and facilities support. We thank Eastman Chemical Company for their kind donation of cellulose acetate and Shin-Etsu Chemical company, LTD for their kind donation of HPMCAS. We also thank Ann Norris (Department of Sustainable Biomaterials, Virginia Tech) for PXRD analyses.

Chapter 4: Overall Summary and Future Opportunities

Research Limitations

In our research we were able to determine the effectiveness of RPT in ASD of modified cellulose polymers. We performed *in vitro* dissolution experiments at three different conditions (pH 1.2, pH 6.8, and pH switch 1.2→6.8) meant to mimic human fasted gastrointestinal conditions. It is important to note that these pH values represent an average and do not account for normal fluctuations in gastrointestinal pH. *In vitro* studies that mimic human digestion are limited in their ability to fully encompass each exact detail that is present in the gut, especially due to constantly changing conditions and intersubject variability (Brenner & Stevens, 2009; Rollins & Klaassen, 2012; Sherwin et al., 2011). This research could possibly be improved with the use of a more encompassing simulation of digestion, meaning that the addition of digestive enzymes, bile salts, or even certain food components may further validate this study. It would be interesting to see how these may affect the results.

The use of *in vivo* animal models is an important predictor of final bioavailability in humans for many compounds (Ting et al., 2015). An *in vivo* study would help to further determine how these results may affect humans. Unfortunately, this was not possible with this research due to time constraints.

Another limiting factor in this research was the use of novel ASD polymers. These polymers are difficult to manufacture and do not yet have an industrial scale-up process that would allow them to be commercially produced. Due to the difficulty in

manufacture, we had to use small volumes for the *in vitro* dissolution experiments. There is the possibility that the use of larger volumes, more similar to those found in the human gastrointestinal tract may affect these results in some way.

Summary

TB is a deadly infection that causes over a million deaths each year. Though TB has been a problem for thousands of years, it is still difficult to treat and cure with the current treatment protocols. *Mycobacterium tuberculosis*, the bacteria that cause the illness, is relatively difficult to kill. The resistant nature of the bacteria in combination with the ease of spread and possibility of latent infection make it difficult to eliminate TB. Current treatment protocols can often require over 6 months of daily dosing with multiple drugs. A treatment like this is extremely challenging for many patients to complete, especially considering that the highest prevalence of TB is in developing countries. Low patient compliance leads to antibiotic resistance and increasingly large numbers of infected patients. Fortunately, RPT has shown great promise in improving the current treatment, that typically uses RIF, and has essentially cut treatment times in half while also increasing patient compliance due to less frequent dosing and decreasing bacterial resistance with the use of higher doses. Although a very effective drug, RPT faces challenges in delivery. Oral bioavailability is limited because this drug is both acid-labile, and is degraded in the gastric environment and is relatively poorly soluble at small intestine pH, where it is absorbed. We aimed to improve the delivery characteristics of RPT with the use of ASD which has shown amazing potential for improvement in

delivery with other drugs. In addition to increasing water solubility, ASD has also shown the potential to protect certain drugs from degradation (Li et al., 2013).

We found that the use of ASD does enhance the delivery characteristics of RPT. However, selecting the correct polymer for optimal delivery is extremely important. We found that the commercially available HPMCAS provided the most optimal results when considering both pH 1.2 and 6.8. This is beneficial because there would be comparatively little development required for these formulations, as commercial production of HPMCAS is common. In general we found better delivery characteristics with a higher amount of polymer in the ASD system. The use of certain ASD formulations greatly reduced the amount of soluble RPT at gastric pH. The decreased solubility was accompanied by a significant reduction in 3-FR, an acidic degradation product of RPT. We also found that the use of certain ASD formulations increased solution concentration at intestinal pH. These large increases may be able to overwhelm metabolic reactions and efflux in enterocytes, leading to higher net absorption of the native form of the drug. The sum of reduced degradation, and enhanced intestinal dissolution *in vitro*, may lead to large improvements of bioavailability, *in vivo*. With the improvements we may see a lower amount of drug required for effective treatment, reduced cost and time of treatment which would increase patient compliance, and reduced antibiotic resistance due to higher circulating levels of the drug *in vivo*, ultimately leading to a better treatment and the elimination of TB.

References

Acocella, G. (1978). Clinical pharmacokinetics of rifampicin. (Vol. 3, pp. 108-127). United States.

Adooq. Rifapentine (Priftin).(2016). http://www.adooq.com/rifapentine-priftin.html Accessed 5-19-2017.

Agrawal, S. (2003). Biopharmaceutics and pharmacokinetics of rifampicin: implications in performance and evaluation of anti-tuberculosis fixed dose combination formulations. PhD Thesis: *National Institute of Pharmaceutical Education and Research*.

Agrawal, S., Ashokraj, Y., Bharatam, P. V., Pillai, O., & Panchagnula, R. (2004). Solid-state characterization of rifampicin samples and its biopharmaceutic relevance. *European Journal of Pharmaceutical Sciences,* 22(2), 127-144.

Agrawal, S., & Panchagnula, R. (2005). Implication of biopharmaceutics and pharmacokinetics of rifampicin in variable bioavailability from solid oral dosage forms. *Biopharmaceutics & Drug Disposition,* 26(8), 321-334.

Anderson, R. J., Groundwater, P. W., Todd, A., & Worsley, A. J. (2012). Rifamycin Antibacterial Agents. In (pp. 63-83). Chichester, UK: John Wiley & Sons, Ltd

Avdeef, A. (2012). Absorption and drug development : solubility, permeability, and charge state: Wiley.

Bender, D. A. (2009). *A dictionary of food and nutrition*. Oxford;New York : Oxford University Press;: Oxford University Press.

Boland, M. (2016). Human digestion – a processing perspective. *Journal of the Science of Food and Agriculture,* 96(7), 2275-2283.

Brenner, G. M., & Stevens, C. (2009). *Pharmacology*: Elsevier Health Sciences.

Brinkmann, U., & Eichelbaum, M. (2001). Polymorphisms in the ABC drug transporter gene MDR1. *The pharmacogenomics journal,* 1(1), 59-64.

CDC. Treatment for TB Disease.(2016). https://www.cdc.gov/tb/topic/treatment/tbdisease.htm Accessed 5/28.2017.

Chakrabarty, D. K. (2010). Solid State Chemistry. Kent: New Academic Science.

Chan, S. L., Yew, W. W., Porter, J. H. D., McAdam, K. P. W. K., Allen, B. W., Dickinson, J. M., . . . Mitchison, D. A. (1994). Comparison of Chinese and Western rifapentines and improvement of bioavailability by prior taking of various meals. *International Journal of Antimicrobial Agents,* 3(4), 267-274.

CITC. Tuberculosis Drug Information Guide, 2nd edition.(2012). http://www.currytbcenter.ucsf.edu/sites/default/files/tb_sg3_chap5_medications.pdf#rifapentine Accessed.2.

Corrigan, O. I., Farvar, M. A., & Higuchi, W. I. (1980). Drug membrane transport enhancement using high energy drug polyvinylpyrrolidone (PVP) co-precipitates. *International Journal of Pharmaceutics,* 5(3), 229-238.

Crespy, V., Morand, C., Besson, C., Cotelle, N., Vézin, H., Demigné, C., & Rémésy, C. (2003). The splanchnic metabolism of flavonoids highly differed according to the nature of the compound. *American Journal of Physiology-Gastrointestinal and Liver Physiology*, 284(6), G980-G988.

Crespy, V., Morand, C., Manach, C., Besson, C., Demigne, C., & Remesy, C. (1999). Part of quercetin absorbed in the small intestine is conjugated and further secreted in the intestinal lumen. *American Journal of Physiology - Gastrointestinal and Liver Physiology*, 277(1), G120-G126.

Cui, X., Mao, S., Liu, M., Yuan, H., & Du, Y. (2008). Mechanism of surfactant micelle formation. *Langmuir : the ACS journal of surfaces and colloids*, 24(19), 10771-10775.

Daintith, J. (2008). *A dictionary of chemistry*. (6th ed.). New York: Oxford University Press.

Daniel, T. M. (2006). The history of tuberculosis. *Respiratory Medicine*, 100(11), 1862-1870.

Desai, K. G. H., & Jin Park, H. (2005). Recent developments in microencapsulation of food ingredients. *Drying technology*, 23(7), 1361-1394.

Dong, Y. F., Mosquera-Giraldo, L. I., Troutman, J., Skogstad, B., Taylor, L. S., & Edgar, K. J. (2016). Amphiphilic hydroxyalkyl cellulose derivatives for amorphous solid dispersion prepared by olefin cross-metathesis. *Polymer Chemistry*, 7(30), 4953-4963.

Dooley, K. E., Bliven-Sizemore, E. E., Weiner, M., Lu, Y., Nuermberger, E. L., Hubbard, W. C., . . . Dorman, S. E. (2012). Safety and Pharmacokinetics of Escalating Daily Doses of the Antituberculosis Drug Rifapentine in Healthy Volunteers. *Clinical Pharmacology & Therapeutics*, 91(5), 881-888.

Dooley, K. E., Savic, R. M., Park, J. G., Cramer, Y., Hafner, R., Hogg, E., . . . Team, A. A. S. (2015). Novel Dosing Strategies Increase Exposures of the Potent Antituberculosis Drug Rifapentine but Are Poorly Tolerated in Healthy Volunteers. *Antimicrobial Agents and Chemotherapy*, 59(6), 3399-3405.

Duanmu, H.-J., Liu, Y.-h., Jiang, G.-l., Wang, S.-m., & Fu, Y.-h. (2005). In vitro study on cross resistance of rifampin and rifapentine for Mycobacterium tuberculosis. *Chinese journal of tuberculosis and respiratory diseases*, 28(3), 192.

Dye, C., Scheele, S., Dolin, P., Pathania, V., Raviglione, M. C., for the, W. H. O. G. S., & Monitoring, P. (1999). Global burden of tuberculosis: Estimated incidence, prevalence, and mortality by country. *JAMA*, 282(7), 677-686.

Ediger, M. D., & Harrowell, P. (2012). Perspective: Supercooled liquids and glasses. *Journal of Chemical Physics*, 137(8), 080901.

Ehret, M. J., Levin, G. M., Narasimhan, M., & Rathinavelu, A. (2007). Venlafaxine induces P - glycoprotein in human Caco - 2 cells. *Human Psychopharmacology: Clinical and Experimental*, 22(1), 49-53.

Emary, W. B., Toren, P. C., Mathews, B., & Huh, K. (1998). Disposition and Metabolism of Rifapentine, a Rifamycin Antibiotic, in Mice, Rats, and Monkeys. *Drug Metabolism and Disposition,* 26(8), 725.

Enogene. Rifapentine(Priftin) Kinase Inhibitor.(2014). http://www.enogene.com/uploads/b6671ecd284a357cb6c967e1ce85f653-1/files/E1KS1760.pdf Accessed 5-19-2017.

Etcheverry, P., Grusak, M. A., & Fleige, L. E. (2012). Application of in vitro bioaccessibility and bioavailability methods for calcium, carotenoids, folate, iron, magnesium, polyphenols, zinc, and vitamins B(6), B(12), D, and E. *Frontiers in Physiology,* 3, 317.

Fang, Z., & Bhandari, B. (2010). Encapsulation of polyphenols – a review. *Trends in Food Science & Technology,* 21(10), 510-523.

FDA. Priftin (rifapentine) Tablets (2010). https://www.accessdata.fda.gov/drugsatfda_docs/label/2010/021024s009lbl.pdf Accessed 5/28.2017.

Fu, Q., Kou, L. F., Gong, C., Li, M., Sun, J., Zhang, D., . . . He, Z. G. (2012). Relationship between dissolution and bioavailability for nimodipine colloidal dispersions: The critical size in improving bioavailability. *International Journal of Pharmaceutics,* 427(2), 358-364.

Gilley, A. D., Arca, H. C., Nichols, B. L. B., Mosquera-Giraldo, L. I., Taylor, L. S., Edgar, K. J., & Neilson, A. P. (2017). Novel cellulose-based amorphous solid dispersions enhance quercetin solution concentrations in vitro. *Carbohydrate Polymers,* 157, 86-93.

Ginsberg, A. M. (2010). Drugs in Development for Tuberculosis. *Drugs* (New York, N.Y.), 70(17), 2201-2214.

Gomez-Orellana, I. (2005). Strategies to improve oral drug bioavailability. *Expert Opinion on Drug Delivery,* 2(3).

Gonçalves, J. E., Ballerini Fernandes, M., Chiann, C., Gai, M. N., De Souza, J., & Storpirtis, S. (2012). Effect of pH, mucin and bovine serum on rifampicin permeability through Caco - 2 cells. *Biopharmaceutics & Drug Disposition,* 33(6), 316-323.

Gonzales, G. S., Guy; Mackie, Alan; Grootaert, Charlotte; Bajka, Balazs; Rigby, Neil; Raes, Katleen; Van Camp, John. (2015). Reports Outline Functional Foods Findings from Institute of Food Research (Use of metabolomics and fluorescence recovery after photobleaching to study the bioavailability and intestinal mucus diffusion of polyphenols from cauliflower waste). *Food Weekly News,* 181.

Hastings, I. M., Watkins, W. M., & White, N. J. (2002). The evolution of drug–resistant malaria: the role of drug elimination half–life. *Philosophical Transactions of the Royal Society of London. Series B: Biological Sciences,* 357(1420), 505-519.

He, X., Wang, J., Liu, X., & Chen, X. (1996). High-performance liquid chromatography assay of rifapentine in human serum. *Journal of chromatography. B, Biomedical applications,* 681(2), 412.

Hedrén, E., Mulokozi, G., Svanberg, U., Chalmers University of, T., Chalmers tekniska, h., Institutionen för kemi och, b., . . . Bioscience. (2002). In vitro accessibility of carotenes from green leafy vegetables cooked with sunflower oil or red palm oil. *International Journal of Food Sciences and Nutrition,* 53(6), 445-453.

Höhne, G. W. H., Hemminger, W., Flammersheim, H. J., & SpringerLink. (1996). *Differential Scanning Calorimetry: An Introduction for Practitioners*. Berlin, Heidelberg: Springer Berlin Heidelberg.

Huang, Y., & Dai, W.-G. (2014). Fundamental aspects of solid dispersion technology for poorly soluble drugs. *Acta Pharmaceutica Sinica B,* 4(1), 18-25.

Ilevbare, G. A., Liu, H., Edgar, K. J., & Taylor, L. S. (2012). Understanding Polymer Properties Important for Crystal Growth Inhibition—Impact of Chemically Diverse Polymers on Solution Crystal Growth of Ritonavir. *Crystal Growth & Design,* 12(6), 3133-3143.

Jamis-Dow, C. A., Katki, A. G., Collins, J. M., & Klecker, R. W. (1997). Rifampin and rifabutin and their metabolism by human liver esterases. *Xenobiotica,* 27(10), 1015-1024.

Jolliffe, D. M. (2009). Practical gastric physiology. *Continuing Education in Anaesthesia, Critical Care & Pain,* 9(6), 173-177.

Kalia, J., & Raines, R. T. (2008). Hydrolytic Stability of Hydrazones and Oximes. *Angewandte Chemie (International ed. in English),* 47(39), 7523-7526.

Kalra, K., Gaur, M., Nainwal, P., Singh, R. P., & Jain, D. A. (2011). Solubility enhancement of rifapentine by inclusion complex. *International Journal of Drug Delivery,* 3(3), 432.

Kamada, N., Seo, S. U., Chen, G. Y., & Nunez, G. (2013). Role of the gut microbiota in immunity and inflammatory disease. *Nature Reviews Immunology,* 13(5), 321-335.

Karavas, E., Ktistis, G., Xenakis, A., & Georgarakis, E. (2006). Effect of hydrogen bonding interactions on the release mechanism of felodipine from nanodispersions with polyvinylpyrrolidone. *European Journal of Pharmaceutics and Biopharmaceutics,* 63(2), 103-114.

Kaunitz, J. D., & Akiba, Y. (2006). Review article: duodenal bicarbonate - mucosal protection, luminal chemosensing and acid-base balance: review: duodenal defence mechanisms. *Alimentary Pharmacology & Therapeutics,* 24, 169-176.

Keung, A., Eller, M. G., McKenzie, K. A., & Weir, S. J. (1999). Single and multiple dose pharmacokinetics of rifapentine in man: Part II. *The International Journal of Tuberculosis and Lung Disease,* 3(5), 437-444.

Keung, A. C. F., Eller, M. G., & Weir, S. J. (1998). Single-dose Pharmacokinetics of Rifapentine in Elderly Men. *Pharmaceutical Research*, 15(8), 1286-1291.

Kohri, T., Nanjo, F., Suzuki, M., Seto, R., Matsumoto, N., Yamakawa, M., . . . Chung, F.-L. (2001). Synthesis of (−)-[4-3H]Epigallocatechin Gallate and Its Metabolic Fate in Rats after Intravenous Administration. *Journal of Agricultural and Food Chemistry*, 49(2), 1042-1048.

Konno, H., Handa, T., Alonzo, D. E., & Taylor, L. S. (2008). Effect of polymer type on the dissolution profile of amorphous solid dispersions containing felodipine. *European Journal of Pharmaceutics and Biopharmaceutics*, 70(2), 493-499.

Kucukatay, V., Bor-Kucukatay, M., Atsak, P., & A Ar, A. (2007). Effect of Ingested Sulfite on Hippocampus Antioxidant Enzyme Activities in Sulfite Oxidase Competent and Deficient Rats. *International Journal of Neuroscience*, 117(7), 971-983.

Lackie, J. M. (2010). *A dictionary of biomedicine*. (1st ed.). Oxford: Oxford University Press.

Lambert, J. D., Sang, S., & Yang, C. S. (2007). Biotransformation of green tea polyphenols and the biological activities of those metabolites. *Molecular Pharmaceutics*, 4(6), 819-825.

Lee, C. A., Ismail, B., & Vickers, Z. M. (2012). The Role of Salivary Proteins in the Mechanism of Astringency. *Journal of Food Science*, 77(4), C381-C387.

Lemke, T. L. (1995). Antimycobacterial agents. *Principles of Medicinal Chemistry*, 4, 756-757.

Leuner, C., & Dressman, J. (2000). Improving drug solubility for oral delivery using solid dispersions. *European Journal of Pharmaceutics and Biopharmaceutics*, 50(1), 47-60.

Li, B., Konecke, S., Harich, K., Wegiel, L., Taylor, L. S., & Edgar, K. J. (2013). Solid dispersion of quercetin in cellulose derivative matrices influences both solubility and stability. *Carbohydrate Polymers*, 92(2), 2033-2040.

Li, B., Harich, K., Wegiel, L., Taylor, L. S., & Edgar, K. J. (2013). Stability and solubility enhancement of ellagic acid in cellulose ester solid dispersions. *Carbohydrate Polymers*, 92(2), 1443-1450.

Li, L., Li, H., Zhao, X., Ma, Y., Zhai, G., & Lou, H. (2009). Enhancement of gastrointestinal absorption of quercetin by solid lipid nanoparticles. *Journal of Controlled Release*, 133(3), 238-244.

Liu, H. (2014). Synthesis and Structure-property Evaluation of Novel Cellulosic Polymers as Amorphous Solid Dispersion Matrices for Enhanced Oral Drug Delivery. PhD Dissertation: *Virginia Tech*.

Liu, H., Ilevbare, G. A., Cherniawski, B. P., Ritchie, E. T., Taylor, L. S., & Edgar, K. J. (2014). Synthesis and structure-property evaluation of cellulose ω-carboxyesters for amorphous solid dispersions. *Carbohydrate Polymers*, 100, 116.

Liu, H., Taylor, L. S., & Edgar, K. J. (2015). The role of polymers in oral bioavailability enhancement; a review. *Polymer*, 77, 399-415.

LoBue, P. (2015). Chapter 3 Infectious Disease Related to Travel: Tuberculosis. *CDC*.

Lumsden, D. (2012). *X-Ray Powder Diffraction*. In *Earth Science. Physics and chemistry of the Earth* (pp. 576-580): Salem Press, Incorporated

Mackie, A. R., Macierzanka, A., Aarak, K., Rigby, N. M., Parker, R., Channell, G. A., . . . Bajka, B. H. (2016). Sodium alginate decreases the permeability of intestinal mucus. *Food Hydrocolloids*, 52, 749-755.

Maldonado-Valderrama, J., Wilde, P., Macierzanka, A., & Mackie, A. (2011). The role of bile salts in digestion. *Advances in colloid and interface science,* 165(1), 36-46.

Marks, J. A., Wegiel, L. A., Taylor, L. S., & Edgar, K. J. (2014). Pairwise Polymer Blends for Oral Drug Delivery. *Journal of Pharmaceutical Sciences,* 103(9), 2871-2883.

Martinez, M. N., & Amidon, G. L. (2002). A mechanistic approach to understanding the factors affecting drug absorption: A review of fundamentals. *Journal of Clinical Pharmacology,* 42(6), 620-643.

Martinsen,Tom C, Bergh, Kare, and Waldum, Helge L. (2005). Gastric Juice: A Barrier Against Infectious Diseases. *Basic & Clinical Pharmacology & Toxicology,* 96(2), 94-102.

McClements, D. J. (2015). Enhancing nutraceutical bioavailability through food matrix design. *Current Opinion in Food Science*, 4, 1-6.

McClements, D. J., Li, F., & Xiao, H. (2015). The Nutraceutical Bioavailability Classification Scheme: Classifying Nutraceuticals According to Factors Limiting their Oral Bioavailability. *Annual Review of Food Science and Technology,* 6(1), 299-327.

Monks, T. J., Jones, D. C., Bai, F., & Lau, S. S. (2004). The role of metabolism in 3, 4-(±)-methylenedioxyamphetamine and 3, 4-(±)-methylenedioxymethamphetamine (Ecstasy) toxicity. *Therapeutic drug monitoring*, 26(2), 132-136.

Mozafari, M. R., Khosravi-Darani, K., Borazan, G. G., Cui, J., Pardakhty, A., & Yurdugul, S. (2008). Encapsulation of Food Ingredients Using Nanoliposome Technology. *International Journal of Food Properties,* 11(4), 833-844.

Neilson, A., Ferruzzi, M., Coulston, A., Boushey, C., & Ferruzzi, M. (2012). Bioavailability and metabolism of bioactive compounds from foods. *Nutrition in the Prevention and Treatment of Disease*, 407-423.

Neilson, A. P., Hopf, A. S., Cooper, B. R., Pereira, M. A., Bomser, J. A., & Ferruzzi, M. G. (2007). Catechin Degradation with Concurrent Formation of Homo- and Heterocatechin Dimers during in Vitro Digestion. *Journal of Agricultural and Food Chemistry*, 55(22), 8941-8949.

Occelli, E., Nebuloni, M., & Cavalleri, B. (1990). Rifapentine hydrohalides. *Google Patents*.

Ostrovskii, K. P., Osipova, N. S., Vanchugova, L. V., Shipulo, E. V., Pereverzeva, É. R., Treshchalin, I. D., . . . Gel'perina, S. É. (2016). Use of Proteins to Increase the Aqueous Solubility of Rifapentine. *Pharmaceutical Chemistry Journal*, 50(6), 407-412.

Patil-Gadhe, A. A., Kyadarkunte, A. Y., Pereira, M., Jejurikar, G., Patole, M. S., Risbud, A., & Pokharkar, V. B. (2014). Rifapentine-proliposomes for inhalation: in vitro and in vivo toxicity. *Toxicology international*, 21(3), 275.

Pereira, J. M., Mejia-Ariza, R., Ilevbare, G. A., McGettigan, H. E., Sriranganathan, N., Taylor, L. S., . . . Edgar, K. J. (2013). Interplay of Degradation, Dissolution and Stabilization of Clarithromycin and Its Amorphous Solid Dispersions. *Molecular Pharmaceutics*, 10(12), 4640-4653.

Pouton, C. W. (2006). Formulation of poorly water-soluble drugs for oral administration: Physicochemical and physiological issues and the lipid formulation classification system. *European Journal of Pharmaceutical Sciences,* 29(3–4), 278-287.

Prasad, B., Bhutani, H., & Singh, S. (2006). Study of the interaction between rifapentine and isoniazid under acid conditions. *Journal of Pharmaceutical and Biomedical Analysis*, 41(4), 1438-1441.

Raina, S. A., Raina, S. A., Zhang, G. G. Z., Alonzo, D. E., & Wu, J. (2014). Enhancements and Limits in Drug Membrane Transport Using Supersaturated Solutions of Poorly Water Soluble Drugs. *Journal of Pharmaceutical Sciences*, 103(9), 2736-2748.

Rastogi, N., Legrand, E., & Sola, C. (2001). The mycobacteria: an introduction to nomenclature and pathogenesis. *Revue Scientifique Et Technique-Office International Des Epizooties,* 20(1), 21-54.

Ribera, E., Azuaje, C., Lopez, R. M., Domingo, P., Curran, A., Feijoo, M., . . . Pahissa, A. (2007). Pharmacokinetic interaction between rifampicin and the once-daily combination of saquinavir and low-dose ritonavir in HIV-infected patients with tuberculosis. *Journal of Antimicrobial Chemotherapy*, 59(4), 690-697.

Rollins, D. E., & Klaassen, C. D. (2012). Biliary Excretion of Drugs in Man. *Clinical Pharmacokinetics,* 4(5), 368-379.

Rosenthal, I. M., Williams, K., Tyagi, S., Peloquin, C. A., Vernon, A. A., Bishai, W. R., . . . Nuermberger, E. L. (2006). Potent Twice-Weekly Rifapentine-containing Regimens in Murine Tuberculosis. *American Journal of Respiratory and Critical Care Medicine,* 174(1), 94-101.

Ruslami, R., Hanneke, M. J. N., Alisjahbana, B., Parwati, I., Crevel, R. v., & Aarnoutse, R. E. (2007). Pharmacokinetics and Tolerability of a Higher Rifampin Dose versus the Standard Dose in Pulmonary Tuberculosis Patients. *Antimicrobial Agents and Chemotherapy,* 51(7), 2546-2551.

Schaschke, C. (2013). *Oxford Paperback Reference: Dictionary of Chemical Engineering*: OUP Oxford.

Serajuddin, A. T. M. (1999). Solid dispersion of poorly water-soluble drugs: Early promises, subsequent problems, and recent breakthroughs. *Journal of Pharmaceutical Sciences,* 88(10), 1058-1066.

Serajuddin, A. T. M. (2007). Salt formation to improve drug solubility. *Advanced Drug Delivery Reviews,* 59(7), 603-616.

Shah, N., Sandhu, H., Choi, D. S., Chokshi, H., Malick, A. W., & SpringerLink. (2014). *Amorphous Solid Dispersions: Theory and Practice*. (2014 ed.). New York, NY: Springer New York.

Sherwin, C. M. T., Fukuda, T., Brunner, H. I., Goebel, J., & Vinks, A. A. (2011). The Evolution of Population Pharmacokinetic Models to Describe the Enterohepatic Recycling of Mycophenolic Acid in Solid Organ Transplantation and Autoimmune Disease. *Clinical Pharmacokinetics,* 50(1), 1-24.

Sirgel, F. A., Fourie, P. B., Donald, P. R., Padayatchi, N., Rustomjee, R., Levin, J., . . . Rifapentine, E. B. A. C. S. G. (2005). The Early Bactericidal Activities of Rifampin and Rifapentine in Pulmonary Tuberculosis. *American Journal of Respiratory and Critical Care Medicine,* 172(1), 128-135.

Srivastava, A., Waterhouse, D., Ardrey, A., & Ward, S. A. (2012). Quantification of rifampicin in human plasma and cerebrospinal fluid by a highly sensitive and rapid liquid chromatographic–tandem mass spectrometric method. *Journal of Pharmaceutical and Biomedical Analysis,* 70, 523-528.

Sun, D. D., & Lee, P. I. (2013) Evolution of supersaturation of amorphous pharmaceuticals: the effect of rate of supersaturation generation. *Molecular Pharmaceutics,* 10(11), 4330-4346.

Tam, C. M., Chan, S. L., Lam, C. W., Dickinson, J. M., & Mitchison, D. A. (1997). Bioavailability of Chinese rifapentine during a clinical trial in Hong Kong. *The International Journal of Tuberculosis and Lung Disease,* 1(5), 411-416.

Tang, V. W., & Goodenough, D. A. (2003). Paracellular Ion Channel at the Tight Junction. *Biophysical Journal,* 84(3), 1660-1673.

Tazina, E. V., Kostin, K. V., & Oborotova, N. A. (2011). Specific features of drug encapsulation in liposomes (A review). *Pharmaceutical Chemistry Journal,* 45(8), 481-490.

Tetko, I. V., Gasteiger, J., Todeschini, R., Mauri, A., Livingstone, D., Ertl, P., . . . Prokopenko, V. V. (2005). Virtual Computational Chemistry Laboratory – Design and Description. *Journal of Computer-Aided Molecular Design,* 19(6), 453-463.

Theil, F., Anantharaman, S., Kyerematen, S. O., van Lishaut, H., Dreis-Kuhne, S. H., Rosenberg, J., . . . Woehrle, G. H. (2017). Frozen in Time: Kinetically Stabilized Amorphous Solid Dispersions of Nifedipine Stable after a Quarter Century of Storage. *Molecular Pharmaceutics,* 14(1), 183-192.

Ting, J. M., Nayale, T. S., Jones, S. D., Bates, F. S., & Reineke, T. M. (2015). Deconstructing HPMCAS: Excipient Design to Tailor Polymer-Drug Interactions

for Oral Drug Delivery. *ACS Biomaterials Science & Engineering*, 1(10), 978-990.

Ting, Y., Zhao, Q., Xia, C., & Huang, Q. (2015). Using in Vitro and in Vivo Models To Evaluate the Oral Bioavailability of Nutraceuticals. *Journal of Agricultural and Food Chemistry*, 63(5), 1332-1338.

Tirona, R. G., & Kim, R. B. (2002). Pharmacogenomics of organic anion-transporting polypeptides (OATP). *Advanced Drug Delivery Reviews*, 54(10), 1343-1352.

Toutain, P. L., & Bousquet - Mélou, A. (2004). Bioavailability and its assessment. *Journal of Veterinary Pharmacology and Therapeutics*, 27(6), 455-466.

Urso, R., Blardi, P., & Giorgi, G. (2002). A short introduction to pharmacokinetics. *European review for medical and pharmacological sciences*, 6(2-3), 33.

Van den Boogaard, J., Kibiki, G. S., Kisanga, E. R., Boeree, M. J., & Aarnoutse, R. E. (2009). New Drugs against Tuberculosis: Problems, Progress, and Evaluation of Agents in Clinical Development. *Antimicrobial Agents and Chemotherapy*, 53(3), 849-862.

Van Itallie, C. M., & Anderson, J. M. (2006). Claudins and epithelial paracellular transport. *Annual Review of Physiology*, 68(1), 403-429.

Vasconcelos, T., Sarmento, B., & Costa, P. (2007). Solid dispersions as strategy to improve oral bioavailability of poor water soluble drugs. *Drug Discovery Today*, 12(23–24), 1068-1075.

Volmink, J., & Garner, P. (2007). Directly observed therapy for treating tuberculosis. *Cochrane Database Syst Rev*, 4.

Wallace, M. N. Your Digestive System and How It Works.(2013). http://www.niddk.nih.gov/health-information/health-topics/Anatomy/your-digestive-system/Pages/anatomy.aspx Accessed.

Washington, N. (2001). *Physiological pharmaceutics : barriers to drug absorption*: Taylor & Francis.

Weiner, M., Bock, N., Peloquin, C. A., Burman, W. J., Khan, A., Vernon, A., . . . Tuberculosis Trials, C. (2004). Pharmacokinetics of Rifapentine at 600, 900, and 1,200 mg during Once-Weekly Tuberculosis Therapy. *American Journal of Respiratory and Critical Care Medicine*, 169(11), 1191-1197.

Wesch, R. (2011). Absolute and Relative Bioavailability. In H. G. Vogel, J. Maas & A. Gebauer (Eds.), *Drug Discovery and Evaluation: Methods in Clinical Pharmacology* (pp. 173-180). Berlin, Heidelberg: Springer Berlin Heidelberg

White, N. J. (2013). Pharmacokinetic and Pharmacodynamic Considerations in Antimalarial Dose Optimization. *Antimicrobial Agents and Chemotherapy*, 57(12), 5792-5807.

WHO. (2014). Global Tuberculosis Report 2014. *World Health Organization*.

WHO. (2015). Guidelines on the Management of Latent Tuberculosis Infection. WHO: *World Health Organization.*

Winchester, L. C., Podany, A. T., Baldwin, J. S., Robbins, B. L., & Fletcher, C. V. (2015). Determination of the rifamycin antibiotics rifabutin, rifampin, rifapentine and their major metabolites in human plasma via simultaneous extraction coupled with LC/MS/MS. *Journal of Pharmaceutical and Biomedical Analysis,* 104, 55-61.

Wolen, R. L., Carmichael, R. H., Ridolfo, A. S., Thompkins, L., & Ziege, E. A. (1979). The effect of crystal size on the bioavailability of benoxaprofen: studies utilizing deuterium labeled drug. *Biomedical mass spectrometry,* 6(4), 173-178.

Xu, J., Jin, H., Zhu, H., Zheng, M., Wang, B., Liu, C., . . . Lu, Y. (2013). Oral bioavailability of rifampicin, isoniazid, ethambutol, and pyrazinamide in a 4-drug fixed-dose combination compared with the separate formulations in healthy Chinese male volunteers. *Clinical therapeutics,* 35(2), 161-168.

Yadav, P., Soni, G., Mahor, A., Alok, S., Singh, P. P., & Verma, A. (2014). Solid Lipid Nanoparticles: An Effective and Promising Drug Delivery System- A Review. *International Journal of Pharmaceutical Sciences and Drug Research,* 5(4), 1152-1152.

Yang, Q., Wang, S., Fan, P., Wang, L., Di, Y., Lin, K., & Xiao, F.-S. (2005). pH-Responsive Carrier System Based on Carboxylic Acid Modified Mesoporous Silica and Polyelectrolyte for Drug Delivery. *Chemistry of Materials,* 17(24), 5999-6003.

Yew, W. (2002). Clinically Significant Interactions with Drugs Used in the Treatment of Tuberculosis. (Vol. 25, pp. 111-133). *Cham*: Adis International.

Yu, L. (2001). Amorphous pharmaceutical solids: preparation, characterization and stabilization. *Advanced Drug Delivery Reviews,* 48(1), 27-42.

Zhou, K., Li, J., Luo, J., & Zheng, D. (2010). Crystal modification of rifapentine using different solvents. *Frontiers of Chemical Engineering in China,* 4(1), 65-69.

Zhou, K., Li, J., & Zheng, D. S. (2010). Growth, characterization and crystal structure analysis of rifapentine. *Journal of Molecular Structure,* 983(1–3), 27-31.

Zvada, S. P., Jan-Stefan Van Der, W., Smith, P. J., Fourie, P. B., Roscigno, G., Mitchison, D., . . . Farmaceutiska, f. (2010). Effects of Four Different Meal Types on the Population Pharmacokinetics of Single-Dose Rifapentine in Healthy Male Volunteers. *Antimicrobial Agents and Chemotherapy,* 54(8), 3390-3394.

Appendix A

Supplementary Information for "Chapter 3: Cellulose-based amorphous solid dispersions enhance rifapentine delivery characteristics in vitro"

Christopher J. Winslow[a], Brittany L.B. Nichols[b], Diana Novo[b], Laura Mosquera-Giraldo[e], Lynne S. Taylor[e], Kevin J. Edgar[c,d], Andrew P. Neilson[a,*]

[a]Department of Food Science and Technology, Virginia Tech, Blacksburg, VA 24060, USA; Christopher Winslow - apples12@vt.edu; Andrew Neilson - andrewn@vt.edu
[b]Department of Chemistry, Virginia Tech; Brittany Nichols - brittan@vt.edu; Diana Novo - dnovo001@vt.edu
[c]Department of Sustainable Biomaterials, Virginia Tech; Kevin Edgar – kjedgar@vt.edu
[d]Macromolecules Innovation Institute, Virginia Tech;
[e]Department of Industrial and Physical Pharmacy, Purdue University, West Lafayette, IN 47907, USA; Lynne Taylor - lstaylor@purdue.edu; Laura Mosquera-Giraldo- lmosquer@purdue.edu

***Corresponding author:** Dr. Andrew P. Neilson, Dept. of Food Science and Technology at Virginia Tech
1981 Kraft Dr., Blacksburg, VA 24060; E-mail: andrewn@vt.edu; Phone: (540) 231-8391.

Materials

KCl (solid, anhydrous, ≥ 99%) sodium hydride (95%, NaH), 5-bromopent-1-ene, anhydrous tetrahydrofuran (THF), acrylic acid (AA), methyl acrylate (MA), 2-hydroxyethyl acrylate (HEA), *tert*-butyl acrylate (*t*BuA), 3,5-di-*tert*-butylhydroxytoluene (BHT), Hoveyda–Grubbs' 2nd generation catalyst, and *p*-toluenesulfonyl hydrazide (*p*TSH) were purchased from Sigma-Aldrich (St. Louis, MO). Acetonitrile (ACN, HPLC-grade), reagent ethanol, sodium phosphate monobasic, monopotassium phosphate (KH_2PO_4), dichloromethane (DCM), isopropanol, *N*,*N*-dimethylformamide (DMF), dialysis tubing (MWCO 3.5 kDa), and sodium hydroxide (NaOH) were purchased from Fisher Scientific (Hampton, NH) and used as received. HCl (12.1 M) was obtained from Macron Chemicals by Avantor (Center Valley, PA). Water was purified by reverse osmosis and ion exchange using a Barnstead RO pure ST from Barnstead/Thermolyne (Ramsey, MN) purification system. LCMS grade ACN, water, and methanol were obtained from VWR (Radnor, PA). Potassium phosphate dibasic (K_2HPO_4) was purchased from Acros Organics (Geel, Belgium). Ethyl vinyl ether was purchased from Fluka Analytical by Honeywell (Mexico City, Mexico).

Methods

Synthesis of ASD polymers

CASub

Preparation of monobenzyl suberate: suberic acid (87 g, 0.5 mol), benzyl alcohol (81 g, 0.75 mol), PTSA (0.95 g, 5 mmol), and toluene (200 mL) were stirred in a flask equipped with Dean-Stark trap and heated at reflux for 3 h until the theoretical amount of water

was collected. The resulting mixture was cooled to room temperature, water (200 mL) was added, and the pH adjusted to 9 with 6M NaOH. The aqueous layer was separated by centrifuge, mixed with ethyl ether (150 mL), and the pH adjusted to 2 with 6M HCl. The ether layer was separated and concentrated under reduced pressure to afford a colorless oil. ^{1}H NMR ($CDCl_3$): δ 1.33 (m, 4H), 1.68 (m, 4H), 2.36 (m, 4H), 5.09 (s, 2H), and 7.32 (m, 5H).

Synthesis of monobenzyl suberoyl chloride: Monobenzyl suberate (30 g, 113 mmol), DMF (3 drops), and 200 mL dichloromethane were cooled in a round bottomed flask to 0°C. Oxalyl chloride (25.4 g, 200 mmol) was added drop by drop under vigorous magnetic stirring, then stirred 2 h at room temperature till gas formation ceased. Solvent was removed under reduced pressure, 10 mL toluene was added, and then it was concentrated again under reduced pressure. The product was a yellow oil. ^{1}H NMR ($CDCl_3$): δ 1.34 (m, 4H), 1.66 (m, 4H), 2.36 (t, 2H), 2.86 (t, 2H), 5.12 (s, 2H), 7.35 (m, 5H).

Benzyl CASub synthesis: CA 320S (1.00 g, 4.19 mmol) was dissolved in DMI (20 mL), Et_3N (1.95 mL, 13.83 mmol, 3.3 eq) was added all at once, then monobenzyl suberoyl chloride (3.7 g, 12.57 mmol, 3 eq) was added. After 20 hours at 90°C under nitrogen, the reaction mixture was cooled, then added to ethanol (250 mL) dropwise to precipitate the product, which was isolated by vacuum filtration, then washed with 200 mL water and re-dissolved with 25 mL THF and re-precipitated in 200 mL hexane. The product was characterized by ^{1}H NMR. δ 1.3 ($COCH_2CH_2CH_2CH_2CH_2CH_2CO$ of suberate), 1.6

($COCH_2CH_2CH_2CH_2CH_2CH_2CO$ of suberate), 2.10–2.46 ($COCH_2CH_2CH_2CH_2CH_2CH_2CO$ of suberate and $COCH_3$ of acetate), 3.00–5.20 (cellulose backbone), 5.10 (s, $CH_2C_6H_5$), 7.35 (CH_2C_6H5).

Hydrogenolysis of benzyl CASub: Benzyl CASub (1 g) was dissolved in 100 mL THF, then $Pd(OH)_2/C$ (500 mg) was added. The mixture was stirred, after removal of the air by vacuum, at a high speed under H_2 (balloon) for 24 h at room temperature. Products were isolated by filtering through Celite, then the same protocol was repeated one more time and, the solvent was removed under reduced pressure, and the product precipitated in ethanol (100 mL). ^{1}H NMR CASub (DMSO): δ 1.2 ($COCH_2CH_2CH_2CH_2CH_2CH_2CO$ of suberate), 1.4-1.6 ($COCH_2CH_2CH_2CH_2CH_2CH_2CO$ of suberate), 2.10–2.46 ($COCH_2CH_2CH_2CH_2CH_2CH_2CO$ of suberate, and $COCH_3$ of acetate), 3.00-5.20 (cellulose backbone).

CHC

Preparation of hydroxypropyl pent-4-enyl cellulose (HPC-Pen106): HPC (1.0 g, 2.40 mmol AGU, 7.19 mmol –OH) was dispersed in 15 mL of anhydrous THF using a mechanical stirrer and with a nitrogen purge. Polymer gradually dissolved to form a clear and transparent solution after overnight stirring. NaH (95%, 0.28 g, 21.6 mmol, 3 equiv./–OH) was added with N_2 protection. The reaction mixture was cooled to 0°C in an ice bath and 5-bromopent-1-ene (1.13 g, 7.2 mmol, 1.0 equiv./–OH) was added dropwise with vigorous stirring. The solution was stirred at room temperature for 1 d and then at 50 °C for 3 d. After cooling to room temperature, isopropanol was gradually added to

deactivate residual catalyst. The solution was added to 300 mL of pH 7.4 buffer solution (3.54 g KH_2PO_4 and 7.14 g KH_2PO_4 in 1000 mL deionized water) to precipitate the product, which was then recovered by filtration. The precipitate was redissolved in THF, then reprecipitated into hexane and recovered by filtration, before vacuum drying at 40°C overnight.

Olefin cross-metathesis reaction with acrylic acid: BHT (5 mg) and 3 mL of THF were added to a flask containing HPC-Pen106 (100 mg; 0.20 mmol AGU; 0.22 mmol terminal olefin). The mixture was stirred under N_2 protection at 37 °C until all reagents were completely dissolved. Acrylic acid (0.82 g; 10.8 mmol; 50 equiv./terminal olefin) was added, followed by the Hoveyda–Grubbs' 2nd generation catalyst (12.8 mg; 8 mol%, dissolved in 4 mL THF). After stirring at 37 °C for 2 h, the reaction was stopped by adding two drops of ethyl vinyl ether. The product solution was concentrated by evaporating the THF solvent with a nitrogen purge and was then added to water to precipitate the product, which was collected by vacuum filtration, then vacuum dried overnight at 40 °C.

Hydrogenation of the CM product HPC-Pen106-AA (CHC) by p-toluenesulfonyl hydrazide (pTSH): BHT (8 mg; 10 wt%) and 4 mL DMF were added to a flask containing HPC-Pen106-AA (CHC) (80 mg; 0.15 mmol AGU; 0.16 mmol olefin). The mixture was stirred under N_2 protection at room temperature until all reagents were completely dissolved. Next, pTSH (0.18 g; 0.95 mmol; 6 equiv./olefin) was added. After refluxing at

135 °C for 5 h, the product was dialyzed against acetone for 3 d and then against water for 2 d, with the acetone and water being changed daily, and then freeze dried.

Preparation of ASDs via Solution Casting

Our convention for naming treatments is to list the % polymer, with the remainder being drug. For example, 90% HPMCAS/10% RPT is referred to as "90 HPMCAS" in the text, or simply "90" in most figures. RPT-loaded ASDs were prepared at 50%, 75%, and 90% by weight for each polymer (HPMCAS, CASub, and CHC) (i.e. 50%, 25%, and 10% RPT by weight). ASD RPT content (loading) was confirmed by UPLC-MS/MS and is presented in Supplementary Table 1. ASD microparticles with formulations 90, 75, and 50 % HPMCAS, CASub, or CHC: rifapentine (RPT) were prepared by film casting. The polymers were either dissolved in acetone (HPMCAS) or tetrahydrofuran (CASub and CHC) and RPT (dissolved in minimal chloroform) was added dropwise with stirring. The solution was allowed to stir overnight before casting films from the solution onto a coated glass plate and allowed to air dry. The films were ground using a Scienceware ® Micro-Mill ® from Bel-Art (Wayne, NJ).

Determination of RPT solubility

Water-circulating jacketed flasks (n=4) were brought to temperature (37°C) and filled with 20 mL sodium phosphate buffer (see "*In Vitro* Dissolution Experiments" below for preparation). A magnetic stir bar was added to each flask and allowed to sit for 2 min. to allow temperature to equalize. An excess of RPT (40 mg) was then added to each flask (2 mg/mL total load, not completely dissolved). These solutions were then stirred for 8 h

(400 rpm), stopping ~1 min. prior to sampling. Samples from each flask were taken at t=1, 2, 4, and 8 h. For each sampling time, 2-250 µL samples were drawn per flask (total *n*=8 from all flasks combined) and centrifuged (17,000 x *g*, 10 min, room temp. ~20°C). Then, 100 µL supernatant was sampled, being careful not to disturb the pellet. Supernatant samples were diluted 10-fold with 900 µL acetonitrile (ACN). Samples were stored at −80°C until further analysis. This study was performed 2 times. Samples were prepared for UPLC and quantified using standard curve with internal standard (see UPLC-MS/MS methods below for details).

Amorphous Solubility of RPT and HPLC Method

Supersaturated RPT solutions were prepared by adding a specific amount of stock solution (10 mg/mL in methanol) to 15 mL buffer at 37 ºC to equal a concentration of 470 µg/mL (RPT). Buffer was sodium phosphate (100 mM, pH 6.8) with 5 µg/mL HPMCAS-MF added. The solutions (*n*=8) were centrifuged at 14,800 rpm (21,100xg), for 45 min., 37 ºC using a Sorvall™ Legend™ Micro 21R Microcentrifuge (ThermoFischer Scientific, Hanover park, IL) equipped with a 24 x 1.5/2.0mL rotor with Click Seal biocontainment lid.

After centrifugation, the supernatant was collected and diluted 1:20 with acetonitrile, and the final concentration was measured using an Agilent HPLC 1260 Infinity system (Agilent Technologies, CA, USA) with an Agilent Eclipse plus C18, 4.6 × 250 mm, 5 µm analytical column (Agilent technologies, CA,USA). Mobile phase was isocratic 50:50 acetonitrile:DI water. All solvents were HPLC grade. An injection volume of 5 µL was

employed with a flow rate of 1 mL/min. Total run time was 10 min., with the retention time for RPT of 6.3 min. A standard curve prepared in methanol was used for quantification with concentrations ranging from 0.005mg/mL - 0.04 mg/mL.

Solid State Characterization of RPT loaded ASDs

DSC

DSC is used in heat measurements and thermal property determination and is especially helpful in determining purity, glass transition temperatures, and crystal structure (Höhne, Hemminger, Flammersheim, & SpringerLink, 1996; Kun Zhou et al., 2010). DSC analyses were performed on a Trios TA Instrument (New Castle, DE) with dry samples (5 mg) loaded into TzeroTM aluminum pans. A heat/cool/heat experiment was done for each sample and the 2nd heating scan was used. Each sample was equilibrated at 25˚C for 5 min., and then heated to 145˚C at 10˚C/min. Sample was kept at isothermal temperature for 1 min. After this, quench cooling occurred at 50˚C/ min. until -50˚C was reached. Finally, sample was heated to 190˚C at 15˚C/min. T_g values were recorded as the step-change inflection point from second heat scans.

PXRD

PXRD is used to analyze the crystalline structure and properties of powders and to distinguish glass states from various crystal forms present in the drug (Lumsden, 2012; Kun Zhou et al., 2010). PXRD patterns were measured with a Bruker D8 Discover X-ray Defractometer (Billerica, MA) with a Lynxeye detector and a KFL CU 2K X-ray source. Samples were run with a 1 mm slit window between a scan range of 10˚ to 50˚ 2θ.

In Vitro Dissolution Experiments

Gastric (pH 1.2) and Small intestinal (pH 6.8) Dissolution experiments

Dissolution experiments were performed under non-sink conditions in order to facilitate observation of apparent solubility at supersaturation levels. We suspected that the ASD formulations would provide higher solution concentrations than RPT alone, so non-sink conditions were necessary. These dissolution experiments were designed to mimic fasted human gastrointestinal conditions. Fasted gastric pH was simulated using pH 1.2 buffer (500 mL of 0.2 M KCl was combined with 850 mL of 0.2 M HCl, and then diluted to 2 L with MilliQ water). Fasting small intestinal pH was simulated using pH 6.8 buffer (6.8 g/L sodium phosphate monobasic in MilliQ Water, adjusted with 0.2 M NaOH to pH 6.8). Dissolution experiments were performed as described by Gilley *et al.* 2017 and Pereira *et al.* 2013, with modifications (Gilley et al., 2017; Pereira et al., 2013). 50 mL water circulating jacketed flasks (n=4) were used to maintain a constant temperature of 37°C. Dissolution medium consisted of 10 mL buffer, either pH 1.2 or 6.8. All treatments contained a fixed amount of RPT (8.2 mg in 10 mL buffer, obtained by varying the amount of ASD added) to ensure treatments were all given equal possibility of supersaturation. 8.2 mg was chosen because it allows for a 5-fold increase in concentration above the determined solubility of RPT, which we calculated by multiplying our experimental (determined) solubility (0.164 mg/mL) by 5 (allowing for up to 5-fold supersaturation) and then multiplied this by the volume of the dissolution (10 mL). The use of small dissolution volumes was also selected in order to minimize the masses of polymers needed. 5X the mass of RPT needed to achieve saturation was

selected to provide conditions where supersaturation was possible, while at the same time limiting the amount of ASD polymers needed to complete the study (due to difficulty in synthesis of CAsub and CHC). However, this limits the obtainable supersaturation to 5X crystalline solubility in these experiments. It should be noted that this is an experimental limitation, not a theoretical one; use of greater masses of RPT in combination with different polymers could potentially provide supersaturation greater than 5X. Flasks were stirred with small magnetic stir bars at 400 rpm over the course of 2 h for gastric pH or 8 h for small intestine pH. Samples were taken at 30, 60, 90, 120 min. for gastric pH or 30, 60, 90, 120, 180, 240, 300, 360, 420, and 480 min. for small intestinal pH. Sample aliquots were 250 μL and each aliquot was immediately replaced with 250 μL of appropriate buffer to maintain a constant volume. Samples were centrifuged (10 min, 37°C, 47,000 x *g*) on a Beckman Coulter Avanti JE high-speed centrifuge (Sunnyvale, CA) in order to pellet out insoluble suspended microparticles to the extent feasible. For gastric dissolution samples, 200 μL of supernatant was drawn from each sample and neutralized with 5 μL of 5N NaOH (no dilution was used due to the lower solution concentrations typically obtained for most samples in gastic dissolution experiments); for small intestinal dissolution samples, 100 μL of supernatant was drawn and an appropriate dilution was performed with ACN (1400 μL for HPMCAS and CHC, 400 μL for CASub and RPT alone). Samples were stored at −80°C prior to analysis by UPLC-MS/MS.

Gastric →Small Intestinal ("pH Switch") Dissolution experiments

To more closely mimic gut transit *in vivo*, pH switch dissolution experiments were performed in order to determine the impact of gastric events on subsequent dissolution in

the small intestine. These dissolution experiments were performed as described by Pereira *et al*. 2013 with modifications (Pereira et al., 2013). In these dissolution experiments, gastrointestinal conditions were simulated with 1 N HCl, instead of potassium chloride buffer. The pH of HCl was adjusted to 1.2 using 1 N NaOH before use. Dissolution medium started with 7.5 mL pH 1.2 1 N HCl, instead of 10 mL. Sample aliquots (250 μL, t=30, 60, 90, 120, 150, 180, 240, 300, 360, 420, and 480 min) were replaced with 250 μL of pH adjusted 1 N HCl for t= 30-120 min. and replaced with 250 μL pH 6.8 buffer from 150-480 min. to maintain a constant volume. After sample at 120 min. was collected, a rapid switch to pH 6.8 was performed. To each flask, 2500 μL of pH 6.8 phosphate buffer and 80 μL of 5N NaOH was added. pH was then adjusted as needed to reach 6.8 with 1 N NaOH and/or 1N HCl. Sampling then continued as if it were a pH 6.8 dissolution but with the addition of a timepoint at 150 min. Samples from gastric and intestinal pH were centrifuged, then neutralized (for gastric) or diluted (for intestinal), and stored prior to analysis as described above for the respective pH conditions.

UPLC Verification of RPT ASD content

RPT loading into ASDs was quantified by UPLC-MS/MS. Each batch of ASDs were evaluated for % loading (n=4). 10 mg of each formulation or RPT alone was accurately weighed and mass recorded. The ASD or RPT was volumetrically dissolved into 50 mL with ACN and sonicated 10 min to break the ASD structure and dissolve RPT. Samples were prepared for UPLC-MS/MS (see UPLC-MS/MS section for details). Samples were analyzed immediately and then stored at −80°C, if further analysis was needed. Loading

was calculated as percent by weight of the total ASD. Loading is reported in Supplementary Table 1.

Neutralization and Freezer Stability

A stability study was performed to determine the effectiveness of neutralization and freezing at preventing 3-formylrifamycin (3-FR) formation after the conclusion of dissolution. 50 mL water-circulating jacketed flasks (*n*=4) were maintained at 37°C. 30 mL of pH 1.2 KCl buffer and a stir bar were added to each flask. RPT was then added to each flask at concentrations that matched dissolution experiments, 5x solubility at saturation (being 24.6 mg for 30 mL) and stirred at 400 rpm for 1 hour. After this time, stirring was stopped and flasks were allowed to settle for 1 min. before drawing 1000 µL aliquots from each flask. Aliquots were centrifuged (47,000 x *g*, 10 min., 37°C). The supernatant from each sample was subsequently divided into 4-200 µL samples (*n*=16 total from 4 flasks). Half of these (*n*=8) were neutralized with 5 µL of 5N NaOH, per the protocol for stabilizing supernatants following gastric dissolution experiments, and the other half (*n*=8) were not neutralized. Each of these (*n*=8 neutralized, *n*=8 non-neutralized) were then divided in half again, of which *n*=4 from both the neutralized and non-neutralized samples were analyzed on UPLC-MS/MS immediately as described below. The remaining half (*n*=4 from both neutralized and non-neutralized) were stored in the freezer (−80°C) for one week prior to analysis as described below. 3-FR levels were quantified as RPT equivalents for each sample. Data were statistically analyzed using Prism v. 6.0d (GraphPad, la Jolla, CA). Statistical significance between treatments was determined using one-way ANOVA with Tukey's HSD *post hoc* test between all

treatment groups. Significance was defined *a priori* as P<0.05. Dixon's Q-test (α = 0.05) was used to identify any outliers as necessary, which were excluded.

UPLC-MS/MS

Filtration Study

Filtration is typically required for optimal UPLC-MS/MS performance and to prevent instrument clogging and column fouling. This study was designed to determine the impact of sample filtration on measured solution concentrations. A solution of 0.166 mg/mL RPT was made up in pH 6.8 sodium phosphate buffer. This concentration was chosen because it is close our calculated saturated solubility of rifapentine (0.164 mg/mL) which provided a value that we thought would represent an average of sample concentrations, with samples at pH 1.2 having much lower concentrations and samples at pH 6.8 much higher concentrations. This solution was stirred for 1 h at 500 rpm. Then 4-1000 μL samples were drawn and placed into two separate tubes. Samples were centrifuged (17,000 x *g*, 10 min, 25°C). 500 μL of sample was drawn from each tube and combined to give a total of 2000 μL. This 2000 μL was used to determine the effects of filtration on sample concentration. Samples were prepared (*n*=4) with the standard protocol of filtering through a PTFE, 0.2 μm, 13mm Dikma filter (Lake Forest, CA). The other samples (*n*=4) were prepared as per standard protocol but without filtration. Data were statistically analyzed using Prism v. 6.0d (GraphPad, la Jolla, CA). Statistical significance between treatments was determined using a t-test between treatment groups. Significance was defined *a priori* as P<0.05. Dixon's Q-test (α = 0.05) was used to identify any outliers as necessary, which were excluded. No significant differences were

found in observed RPT concentrations between treatments (see Supplementary Figure 1 below). Therefore, filtration was employed for all samples reported in this manuscript.

RPT and RIF Sample Preparation

Sample preparation was performed the same way for all experimental samples and standard curves. The internal standard (IS) solution was rifampin (0.0504mg/mL) in ACN. Experimental samples were vortexted thoroughly before use to ensure even mixing. Samples were prepared for analysis by combining 100 µL sample (diluted dissolution supernatant or ASD extract), 100 µL IS (0.0504 mg/mL RIF in ACN), and 600 µL mobile phase A (0.1% formic acid in water) to give conditions similar to starting conditions in the UPLC (~75% aqueous, ~25% ACN). These were combined into 2 mL tubes and vortexed. Since it was previously determined that filtration through 13 mm, 0.22 um, PTFE filters did not significantly affect measured concentrations of analytes, samples were drawn with a syringe and filtered (13 mm Luer-Lok PTFE syringe filters, 0.22 µm pore size) into Waters UPLC vials (Milford, MA).

Analyses were performed on a Waters Acquity H-class UPLC separation module (Milford, MA) equipped with a Waters Acquity UPLC BEH C18 column (2.1 mm x 50 mm, 1.7 µm particle size). Column temperature was maintained at 40°C and samples were kept at 25°C in the autosampler. The binary mobile phase consisted of 0.1% (v/v) aqueous formic acid (phase A) and 0.1% (v/v) formic acid in ACN (phase B) (all solvents LC-MS grade, except formic acid). System flow rate was 0.4 mL/min. A linear elution gradient was employed as follows: 75% A at 0 min, 5% A at 2 min, 0% A at 3 min. An

injection volume of 5 μL was employed. A second injection of 100 μL methanol was used in between sample injections to remove any carryover RPT, with gradient 0% A initially, 75% A at 1 min for 1.5 min. A prerun re-equilibration period (75% A, 2 min) was then used to restore the initial conditions for the next injection. Electrospray (ESI)-MS/MS analysis was performed in positive mode on a Waters Acquity TQD (triple quadrupole) mass spectrometer equipped with a Z-spray electrospray interface. Capillary voltage was 1.5 kV, source temperature was 150°C, and desolvation temperature was 500°C. Desolvation and cone gasses were N_2 at flow rates of 900 and 30 L/hr, respectively. Detection was performed by multi-reaction monitoring (MRM) of parent psuedomolecular ($[M-H]^-$) ion to daughter (fragment) ion transitions during collision-induced dissociation (CID, Ar gas: 0.25 mL/min).

The MRM transitions were developed using the Intellistart function of Masslynx (Waters) software. The MRMs for RIF and RPT were 823.71 m/z → 791.50 m/z and 877.71 m/z → 845.56 m/z, respectively, with collision energies of 12 eV (RIF) and 14 eV (RPT), and cone voltages were 32 V (RIF) and 44 V (RPT). Quantification was based on an internal standard curve prepared using varying levels of RPT with the fixed internal standard, RIF.

3-formylrifamycin

To produce a high concentration of 3-FR, an excess of RPT (0.1632 g) was added to 50 mL of 1 N HCl and left at room temperature for 3 d. This excess amount of RPT in the acidic solution was likely to give a large amount of 3-FR. The degraded sample was

freeze dried, solubilized in 25 mL ACN, centrifuged (3500 x *g*, 5 min, 20°C) and the supernatant was used to develop a UPLC-MS/MS method for 3-FR. Direct infusion MS was employed to optimize ionization parameters (negative mode was optimum for 3-FR, whereas positive mode was optimal for RPT). First, an MS (parent ion, $[M-H^-]$) spectrum of the degraded sample was obtained (m/z 100-1000), followed by an MS/MS spectrum of degraded sample (m/z 100-750) (**Fig. 3.6**). After confirming the presence of the expected $[M-H^-]$ (MW = 725.8, observed $[M-H^-]$ = 724.1), an MS/MS (daughter ion) spectrum was obtained for this parent using a collision energy ramp (5-60 eV). Finally, a multi-reaction monitoring (MRM) MS/MS method was developed for 3-FR using the Waters Masslynx Intellistart function, and the UPLC-MS/MS method employed for RPT was modified to detect 3-FR.

UPLC-MS/MS conditions were largely unchanged but were optimized for detection of 3-FR in gastric dissolution experiments samples. The UPLC run was extended to 5 min , with detection of RIF and RPT from 0-3 min per the standard method, and with the MRM for 3-FR spanning from 3-5 min. The same linear elution gradient was employed as the rifapentine method, with the only difference being the extension period; after 3 min., the gradient was kept at 100% B (0.1% formic acid in ACN) until completion at 5 min. Optimization of ionization for 3-FR resulted in slightly different conditions compared to RIF and RPT: ion mode was negative, capillary voltage was 2.1 kV, cone voltage was 55 V, cone gas was N_2 at a flow rate of 50 L/hr. The MRM transition for 3-formylrifamycin (3-FR) was 724.08 m/z → 392.95 m/z, with collision energy of 38 eV. 3-FR was quantified as RPT equivalents

Results

Filtration Study

The use of filtration in UPLC analysis is common practice. Filtering samples prevents problems of UPLC contamination and other damage as well as reduces chances of clogging the instrument and column fouling. The use of filtration can increase throughput, reduce downtime, and lead to higher performance in analysis. However, not all filters are optimal for all analytes and for this reason it is important to determine if the specific filter used causes differences in measured concentration of specific samples. Furthermore, filtration could adsorb soluble RPT and catch insoluble RPT microparticles. Therefore, it was necessary to determine whether filtration would affect measured RPT concentrations and thus calculated solution concentrations. In this study, we determined that filtration through PTFE, 0.2 μm, 13mm filters did not significantly affect measured concentration of our analytes (Supplementary Figure 1).

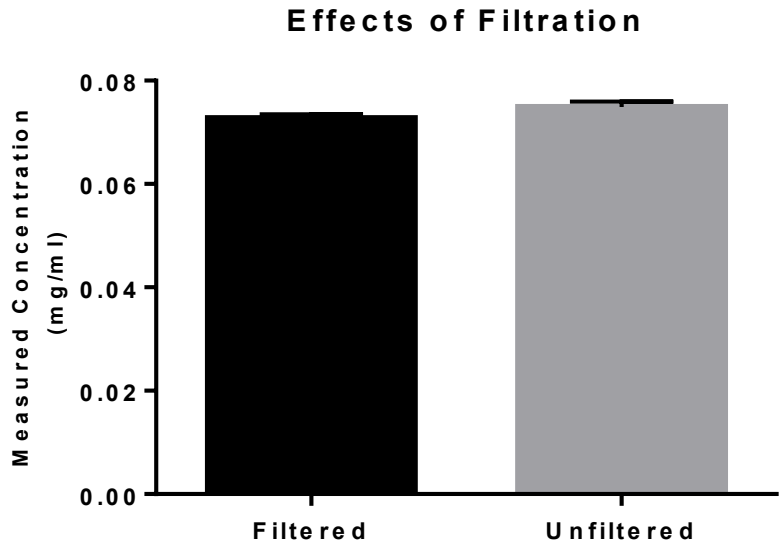

Supplementary Figure 1: The effect of sample filtration on measured RPT concentration. Values represent mean ± SEM [n=3(filtered), n=4(unfiltered]). No significant differences were found (t-test, p<0.05).

Neutralization and Freezer Stability

This study was performed to determine the effectiveness of neutralization and freezing at preventing 3-formylrifamycin (3-FR) formation after the conclusion of dissolution. The results clearly show that both neutralization and freezing significantly reduce formation of 3-FR post-dissolution compared to analyzing fresh, non-neutralized samples (Supplementary Figure 2). These results confirm that our standard practice of freezing and neutralizing samples before analysis effectively reduced formation of 3-FR, and that 3-FR concentrations are primarily due to dissolution and are not artifacts of subsequent post-dissolution storage. We also found that the measured 3-FR concentration from thedissolution experiment employing 90 HPMCAS did not show significantly higher concentration of 3-FR compared to RPT analyzed directly from the bottle (Supplementary Figure 3). This indicates that the 90 HPMCAS ASD essentially showed

no degradation due to the actual dissolution experiment and 3-FR concentration was primarily due to concentration previously found in the RPT.

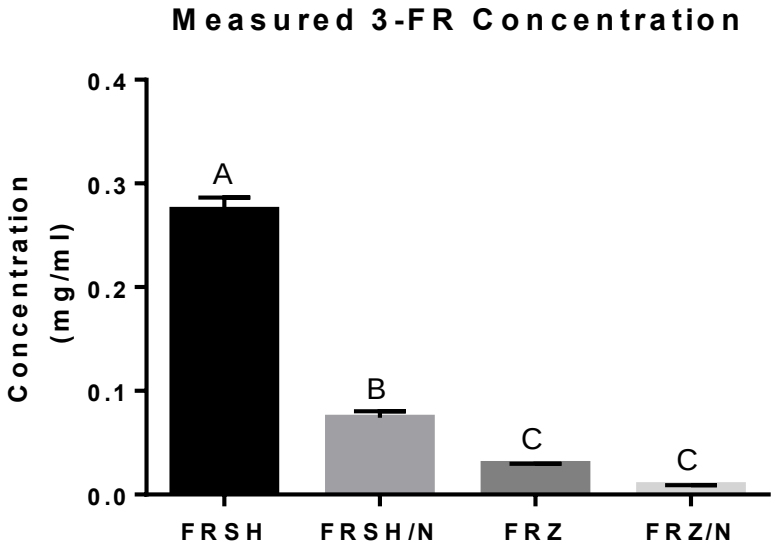

Supplementary Figure 2: Measured concentration of 3-formylrifamycin[1] (3-FR) after differing treatments of freezing and neutralization, after dissolution at gastric pH. FRSH represent samples prepared immediately after the dissolution and FRZ represents samples that were frozen for 1 week prior to analysis. /N represents neutralization of sample with 5N NaOH. Values represent mean ± SEM (n=4). Values on the graph not sharing a common superscript are significantly different (1-way ANOVA with Tukey's post hoc test for all possible comparisons, $p<0.05$).

[1]3-FR was quantified as RPT equivalents

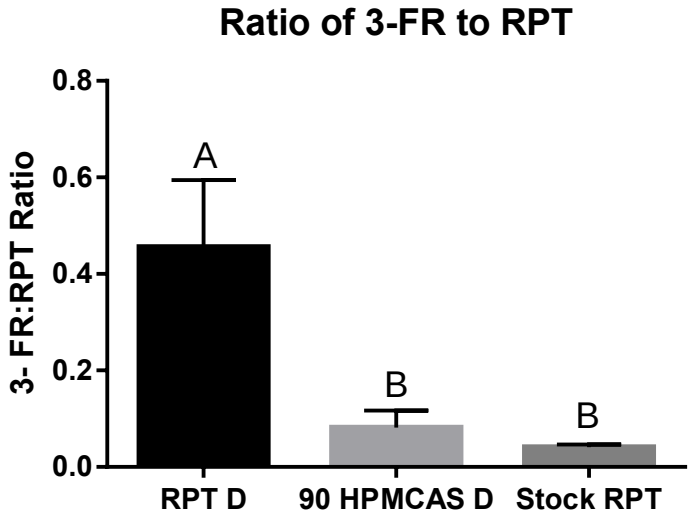

Supplementary Figure 3: Measured concentration of 3-FR[1,2] expressed as a fraction of the highest possible solution concentration of RPT as measured in gastric dissolution (pH 1.2) after 30 min. of exposure for RPT alone (RPT D), 90 HPMCAS (90 HPMCAS D), and as measured directly from the bottle of untreated RPT without dissolution (Stock RPT)[3]. Values represent mean ± SEM (n=3-4). Values on the graph not sharing a common superscript are significantly different (1-way ANOVA with Tukey's post hoc test for all possible comparisons, $p<0.05$).

[1]This figure is representative only of soluble 3-FR

[2]3-FR was quantified as RPT equivalents

[3]The concentration of 3-FR in untreated RPT powder was found to be 5.58 ± 0.621(mean ± SEM) % weight

UPLC Verification of RPT ASD content

RPT content in each ASD formulation was verified before use to ensure correct loading (% by weight).

Supplementary Table 1: Measured RPT content of prepared ASD formulations.

ASD Formulation[a]	Formulated RPT (%weight)	Measured RPT (%weight)[bc]
RPT[b]	100[d]	95.8 ± 2.77[d]
90 HPMCAS	10	9.11 ± 0.207
75 HPMCAS	25	20.1 ± 1.24
50 HPMCAS[b]	50	45.2 ± 3.54
90 CASub	10	7.74 ± 0.0616
75 CASub	25	22.1 ± 0.592
50 CASub	50	49.6 ± 1.31
90 CHC	10	7.72 ± 1.83
75 CHC	25	23.7 ± 0.636
50 CHC	50	43.5 ± 1.42

[a]Convention for naming treatments is to list the % polymer, with the remainder being RPT

[b]Data shown are mean ± SEM (n = 4), except RPT which represents n = 8, and 50 HPMCAS which represents n = 5

[c]Note that the seemingly low contents of RPT in the ASDs is likely due to polymers not being fully solubilized during testing, due to clumping. Analytical error is another possible contributing cause to these low values.

[d]Supplier indicated 98.2% purity

Solid State ASD Characterization Results

DSC and PXRD were used to characterize RPT loaded ASDs and ensure that the RPT was in the amorphous form. Supplementary Figure 4 shows that the DSC and PXRD data clearly confirm the amorphous nature of the RPT loaded ASDs. The DSC data show a T_g for all ASDs and a steep crystalline melting peak for RPT alone, indicative of amorphous

and crystalline forms, respectively. Evidence from PXRD also confirms that the RPT loaded ASDs were in their amorphous form. RPT alone showed steep peaks indicating the diffraction of the X-rays due to the crystalline structure whereas the ASDs only show amorphous halos.

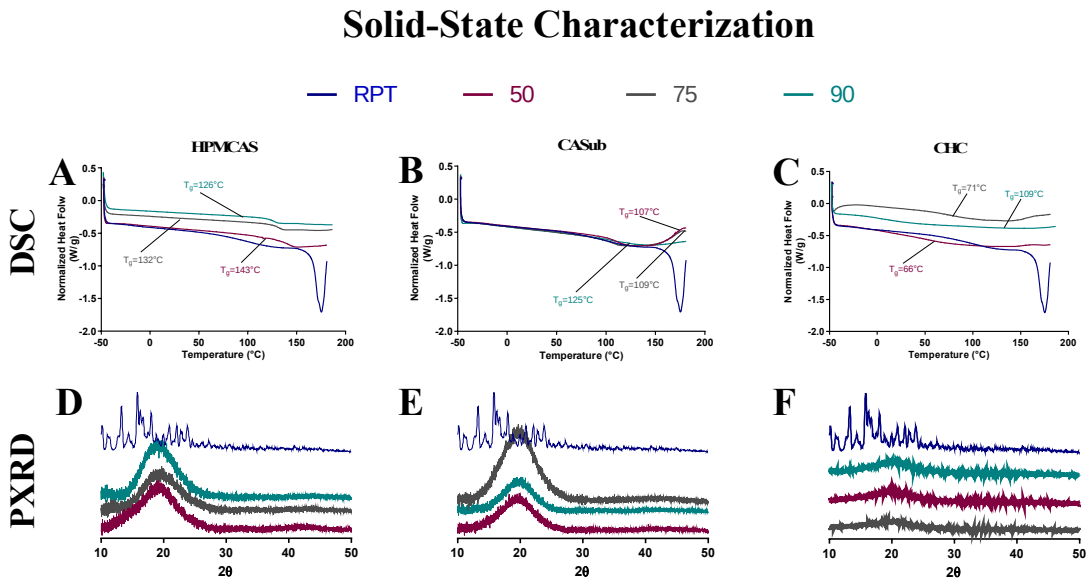

Supplementary Figure 4: Results of solid state characterization of crystalline RPT and RPT-loaded ASD from various polymers: HPMCAS (A, D), CASub (B, E) and CHC (C, F) as measured by differential scanning calorimetry (DSC) and X-ray powder diffraction (PXRD). These data confirm the amorphous nature of RPT in the ASDs as opposed to the crystallinity of RPT alone.

In Vitro Dissolution Experiments

Pseudo-pharmacokinetic parameters have been provided in this section in tabular form below.

Supplementary Table 2: Pseudo-pharmacokinetic parameters at pH 1.2

ASD Formulation	AUC[a] ((mg)(min)/mL)	C_{max}[a] (mg/mL)
RPT[b]	0.952 ± 0.110	0.0130 ± 0.00193
90 HPMCAS	0.0489 ± 0.00219	0.000737 ± 0.000105
75 HPMCAS	0.174 ± 0.0671	0.00310 ± 0.00145
50 HPMCAS	0.539 ± 0.0250	0.00587 ± 0.000360
90 CASub	0.0300 ± 0.00413	0.000500 ± 0.000185
75 CASub	0.251 ± 0.0527	0.00324 ± 0.000724
50 CASub	0.228 ± 0.0550	0.00416 ± 0.00181
90 CHC	0.339 ± 0.00996	0.00403 ± 0.000182
75 CHC	0.764 ±0.0139	0.0122 ± 0.000567
50 CHC[b]	1.41 ±0.0586	0.0222 ± 0.00186

[a]Data are mean ± SEM; AUC and C_{max} (n = 4 except where indicated)
[b]n = 3

Supplementary Table 3: Pseudo-pharmacokinetic parameters at pH 6.8

ASD Formulation	AUC[a] ((mg*min)/mL)	C_{max}[a] (mg/mL)
RPT	46.5 ± 3.48	0.141 ± 0.00721
90 HPMCAS[b]	180 ± 1.92	0.466 ± 0.0140
75 HPMCAS[b]	147 ± 2.68	0.497 ± 0.0435
50 HPMCAS[b]	124 ± 2.13	0.298 ± 0.00995
90 CASub	11.3 ±0 .381	0.0300 ± 0.00215
75 CASub	8.29 ± 0.378	0.0257 ± 0.00222
50 CASub	13.9 ± 0.894	0.0488 ± 0.00364
90 CHC	65.7 ± 5.08	0.2586 ± 0.0470
75 CHC	123 ± 4.19	0.287 ± 0.0136
50 CHC	106 ± 1.19	0.251 ± 0.00404

[a]Data are mean ± SEM; AUC and C_{max} (n = 4 except where indicated)
[b]n = 3

Suplementary Table 4: Pseudo-pharmacokinetic parameters after pH switch[a]

ASD Formulation	AUC[b] ((mg*min)/mL)	C_{max}[b](mg/mL)
RPT	26.5 ± 2.91	0.0975 ± 0.00678
90 HPMCAS	127 ± 3.67	0.488 ± 0.0338
75 HPMCAS	44.9 ± 4.44	0.164 ± 0.0157
50 HPMCAS	15.5 ± 1.03	0.0622 ± 0.00255
90 CASub[c]	14.3 ± 2.92	0.0676 ± 0.0148
75 CASub	15.4 ± 1.48	0.0561 ± 0.00358
50 CASub	20.1 ± 1.27	0.0777 ± 0.00737
90 CHC	64.2 ± 3.03	0.3039 ± 0.0398
75 CHC	59.2 ± 3.58	0.213 ± 0.0177
50 CHC	38.2 ± 2.08	0.176 ± 0.0204

[a]Values are calculated only from 120 min to 480 min with 120 min as a zero point
[b]Data are mean ± SEM; AUC and C_{max} (n = 4 except where indicated)
[c]n = 3